Contents

ROMAI J., v.19, no.1(2023), 1–24

MULTIVARIATE FUZZY-RANDOM AND STOCHASTIC GENERAL SIGMOID ACTIVATION FUNCTION INDUCED NEURAL NETWORK APPROXIMATIONS

George A. Anastassiou

Department of Mathematical Sciences, University of Memphis, Memphis, U.S.A.

ganastss@memphis.edu

Abstract In this article we research the degree of approximation of multivariate pointwise and uniform convergences in the q-mean to the Fuzzy-Random unit operator of multivariate Fuzzy-Random Quasi-Interpolation general sigmoid activation function based neural network operators. These multivariate Fuzzy-Random operators arise in a natural way among multivariate Fuzzy-Random neural networks. The rates are given through multivariate Probabilistic-Jackson type inequalities involving the multivariate Fuzzy-Random modulus of continuity of the engaged multivariate Fuzzy-Random function. The plain stochastic extreme analog of this theory is also met in detail for the stochastic analogs of the operators: the stochastic full quasi-interpolation operators, the stochastic Kantorovich type operators and the stochastic quadrature type operators.

Keywords: Fuzzy-Random analysis, Fuzzy-Random neural networks and operators, Fuzzy-Random modulus of continuity, Fuzzy-Random functions, Stochastic processes, Jackson type fuzzy and probabilistic inequalities, general sigmoid function.

2020 MSC: 26A15, 26E50, 41A17, 41A25, 41A99, 47S40, 60H25, 60H30.

1. FUZZY-RANDOM FUNCTIONS AND STOCHASTIC PROCESSES BACKGROUND

See also [18], Ch. 22, pp. 497-501.

We start with

Definition 1.1. *(see* [28]*) Let $\mu : \mathbb{R} \to [0,1]$ with the following properties:*

(i) is normal, i.e., $\exists\ x_0 \in \mathbb{R} : \mu(x_0) = 1$.

(ii) $\mu(\lambda x + (1-\lambda) y) \geq \min\{\mu(x), \mu(y)\}$, $\forall\ x, y \in \mathbb{R}$, $\forall\ \lambda \in [0,1]$ (μ is called a convex fuzzy subset).

(iii) μ is upper semicontinuous on $\mathbb{R}$, i.e., $\forall\ x_0 \in \mathbb{R}$ and $\forall\ \varepsilon > 0$, $\exists$ neighborhood $V(x_0) : \mu(x) \leq \mu(x_0) + \varepsilon$, $\forall\ x \in V(x_0)$.

(iv) the set $\overline{supp(\mu)}$ is compact in $\mathbb{R}$ (where $supp(\mu) := \{x \in \mathbb{R}; \mu(x) > 0\}$).

We call μ a fuzzy real number. Denote the set of all μ with $\mathbb{R}_{\mathcal{F}}$.

E.g., $\chi_{\{x_0\}} \in \mathbb{R}_{\mathcal{F}}$, *for any* $x_0 \in \mathbb{R}$, *where* $\chi_{\{x_0\}}$ *is the characteristic function at* x_0.

For $0 < r \leq 1$ *and* $\mu \in \mathbb{R}_{\mathcal{F}}$ *define* $[\mu]^r := \{x \in \mathbb{R} : \mu(x) \geq r\}$ *and* $[\mu]^0 := \overline{\{x \in \mathbb{R} : \mu(x) > 0\}}$.

Then it is well known that for each $r \in [0,1]$, $[\mu]^r$ is a closed and bounded interval of $\mathbb{R}$. For $u, v \in \mathbb{R}_{\mathcal{F}}$ and $\lambda \in \mathbb{R}$, we define uniquely the sum $u \oplus v$ and the product $\lambda \odot u$ by

$$[u \oplus v]^r = [u]^r + [v]^r, \quad [\lambda \odot u]^r = \lambda [u]^r, \quad \forall\, r \in [0,1],$$

where $[u]^r + [v]^r$ means the usual addition of two intervals (as subsets of $\mathbb{R}$) and $\lambda [u]^r$ means the usual product between a scalar and a subset of $\mathbb{R}$ (see, e.g., [28]). Notice $1 \odot u = u$ and it holds $u \oplus v = v \oplus u$, $\lambda \odot u = u \odot \lambda$. If $0 \leq r_1 \leq r_2 \leq 1$ then $[u]^{r_2} \subseteq [u]^{r_1}$. Actually $[u]^r = \left[u_-^{(r)}, u_+^{(r)}\right]$, where $u_-^{(r)} < u_+^{(r)}$, $u_-^{(r)}, u_+^{(r)} \in \mathbb{R}$, $\forall\, r \in [0,1]$.

Define

$$D : \mathbb{R}_{\mathcal{F}} \times \mathbb{R}_{\mathcal{F}} \to \mathbb{R}_+ \cup \{0\}$$

by

$$D(u,v) := \sup_{r \in [0,1]} \max\left\{\left|u_-^{(r)} - v_-^{(r)}\right|, \left|u_+^{(r)} - v_+^{(r)}\right|\right\},$$

where $[v]^r = \left[v_-^{(r)}, v_+^{(r)}\right]$; $u, v \in \mathbb{R}_{\mathcal{F}}$. We have that D is a metric on $\mathbb{R}_{\mathcal{F}}$. Then $(\mathbb{R}_{\mathcal{F}}, D)$ is a complete metric space, see [28], with the properties

$$\begin{gathered} D(u \oplus w, v \oplus w) = D(u,v), \quad \forall\, u, v, w \in \mathbb{R}_{\mathcal{F}}, \\ D(k \odot u, k \odot v) = |k|\, D(u,v), \quad \forall\, u, v \in \mathbb{R}_{\mathcal{F}}, \forall\, k \in \mathbb{R}, \\ D(u \oplus v, w \oplus e) \leq D(u,w) + D(v,e), \quad \forall\, u, v, w, e \in \mathbb{R}_{\mathcal{F}}. \end{gathered} \tag{1}$$

Let (M,d) metric space and $f, g : M \to \mathbb{R}_{\mathcal{F}}$ be fuzzy real number valued functions. The distance between f, g is defined by

$$D^*(f,g) := \sup_{x \in M} D(f(x), g(x)).$$

On $\mathbb{R}_{\mathcal{F}}$ we define a partial order by "$\leq$": $u, v \in \mathbb{R}_{\mathcal{F}}$, $u \leq v$ iff $u_-^{(r)} \leq v_-^{(r)}$ and $u_+^{(r)} \leq v_+^{(r)}$, $\forall\, r \in [0,1]$.

$\overset{*}{\sum}$ denotes the fuzzy summation, $\widetilde{o} := \chi_{\{0\}} \in \mathbb{R}_{\mathcal{F}}$ the neutral element with respect to $\oplus$. For more see also [29], [30].

We need

Definition 1.2. *(see also* [24]*, Definition 13.16, p. 654) Let* $(X, \mathcal{B}, P)$ *be a probability space. A fuzzy-random variable is a* $\mathcal{B}$*-measurable mapping* g :

$X \to \mathbb{R}_{\mathcal{F}}$ *(i.e., for any open set* $U \subseteq \mathbb{R}_{\mathcal{F}}$*, in the topology of* $\mathbb{R}_{\mathcal{F}}$ *generated by the metric* D*, we have*

$$g^{-1}(U) = \{s \in X; g(s) \in U\} \in \mathcal{B}). \tag{2}$$

The set of all fuzzy-random variables is denoted by $\mathcal{L}_{\mathcal{F}}(X, \mathcal{B}, P)$*. Let* $g_n, g \in \mathcal{L}_{\mathcal{F}}(X, \mathcal{B}, P)$*,* $n \in \mathbb{N}$ *and* $0 < q < +\infty$*. We say* $g_n(s) \overset{\text{"q-mean"}}{\underset{n\to+\infty}{\to}} g(s)$ *if*

$$\lim_{n\to+\infty} \int_X D(g_n(s), g(s))^q P(ds) = 0. \tag{3}$$

Remark 1.1. *(see* [24]*, p. 654) If* $f, g \in \mathcal{L}_{\mathcal{F}}(X, \mathcal{B}, P)$*, let us denote* $F : X \to \mathbb{R}_+ \cup \{0\}$ *by* $F(s) = D(f(s), g(s))$*,* $s \in X$*. Here,* F *is* $\mathcal{B}$*-measurable, because* $F = G \circ H$*, where* $G(u, v) = D(u, v)$ *is continuous on* $\mathbb{R}_{\mathcal{F}} \times \mathbb{R}_{\mathcal{F}}$*, and* $H : X \to \mathbb{R}_{\mathcal{F}} \times \mathbb{R}_{\mathcal{F}}$*,* $H(s) = (f(s), g(s))$*,* $s \in X$*, is* $\mathcal{B}$*-measurable. This shows that the above convergence in q-mean makes sense.*

Definition 1.3. *(see* [24]*, p. 654, Definition 13.17) Let* $(T, \mathcal{T})$ *be a topological space. A mapping* $f : T \to \mathcal{L}_{\mathcal{F}}(X, \mathcal{B}, P)$ *will be called fuzzy-random function (or fuzzy-stochastic process) on* T*. We denote* $f(t)(s) = f(t, s)$*,* $t \in T$*,* $s \in X$*.*

Remark 1.2. *(see* [24]*, p. 655) Any usual fuzzy real function* $f : T \to \mathbb{R}_{\mathcal{F}}$ *can be identified with the degenerate fuzzy-random function* $f(t, s) = f(t)$*,* $\forall$ $t \in T$*,* $s \in X$*.*

Remark 1.3. *(see* [24]*, p. 655) Fuzzy-random functions that coincide with probability one for each* $t \in T$ *will be consider equivalent.*

Remark 1.4. *(see* [24]*, p. 655) Let* $f, g : T \to \mathcal{L}_{\mathcal{F}}(X, \mathcal{B}, P)$*. Then* $f \oplus g$ *and* $k \odot f$ *are defined pointwise, i.e.,*

$$\begin{aligned} (f \oplus g)(t, s) &= f(t, s) \oplus g(t, s), \\ (k \odot f)(t, s) &= k \odot f(t, s), \ \ t \in T, s \in X, \ k \in \mathbb{R}. \end{aligned}$$

Definition 1.4. *(see also Definition 13.18, pp. 655-656,* [24]*) For a fuzzy-random function* $f : W \subseteq \mathbb{R}^N \to \mathcal{L}_{\mathcal{F}}(X, \mathcal{B}, P)$*,* $N \in \mathbb{N}$*, we define the (first) fuzzy-random modulus of continuity*

$$\Omega_1^{(\mathcal{F})}(f, \delta)_{L^q} =$$

$$\sup\left\{\left(\int_X D^q(f(x, s), f(y, s)) P(ds)\right)^{\frac{1}{q}} : x, y \in W, \ \ \|x - y\|_\infty \le \delta\right\},$$

$0 < \delta$*,* $1 \le q < \infty$*.*

Definition 1.5. *([16]) Here $1 \leq q < +\infty$. Let $f : W \subseteq \mathbb{R}^N \to \mathcal{L}_{\mathcal{F}}(X, \mathcal{B}, P)$, $N \in \mathbb{N}$, be a fuzzy random function. We call f a (q-mean) uniformly continuous fuzzy random function over W, iff $\forall\ \varepsilon > 0\ \exists\ \delta > 0$:whenever $\|x - y\|_\infty \leq \delta$, $x, y \in W$, implies that*

$$\int_X (D(f(x,s), f(y,s)))^q P(ds) \leq \varepsilon.$$

We denote it as $f \in C_{FR}^{U_q}(W)$.

Proposition 1.1. *([16]) Let $f \in C_{FR}^{U_q}(W)$, where $W \subseteq \mathbb{R}^N$ is convex.*
Then $\Omega_1^{(\mathcal{F})}(f, \delta)_{L^q} < \infty$, any $\delta > 0$.

Proposition 1.2. *([16]) Let $f, g : W \subseteq \mathbb{R}^N \to \mathcal{L}_{\mathcal{F}}(X, \mathcal{B}, P)$, $N \in \mathbb{N}$, be fuzzy random functions. It holds*
(i) $\Omega_1^{(\mathcal{F})}(f, \delta)_{L^q}$ is nonnegative and nondecreasing in $\delta > 0$.
(ii) $\lim_{\delta \downarrow 0} \Omega_1^{(\mathcal{F})}(f, \delta)_{L^q} = \Omega_1^{(\mathcal{F})}(f, 0)_{L^q} = 0$, iff $f \in C_{FR}^{U_q}(W)$.

We mention

Definition 1.6. *(see also [6]) Let $f(t, s)$ be a random function (stochastic process) from $W \times (X, \mathcal{B}, P)$, $W \subseteq \mathbb{R}^N$, into $\mathbb{R}$, where $(X, \mathcal{B}, P)$ is a probability space. We define the q-mean multivariate first modulus of continuity of f by*

$$\Omega_1(f, \delta)_{L^q} :=$$

$$\sup \left\{ \left(\int_X |f(x,s) - f(y,s)|^q P(ds) \right)^{\frac{1}{q}} : x, y \in W,\ \ \|x - y\|_\infty \leq \delta \right\}, \quad (4)$$

$\delta > 0$, $1 \leq q < \infty$.

The concept of f being (q-mean) uniformly continuous random function is defined the same way as in Definition 1.5, just replace D by $|\cdot|$, etc. We denote it as $f \in C_{\mathbb{R}}^{U_q}(W)$.

Similar properties as in Propositions 1.1, 1.2 are valid for $\Omega_1(f, \delta)_{L^q}$.

Also we have

Proposition 1.3. *([3]) Let $Y(t, \omega)$ be a real valued stochastic process such that Y is continuous in $t \in [a, b]$. Then Y is jointly measurable in (t, ω).*

According to [23], p. 94 we have the following

Definition 1.7. *Let $(Y, \mathcal{T})$ be a topological space, with its σ-algebra of Borel sets $\mathcal{B} := \mathcal{B}(Y, \mathcal{T})$ generated by $\mathcal{T}$. If $(X, \mathcal{S})$ is a measurable space, a function $f : X \to Y$ is called measurable iff $f^{-1}(B) \in \mathcal{S}$ for all $B \in \mathcal{B}$.*

By Theorem 4.1.6 of [23], p. 89 f as above is measurable iff

$$f^{-1}(C) \in \mathcal{S} \text{ for all } C \in \mathcal{T}.$$

We mention

Theorem 1.1. *(see* [23]*, p. 95) Let $(X, \mathcal{S})$ be a measurable space and (Y, d) be a metric space. Let f_n be measurable functions from X into Y such that for all $x \in X$, $f_n(x) \to f(x)$ in Y. Then f is measurable. I.e., $\lim_{n\to\infty} f_n = f$ is measurable.*

We need also

Proposition 1.4. *(*[16]*) Let f, g be fuzzy random variables from $\mathcal{S}$ into $\mathbb{R}_{\mathcal{F}}$. Then*

(i) Let $c \in \mathbb{R}$, then $c \odot f$ is a fuzzy random variable.

(ii) $f \oplus g$ is a fuzzy random variable.

Proposition 1.5. *Let $Y\left(\overrightarrow{t}, \omega\right)$ be a real valued multivariate random function (stochastic process) such that Y is continuous in $\overrightarrow{t} \in \prod_{i=1}^{N} [a_i, b_i]$. Then Y is jointly measurable in $\left(\overrightarrow{t}, \omega\right)$ and $\int_{\prod_{i=1}^{N}[a_i,b_i]} Y\left(\overrightarrow{t}, \omega\right) d\overrightarrow{t}$ is a real valued random variable.*

Proof. Similar to Proposition 18.14, p. 353 of [7]. ∎

2. ABOUT REAL NEURAL NETWORKS BACKGROUND

Here we follow [21].

Let $h : \mathbb{R} \to [-1, 1]$ be a general sigmoid function, such that it is strictly increasing, $h(0) = 0$, $h(-x) = -h(x)$, $h(+\infty) = 1$, $h(-\infty) = -1$. Also h is strictly convex over $(-\infty, 0]$ and strictly concave over $[0, +\infty)$, with $h^{(2)} \in C(\mathbb{R})$.

We consider the activation function

$$\psi(x) := \frac{1}{4}\left(h(x+1) - h(x-1)\right), \quad x \in \mathbb{R}, \tag{5}$$

As in [20], p. 88, we get that $\psi(-x) = \psi(x)$, thus ψ is an even function. Since $x + 1 > x - 1$, then $h(x+1) > h(x-1)$, and $\psi(x) > 0$, all $x \in \mathbb{R}$.

We see that

$$\psi(0) = \frac{h(1)}{2}. \tag{6}$$

Let $x > 1$, we have that

$$\psi'(x) = \frac{1}{4}\left(h'(x+1) - h'(x-1)\right) < 0,$$

by h' being strictly decreasing over $[0, +\infty)$.

Let now $0 < x < 1$, then $1 - x > 0$ and $0 < 1 - x < 1 + x$. It holds $h'(x-1) = h'(1-x) > h'(x+1)$, so that again $\psi'(x) < 0$. Consequently ψ is stritly decreasing on $(0, +\infty)$.

Clearly, ψ is strictly increasing on $(-\infty, 0)$, and $\psi'(0) = 0$.

See that

$$\lim_{x \to +\infty} \psi(x) = \frac{1}{4}\left(h(+\infty) - h(+\infty)\right) = 0, \tag{7}$$

and

$$\lim_{x \to -\infty} \psi(x) = \frac{1}{4}\left(h(-\infty) - h(-\infty)\right) = 0. \tag{8}$$

That is the x-axis is the horizontal asymptote on ψ.

Conclusion, ψ is a bell symmetric function with maximum

$$\psi(0) = \frac{h(1)}{2}.$$

We need

Theorem 2.1. *([21]) We have that*

$$\sum_{i=-\infty}^{\infty} \psi(x - i) = 1, \ \ \forall\ x \in \mathbb{R}. \tag{9}$$

Theorem 2.2. *([21]) It holds*

$$\int_{-\infty}^{\infty} \psi(x)\, dx = 1. \tag{10}$$

Thus $\psi(x)$ is a density function on $\mathbb{R}$.

We give

Theorem 2.3. *([21]) Let $0 < \alpha < 1$, and $n \in \mathbb{N}$ with $n^{1-\alpha} > 2$. It holds*

$$\sum_{\substack{k=-\infty \\ :\, |nx-k| \geq n^{1-\alpha}}}^{\infty} \psi(nx - k) < \frac{\left(1 - h\left(n^{1-\alpha} - 2\right)\right)}{2}. \tag{11}$$

Notice that

$$\lim_{n \to +\infty} \frac{\left(1 - h\left(n^{1-\alpha} - 2\right)\right)}{2} = 0.$$

Denote by $\lfloor \cdot \rfloor$ the integral part of the number and by $\lceil \cdot \rceil$ the ceiling of the number.

We further give

Theorem 2.4. *([21]) Let $x \in [a,b] \subset \mathbb{R}$ and $n \in \mathbb{N}$ so that $\lceil na \rceil \leq \lfloor nb \rfloor$. It holds*

$$\frac{1}{\sum_{k=\lceil na \rceil}^{\lfloor nb \rfloor} \psi(nx-k)} < \frac{1}{\psi(1)}, \quad \forall\, x \in [a,b]. \tag{12}$$

Remark 2.1. *([21]) i) We have that*

$$\lim_{n\to\infty} \sum_{k=\lceil na \rceil}^{\lfloor nb \rfloor} \psi(nx-k) \neq 1, \tag{13}$$

for at least some $x \in [a,b]$.

ii) For large enough $n \in \mathbb{N}$ we always obtain $\lceil na \rceil \leq \lfloor nb \rfloor$. Also $a \leq \frac{k}{n} \leq b$, iff $\lceil na \rceil \leq k \leq \lfloor nb \rfloor$.

In general, by Theorem 2.1, it holds

$$\sum_{k=\lceil na \rceil}^{\lfloor nb \rfloor} \psi(nx-k) \leq 1. \tag{14}$$

We introduce

$$Z(x_1,...,x_N) := Z(x) := \prod_{i=1}^{N} \psi(x_i), \quad x = (x_1,...,x_N) \in \mathbb{R}^N,\ N \in \mathbb{N}. \tag{15}$$

It has the properties:

(i) $Z(x) > 0,\ \forall\, x \in \mathbb{R}^N$,

(ii)

$$\sum_{k=-\infty}^{\infty} Z(x-k) := \sum_{k_1=-\infty}^{\infty} \sum_{k_2=-\infty}^{\infty} ... \sum_{k_N=-\infty}^{\infty} Z(x_1-k_1,...,x_N-k_N) = 1, \tag{16}$$

where $k := (k_1,...,k_n) \in \mathbb{Z}^N$, $\forall\, x \in \mathbb{R}^N$,

hence

(iii)

$$\sum_{k=-\infty}^{\infty} Z(nx-k) = 1, \tag{17}$$

$\forall\, x \in \mathbb{R}^N$; $n \in \mathbb{N}$,

and

(iv)

$$\int_{\mathbb{R}^N} Z(x)\,dx = 1, \tag{18}$$

that is Z is a multivariate density function.

Here denote $\|x\|_\infty := \max\{|x_1|, ..., |x_N|\}$, $x \in \mathbb{R}^N$, also set $\infty := (\infty, ..., \infty)$, $-\infty := (-\infty, ..., -\infty)$ upon the multivariate context, and

$$\begin{gathered} \lceil na \rceil := (\lceil na_1 \rceil, ..., \lceil na_N \rceil), \\ \lfloor nb \rfloor := (\lfloor nb_1 \rfloor, ..., \lfloor nb_N \rfloor), \end{gathered} \tag{19}$$

where $a := (a_1, ..., a_N)$, $b := (b_1, ..., b_N)$.

We obviously see that

$$\sum_{k=\lceil na \rceil}^{\lfloor nb \rfloor} Z(nx-k) = \sum_{k=\lceil na \rceil}^{\lfloor nb \rfloor} \left(\prod_{i=1}^{N} \psi(nx_i - k_i) \right) =$$

$$\sum_{k_1=\lceil na_1 \rceil}^{\lfloor nb_1 \rfloor} ... \sum_{k_N=\lceil na_N \rceil}^{\lfloor nb_N \rfloor} \left(\prod_{i=1}^{N} \psi(nx_i - k_i) \right) = \prod_{i=1}^{N} \left(\sum_{k_i=\lceil na_i \rceil}^{\lfloor nb_i \rfloor} \psi(nx_i - k_i) \right). \tag{20}$$

For $0 < \beta < 1$ and $n \in \mathbb{N}$, a fixed $x \in \mathbb{R}^N$, we have that

$$\sum_{k=\lceil na \rceil}^{\lfloor nb \rfloor} Z(nx-k) =$$

$$\sum_{\substack{k=\lceil na \rceil \\ \left\| \frac{k}{n} - x \right\|_\infty \le \frac{1}{n^\beta}}}^{\lfloor nb \rfloor} Z(nx-k) + \sum_{\substack{k=\lceil na \rceil \\ \left\| \frac{k}{n} - x \right\|_\infty > \frac{1}{n^\beta}}}^{\lfloor nb \rfloor} Z(nx-k). \tag{21}$$

In the last two sums the counting is over disjoint vector sets of k's, because the condition $\left\| \frac{k}{n} - x \right\|_\infty > \frac{1}{n^\beta}$ implies that there exists at least one $\left| \frac{k_r}{n} - x_r \right| > \frac{1}{n^\beta}$, where $r \in \{1, ..., N\}$.

(v) As in [18], pp. 379-380, we derive that

$$\sum_{\substack{k=\lceil na \rceil \\ \left\| \frac{k}{n} - x \right\|_\infty > \frac{1}{n^\beta}}}^{\lfloor nb \rfloor} Z(nx-k) \overset{(11)}{<} \frac{1 - h\left(n^{1-\beta} - 2\right)}{2}, \quad 0 < \beta < 1, \tag{22}$$

with $n \in \mathbb{N} : n^{1-\beta} > 2$, $x \in \prod_{i=1}^{N} [a_i, b_i]$.

(vi) By Theorem 2.4 we get that

$$0 < \frac{1}{\sum_{k=\lceil na \rceil}^{\lfloor nb \rfloor} Z(nx-k)} < \frac{1}{(\psi(1))^N} =: \gamma(N), \tag{23}$$

$\forall\, x \in \left(\prod_{i=1}^{N} [a_i, b_i]\right)$, $n \in \mathbb{N}$.

It is also clear that

(vii)

$$\sum_{\substack{k=-\infty \\ \left\|\frac{k}{n}-x\right\|_\infty > \frac{1}{n^\beta}}}^{\infty} Z(nx-k) < \frac{1-h\left(n^{1-\beta}-2\right)}{2} =: c(\beta, n), \tag{24}$$

$0 < \beta < 1$, $n \in \mathbb{N} : n^{1-\beta} > 2$, $x \in \mathbb{R}^N$.

Furthermore it holds

$$\lim_{n\to\infty} \sum_{k=\lceil na \rceil}^{\lfloor nb \rfloor} Z(nx-k) \neq 1, \tag{25}$$

for at least some $x \in \left(\prod_{i=1}^{N} [a_i, b_i]\right)$.

Let $f \in C\left(\prod_{i=1}^{N} [a_i, b_i]\right)$, and $n \in \mathbb{N}$ such that $\lceil na_i \rceil \leq \lfloor nb_i \rfloor$, $i = 1, ..., N$.

We define the multivariate averaged positive linear neural network operators ($x := (x_1, ..., x_N) \in \left(\prod_{i=1}^{N} [a_i, b_i]\right)$):

$$A_n(f, x_1, ..., x_N) := A_n(f, x) := \frac{\sum_{k=\lceil na \rceil}^{\lfloor nb \rfloor} f\left(\frac{k}{n}\right) Z(nx-k)}{\sum_{k=\lceil na \rceil}^{\lfloor nb \rfloor} Z(nx-k)} = \tag{26}$$

$$\frac{\sum_{k_1=\lceil na_1 \rceil}^{\lfloor nb_1 \rfloor} \sum_{k_2=\lceil na_2 \rceil}^{\lfloor nb_2 \rfloor} \cdots \sum_{k_N=\lceil na_N \rceil}^{\lfloor nb_N \rfloor} f\left(\frac{k_1}{n}, ..., \frac{k_N}{n}\right) \left(\prod_{i=1}^{N} \psi(nx_i - k_i)\right)}{\prod_{i=1}^{N} \left(\sum_{k_i=\lceil na_i \rceil}^{\lfloor nb_i \rfloor} \psi(nx_i - k_i)\right)}.$$

For large enough $n \in \mathbb{N}$ we always obtain $\lceil na_i \rceil \leq \lfloor nb_i \rfloor$, $i = 1, ..., N$. Also $a_i \leq \frac{k_i}{n} \leq b_i$, iff $\lceil na_i \rceil \leq k_i \leq \lfloor nb_i \rfloor$, $i = 1, ..., N$.

When $f \in C_B\left(\mathbb{R}^N\right)$ we define

$$B_n(f, x) := B_n(f, x_1, ..., x_N) := \sum_{k=-\infty}^{\infty} f\left(\frac{k}{n}\right) Z(nx-k) := \tag{27}$$

$$\sum_{k_1=-\infty}^{\infty} \sum_{k_2=-\infty}^{\infty} \cdots \sum_{k_N=-\infty}^{\infty} f\left(\frac{k_1}{n}, \frac{k_2}{n}, ..., \frac{k_N}{n}\right) \left(\prod_{i=1}^{N} \psi(nx_i - k_i)\right),$$

$n \in \mathbb{N}$, $\forall\, x \in \mathbb{R}^N$, $N \in \mathbb{N}$, the multivariate quasi-interpolation neural network operators.

Also for $f \in C_B\left(\mathbb{R}^N\right)$ we define the multivariate Kantorovich type neural network operators

$$C_n\left(f,x\right) := C_n\left(f, x_1, ..., x_N\right) := \sum_{k=-\infty}^{\infty} \left(n^N \int_{\frac{k}{n}}^{\frac{k+1}{n}} f\left(t\right) dt \right) Z\left(nx - k\right) := \tag{28}$$

$$\sum_{k_1=-\infty}^{\infty} \sum_{k_2=-\infty}^{\infty} ... \sum_{k_N=-\infty}^{\infty} \left(n^N \int_{\frac{k_1}{n}}^{\frac{k_1+1}{n}} \int_{\frac{k_2}{n}}^{\frac{k_2+1}{n}} ... \int_{\frac{k_N}{n}}^{\frac{k_N+1}{n}} f\left(t_1, ..., t_N\right) dt_1 ... dt_N \right)$$

$$\cdot \left(\prod_{i=1}^{N} \psi\left(nx_i - k_i\right) \right),$$

$n \in \mathbb{N}$, $\forall\, x \in \mathbb{R}^N$.

Again for $f \in C_B\left(\mathbb{R}^N\right)$, $N \in \mathbb{N}$, we define the multivariate neural network operators of quadrature type $D_n\left(f,x\right)$, $n \in \mathbb{N}$, as follows. Let $\theta = \left(\theta_1, ..., \theta_N\right) \in \mathbb{N}^N$, $\overline{r} = \left(r_1, ..., r_N\right) \in \mathbb{Z}_+^N$, $w_{\overline{r}} = w_{r_1, r_2, ... r_N} \geq 0$, such that $\sum\limits_{\overline{r}=0}^{\theta} w_{\overline{r}} = \sum\limits_{r_1=0}^{\theta_1} \sum\limits_{r_2=0}^{\theta_2} ... \sum\limits_{r_N=0}^{\theta_N} w_{r_1, r_2, ... r_N} = 1$; $k \in \mathbb{Z}^N$ and

$$\delta_{nk}\left(f\right) := \delta_{n, k_1, k_2, ..., k_N}\left(f\right) := \sum_{\overline{r}=0}^{\theta} w_{\overline{r}} f\left(\frac{k}{n} + \frac{\overline{r}}{n\theta}\right) :=$$

$$\sum_{r_1=0}^{\theta_1} \sum_{r_2=0}^{\theta_2} ... \sum_{r_N=0}^{\theta_N} w_{r_1, r_2, ... r_N} f\left(\frac{k_1}{n} + \frac{r_1}{n\theta_1}, \frac{k_2}{n} + \frac{r_2}{n\theta_2}, ..., \frac{k_N}{n} + \frac{r_N}{n\theta_N}\right), \tag{29}$$

where $\frac{\overline{r}}{\theta} := \left(\frac{r_1}{\theta_1}, \frac{r_2}{\theta_2}, ..., \frac{r_N}{\theta_N}\right)$.

We put

$$D_n\left(f,x\right) := D_n\left(f, x_1, ..., x_N\right) := \sum_{k=-\infty}^{\infty} \delta_{nk}\left(f\right) Z\left(nx - k\right) := \tag{30}$$

$$\sum_{k_1=-\infty}^{\infty} \sum_{k_2=-\infty}^{\infty} ... \sum_{k_N=-\infty}^{\infty} \delta_{n, k_1, k_2, ..., k_N}\left(f\right) \left(\prod_{i=1}^{N} \psi\left(nx_i - k_i\right) \right),$$

$\forall\, x \in \mathbb{R}^N$.

For the next we need, for $f \in C\left(\prod_{i=1}^{N}[a_i,b_i]\right)$ the first multivariate modulus of continuity

$$\omega_1(f,h) := \sup_{\substack{x,y\in\prod_{i=1}^{N}[a_i,b_i]\\ \|x-y\|_\infty\le h}} |f(x)-f(y)|, \quad h>0.$$

A totally similar definition applies to $f \in C_B\left(\mathbb{R}^N\right)$.

Above $\|\cdot\|_\infty$ is the supremum norm.

In [20] we studied the basic approximation properties of A_n, B_n, C_n, D_n neural network operators and as well of their iterates for Banach space valued functions. That is, the quantitative pointwise and uniform convergence of these operators to the unit operator I.

We need

Theorem 2.5. *Let $f \in C\left(\prod_{i=1}^{N}[a_i,b_i]\right)$, $0<\beta<1$, $x \in \left(\prod_{i=1}^{N}[a_i,b_i]\right)$, $N,n\in\mathbb{N}$ with $n^{1-\beta}>2$. Then*

1)

$$|A_n(f,x)-f(x)| \le \gamma(N)\left[\omega_1\left(f,\frac{1}{n^\beta}\right)+2c(\beta,n)\|f\|_\infty\right] =: \lambda_1, \tag{31}$$

and

2)

$$\|A_n(f)-f\|_\infty \le \lambda_1. \tag{32}$$

We notice that $\lim_{n\to\infty} A_n(f)=f$, pointwise and uniformly.

Proof. Similar to [20], p. 118. ∎

We need

Theorem 2.6. *Let $f \in C_B\left(\mathbb{R}^N\right)$, $0<\beta<1$, $x\in\mathbb{R}^N$, $N,n\in\mathbb{N}$ with $n^{1-\beta}>2$. Then*

1)

$$|B_n(f,x)-f(x)| \le \omega_1\left(f,\frac{1}{n^\beta}\right)+2c(\beta,n)\|f\|_\infty =: \lambda_2, \tag{33}$$

2)

$$\|B_n(f)-f\|_\infty \le \lambda_2. \tag{34}$$

Given that $f \in \left(C_U\left(\mathbb{R}^N\right)\cap C_B\left(\mathbb{R}^N\right)\right)$, we obtain $\lim_{n\to\infty} B_n(f)=f$, uniformly.

Proof. Similar to [20], p. 128. ∎

We also need

Theorem 2.7. *Let* $f \in C_B\left(\mathbb{R}^N\right)$, $0 < \beta < 1$, $x \in \mathbb{R}^N$, $N, n \in \mathbb{N}$ *with* $n^{1-\beta} > 2$. *Then*

1)

$$|C_n(f,x) - f(x)| \leq \omega_1\left(f, \frac{1}{n} + \frac{1}{n^\beta}\right) + 2c(\beta,n)\|f\|_\infty =: \lambda_3, \tag{35}$$

2)

$$\|C_n(f) - f\|_\infty \leq \lambda_3. \tag{36}$$

Given that $f \in \left(C_U\left(\mathbb{R}^N\right) \cap C_B\left(\mathbb{R}^N\right)\right)$, *we obtain* $\lim_{n\to\infty} C_n(f) = f$, *uniformly.*

Proof. Similar to [20], p. 129. ∎

We also need

Theorem 2.8. *Let* $f \in C_B\left(\mathbb{R}^N\right)$, $0 < \beta < 1$, $x \in \mathbb{R}^N$, $N, n \in \mathbb{N}$ *with* $n^{1-\beta} > 2$. *Then*

1)

$$|D_n(f,x) - f(x)| \leq \omega_1\left(f, \frac{1}{n} + \frac{1}{n^\beta}\right) + 2c(\beta,n)\|f\|_\infty = \lambda_3, \tag{37}$$

2)

$$\|D_n(f) - f\|_\infty \leq \lambda_3. \tag{38}$$

Given that $f \in \left(C_U\left(\mathbb{R}^N\right) \cap C_B\left(\mathbb{R}^N\right)\right)$, *we obtain* $\lim_{n\to\infty} D_n(f) = f$, *uniformly.*

Proof. Similar to [20], p. 131. ∎

In this article we extend Theorems 2.5, 2.6, 2.7, 2.8 to the random level.

We are also motivated by [1] - [16] and continuing [17]. For general knowledge on neural networks we recommend [25], [26], [27].

3. MAIN RESULTS

I) q-mean Approximation by Fuzzy-Random general sigmoid activation function based Quasi-Interpolation Neural Network Operators

All terms and assumptions here as in Sections 1, 2.

Let $f \in C_{\mathcal{FR}}^{U_q}\left(\prod_{i=1}^N [a_i, b_i]\right)$, $1 \leq q < +\infty$, $n, N \in \mathbb{N}$, $0 < \beta < 1$, $\overrightarrow{x} \in \left(\prod_{i=1}^N [a_i, b_i]\right)$, $(X, \mathcal{B}, P)$ probability space, $s \in X$.

We define the following multivariate fuzzy random general sigmoid activation function based quasi-interpolation linear neural network operators

$$\left(A_n^{\mathcal{FR}}(f)\right)(\overrightarrow{x},s) := \sum_{\overrightarrow{k}=\lceil na\rceil}^{\lfloor nb\rfloor *} f\left(\frac{\overrightarrow{k}}{n},s\right)\odot \frac{Z\left(n\overrightarrow{x}-\overrightarrow{k}\right)}{\sum_{\overrightarrow{k}=\lceil na\rceil}^{\lfloor nb\rfloor} Z\left(n\overrightarrow{x}-\overrightarrow{k}\right)}, \tag{39}$$

(see also (26).

We present

Theorem 3.1. *Let* $f\in C_{\mathcal{FR}}^{U_q}\left(\prod_{i=1}^{N}[a_i,b_i]\right)$, $0<\beta<1$, $\overrightarrow{x}\in\left(\prod_{i=1}^{N}[a_i,b_i]\right)$, $n,N\in\mathbb{N}$, *with* $n^{1-\beta}>2$, $1\leq q<+\infty$. *Assume that* $\int_X (D^*(f(\cdot,s),\widetilde{o}))^q P(ds)<\infty$. *Then*

1)

$$\left(\int_X D^q\left(\left(A_n^{\mathcal{FR}}(f)\right)(\overrightarrow{x},s),f(\overrightarrow{x},s)\right)P(ds)\right)^{\frac{1}{q}}\leq \tag{40}$$

$$\gamma(N)\left\{\Omega_1\left(f,\frac{1}{n^\beta}\right)_{L^q}+2c(\beta,n)\left(\int_X (D^*(f(\cdot,s),\widetilde{o}))^q P(ds)\right)^{\frac{1}{q}}\right\}=:\lambda_1^{(\mathcal{FR})},$$

2)

$$\left\|\left(\int_X D^q\left(\left(A_n^{\mathcal{FR}}(f)\right)(\overrightarrow{x},s),f(\overrightarrow{x},s)\right)P(ds)\right)^{\frac{1}{q}}\right\|_{\infty,\left(\prod_{i=1}^{N}[a_i,b_i]\right)}\leq\lambda_1^{(\mathcal{FR})}, \tag{41}$$

where $\gamma(N)$ *as in (23) and* $c(\beta,n)$ *as in (24).*

Proof. We notice that

$$D\left(f\left(\frac{\overrightarrow{k}}{n},s\right),f(\overrightarrow{x},s)\right)\leq D\left(f\left(\frac{\overrightarrow{k}}{n},s\right),\widetilde{o}\right)+D(f(\overrightarrow{x},s),\widetilde{o}) \tag{42}$$

$$\leq 2D^*(f(\cdot,s),\widetilde{o}).$$

Hence

$$D^q\left(f\left(\frac{\overrightarrow{k}}{n},s\right),f(\overrightarrow{x},s)\right)\leq 2^q D^{*q}(f(\cdot,s),\widetilde{o}), \tag{43}$$

and

$$\left(\int_X D^q\left(f\left(\frac{\overrightarrow{k}}{n},s\right),f(\overrightarrow{x},s)\right)P(ds)\right)^{\frac{1}{q}}\leq 2\left(\int_X (D^*(f(\cdot,s),\widetilde{o}))^q P(ds)\right)^{\frac{1}{q}}. \tag{44}$$

We observe that

$$D\left(\left(A_n^{\mathcal{FR}}(f)\right)(\overrightarrow{x},s),f(\overrightarrow{x},s)\right)= \tag{45}$$

$$D\left(\sum_{\overrightarrow{k}=\lceil na\rceil}^{\lfloor nb\rfloor *} f\left(\frac{\overrightarrow{k}}{n},s\right)\odot\frac{Z(nx-k)}{\sum_{\overrightarrow{k}=\lceil na\rceil}^{\lfloor nb\rfloor} Z(nx-k)},f(\overrightarrow{x},s)\odot 1\right)=$$

$$D\left(\sum_{\overrightarrow{k}=\lceil na\rceil}^{\lfloor nb\rfloor *} f\left(\frac{\overrightarrow{k}}{n},s\right)\odot\frac{Z(nx-k)}{\sum_{\overrightarrow{k}=\lceil na\rceil}^{\lfloor nb\rfloor} Z(nx-k)},f(\overrightarrow{x},s)\odot\frac{\sum_{\overrightarrow{k}=\lceil na\rceil}^{\lfloor nb\rfloor} Z(nx-k)}{\sum_{\overrightarrow{k}=\lceil na\rceil}^{\lfloor nb\rfloor} Z(nx-k)}\right)= \tag{46}$$

$$D\left(\sum_{\overrightarrow{k}=\lceil na\rceil}^{\lfloor nb\rfloor *} f\left(\frac{\overrightarrow{k}}{n},s\right)\odot\frac{Z(nx-k)}{\sum_{\overrightarrow{k}=\lceil na\rceil}^{\lfloor nb\rfloor} Z(nx-k)},\sum_{\overrightarrow{k}=\lceil na\rceil}^{\lfloor nb\rfloor *} f(\overrightarrow{x},s)\odot\frac{Z(nx-k)}{\sum_{\overrightarrow{k}=\lceil na\rceil}^{\lfloor nb\rfloor} Z(nx-k)}\right)$$

$$\leq\sum_{\overrightarrow{k}=\lceil na\rceil}^{\lfloor nb\rfloor}\left(\frac{Z(nx-k)}{\sum_{\overrightarrow{k}=\lceil na\rceil}^{\lfloor nb\rfloor} Z(nx-k)}\right)D\left(f\left(\frac{\overrightarrow{k}}{n},s\right),f(\overrightarrow{x},s)\right). \tag{47}$$

So that

$$D\left(\left({}_jA_n^{\mathcal{FR}}(f)\right)(\overrightarrow{x},s),f(\overrightarrow{x},s)\right)\leq$$

$$\sum_{\overrightarrow{k}=\lceil na\rceil}^{\lfloor nb\rfloor}\left(\frac{Z(nx-k)}{\sum_{\overrightarrow{k}=\lceil na\rceil}^{\lfloor nb\rfloor} Z(nx-k)}\right)D\left(f\left(\frac{\overrightarrow{k}}{n},s\right),f(\overrightarrow{x},s)\right)= \tag{48}$$

$$\sum_{\substack{\overrightarrow{k}=\lceil na\rceil\\ \left\|\frac{\overrightarrow{k}}{n}-\overrightarrow{x}\right\|_\infty\leq\frac{1}{n^\beta}}}^{\lfloor nb\rfloor}\left(\frac{Z(nx-k)}{\sum_{\overrightarrow{k}=\lceil na\rceil}^{\lfloor nb\rfloor} Z(nx-k)}\right)D\left(f\left(\frac{\overrightarrow{k}}{n},s\right),f(\overrightarrow{x},s)\right)+$$

$$\sum_{\substack{\overrightarrow{k}=\lceil na\rceil \\ \left\|\frac{\overrightarrow{k}}{n}-\overrightarrow{x}\right\|_\infty > \frac{1}{n^\beta}}}^{\lfloor nb\rfloor} \left(\frac{Z\left(nx-k\right)}{\sum\limits_{\overrightarrow{k}=\lceil na\rceil}^{\lfloor nb\rfloor} Z\left(nx-k\right)} \right) D\left(f\left(\frac{\overrightarrow{k}}{n}, s \right), f\left(\overrightarrow{x}, s\right) \right).$$

Hence it holds

$$\left(\int_X D^q \left(\left(A_n^{\mathcal{FR}}\left(f\right) \right)\left(\overrightarrow{x}, s\right), f\left(\overrightarrow{x}, s\right) \right) P\left(ds\right) \right)^{\frac{1}{q}} \leq \tag{49}$$

$$\sum_{\substack{\overrightarrow{k}=\lceil na\rceil \\ \left\|\frac{\overrightarrow{k}}{n}-\overrightarrow{x}\right\|_\infty \leq \frac{1}{n^\beta}}}^{\lfloor nb\rfloor} \left(\frac{Z\left(nx-k\right)}{\sum\limits_{\overrightarrow{k}=\lceil na\rceil}^{\lfloor nb\rfloor} Z\left(nx-k\right)} \right) \left(\int_X D^q \left(f\left(\frac{\overrightarrow{k}}{n}, s \right), f\left(\overrightarrow{x}, s\right) \right) P\left(ds\right) \right)^{\frac{1}{q}} +$$

$$\sum_{\substack{\overrightarrow{k}=\lceil na\rceil \\ \left\|\frac{\overrightarrow{k}}{n}-\overrightarrow{x}\right\|_\infty > \frac{1}{n^\beta}}}^{\lfloor nb\rfloor} \left(\frac{Z\left(nx-k\right)}{\sum\limits_{\overrightarrow{k}=\lceil na\rceil}^{\lfloor nb\rfloor} Z\left(nx-k\right)} \right) \left(\int_X D^q \left(f\left(\frac{\overrightarrow{k}}{n}, s \right), f\left(\overrightarrow{x}, s\right) \right) P\left(ds\right) \right)^{\frac{1}{q}} \leq$$

$$\left(\frac{1}{\sum\limits_{\overrightarrow{k}=\lceil na\rceil}^{\lfloor nb\rfloor} Z\left(nx-k\right)} \right) \cdot \left\{ \Omega_1^{(\mathcal{F})}\left(f, \frac{1}{n^\beta} \right)_{L^q} + \right. \tag{50}$$

$$\left. 2\left(\int_X \left(D^*\left(f\left(\cdot, s\right), \widetilde{o}\right)\right)^q P\left(ds\right) \right)^{\frac{1}{q}} \left(\sum_{\substack{\overrightarrow{k}=\lceil na\rceil \\ \left\|\frac{\overrightarrow{k}}{n}-\overrightarrow{x}\right\|_\infty > \frac{1}{n^\beta}}}^{\lfloor nb\rfloor} Z\left(nx-k\right) \right) \right\}$$

(by (23), (24))

$$\leq \gamma\left(N\right) \left\{ \Omega_1^{(\mathcal{F})}\left(f, \frac{1}{n^\beta} \right)_{L^q} + 2c\left(\beta, n\right) \left(\int_X \left(D^*\left(f\left(\cdot, s\right), \widetilde{o}\right)\right)^q P\left(ds\right) \right)^{\frac{1}{q}} \right\}. \tag{51}$$

We have proved claim. ∎

Conclusion 1. *By Theorem 3.1 we obtain the pointwise and uniform convergences with rates in the q-mean and D-metric of the operator $A_n^{\mathcal{FR}}$ to the unit operator for $f \in C_{\mathcal{FR}}^{U_q}\left(\prod_{i=1}^{N}[a_i,b_i]\right)$.*

II) 1-mean Approximation by Stochastic general sigmoid activation function based full Quasi-Interpolation Neural Network Operators

Let $g \in C_{\mathcal{R}}^{U_1}\left(\mathbb{R}^N\right)$, $0<\beta<1$, $\overrightarrow{x} \in \mathbb{R}^N$, $n, N \in \mathbb{N}$, with $\|g\|_{\infty,\mathbb{R}^N,X} < \infty$, $(X, \mathcal{B}, P)$ probability space, $s \in X$.

We define

$$B_n^{(\mathcal{R})}(g)(\overrightarrow{x},s) := \sum_{\overrightarrow{k}=-\infty}^{\infty} g\left(\frac{\overrightarrow{k}}{n},s\right) Z\left(n\overrightarrow{x}-\overrightarrow{k}\right), \tag{52}$$

(see also (27)).

We give

Theorem 3.2. *Let $g \in C_{\mathcal{R}}^{U_1}\left(\mathbb{R}^N\right)$, $0<\beta<1$, $\overrightarrow{x} \in \mathbb{R}^N$, $n, N \in \mathbb{N}$, with $n^{1-\beta} > 2$, $\|g\|_{\infty,\mathbb{R}^N,X} < \infty$. Then*

1)

$$\int_X \left|\left(B_n^{(\mathcal{R})}(g)\right)(\overrightarrow{x},s) - g(\overrightarrow{x},s)\right| P(ds) \leq \tag{53}$$

$$\left\{\Omega_1\left(g,\frac{1}{n^\beta}\right)_{L^1} + 2c(\beta,n)\|g\|_{\infty,\mathbb{R}^N,X}\right\} =: \mu_1^{(\mathcal{R})},$$

2)

$$\left\|\int_X \left|\left(B_n^{(\mathcal{R})}(g)\right)(\overrightarrow{x},s) - g(\overrightarrow{x},s)\right| P(ds)\right\|_{\infty,\mathbb{R}^N} \leq \mu_1^{(\mathcal{R})}. \tag{54}$$

Proof. Since $\|g\|_{\infty,\mathbb{R}^N,X} < \infty$, then

$$\left|g\left(\frac{\overrightarrow{k}}{n},s\right) - g(\overrightarrow{x},s)\right| \leq 2\|g\|_{\infty,\mathbb{R}^N,X} < \infty. \tag{55}$$

Hence

$$\int_X \left|g\left(\frac{\overrightarrow{k}}{n},s\right) - g(\overrightarrow{x},s)\right| P(ds) \leq 2\|g\|_{\infty,\mathbb{R}^N,X} < \infty. \tag{56}$$

We observe that

$$\left(B_n^{(\mathcal{R})}(g)\right)(\overrightarrow{x},s) - g(\overrightarrow{x},s) =$$

$$\sum_{\overrightarrow{k}=-\infty}^{\infty} g\left(\frac{\overrightarrow{k}}{n},s\right) Z\left(nx-k\right) - g\left(\overrightarrow{x},s\right) \sum_{\overrightarrow{k}=-\infty}^{\infty} Z\left(nx-k\right) = \tag{57}$$

$$\left(\sum_{\overrightarrow{k}=-\infty}^{\infty} g\left(\frac{\overrightarrow{k}}{n},s\right) - g\left(\overrightarrow{x},s\right)\right) Z\left(nx-k\right).$$

However it holds

$$\sum_{\overrightarrow{k}=-\infty}^{\infty} \left| g\left(\frac{\overrightarrow{k}}{n},s\right) - g\left(\overrightarrow{x},s\right)\right| Z\left(nx-k\right) \leq 2\left\|g\right\|_{\infty,\mathbb{R}^N,X} < \infty. \tag{58}$$

Hence

$$\left|\left(B_n^{(\mathcal{R})}\left(g\right)\right)\left(\overrightarrow{x},s\right) - g\left(\overrightarrow{x},s\right)\right| \leq$$

$$\sum_{\overrightarrow{k}=-\infty}^{\infty} \left| g\left(\frac{\overrightarrow{k}}{n},s\right) - g\left(\overrightarrow{x},s\right)\right| Z\left(nx-k\right) = \tag{59}$$

$$\sum_{\substack{\overrightarrow{k}=-\infty \\ \left\|\frac{\overrightarrow{k}}{n}-\overrightarrow{x}\right\|_\infty \leq \frac{1}{n^\beta}}}^{\infty} \left| g\left(\frac{\overrightarrow{k}}{n},s\right) - g\left(\overrightarrow{x},s\right)\right| Z\left(nx-k\right) +$$

$$\sum_{\substack{\overrightarrow{k}=-\infty \\ \left\|\frac{\overrightarrow{k}}{n}-\overrightarrow{x}\right\|_\infty > \frac{1}{n^\beta}}}^{\infty} \left| g\left(\frac{\overrightarrow{k}}{n},s\right) - g\left(\overrightarrow{x},s\right)\right| Z\left(nx-k\right).$$

Furthermore it holds

$$\left(\int_X \left|\left(B_n^{(\mathcal{R})}\left(g\right)\right)\left(\overrightarrow{x},s\right) - g\left(\overrightarrow{x},s\right)\right| P\left(ds\right)\right) \leq$$

$$\sum_{\substack{\overrightarrow{k}=-\infty \\ \left\|\frac{\overrightarrow{k}}{n}-\overrightarrow{x}\right\|_\infty \leq \frac{1}{n^\beta}}}^{\infty} \left(\int_X \left| g\left(\frac{\overrightarrow{k}}{n},s\right) - g\left(\overrightarrow{x},s\right)\right| P\left(ds\right)\right) Z\left(nx-k\right) + \tag{60}$$

$$\sum_{\substack{\overrightarrow{k}=-\infty \\ \left\|\frac{\overrightarrow{k}}{n}-\overrightarrow{x}\right\|_\infty > \frac{1}{n^\beta}}}^{\infty} \left(\int_X \left| g\left(\frac{\overrightarrow{k}}{n},s\right) - g\left(\overrightarrow{x},s\right)\right| P\left(ds\right)\right) Z\left(nx-k\right) \leq$$

$$\Omega_1\left(g,\frac{1}{n^\beta}\right)_{L^1}+2\left\|g\right\|_{\infty,\mathbb{R}^N,X}\sum_{\substack{\overrightarrow{k}=-\infty\\ \left\|\frac{\overrightarrow{k}}{n}-\overrightarrow{x}\right\|_\infty>\frac{1}{n^\beta}}}^{\infty}Z\left(nx-k\right)\leq$$

$$\Omega_1\left(g,\frac{1}{n^\beta}\right)_{L^1}+2c\left(\beta,n\right)\left\|g\right\|_{\infty,\mathbb{R}^N,X},$$

proving the claim. ∎

Conclusion 2. *By Theorem 3.2 we obtain pointwise and uniform convergences with rates in the* 1*-mean of random operators* $B_n^{(\mathcal{R})}$ *to the unit operator for* $g\in C_{\mathcal{R}}^{U_1}\left(\mathbb{R}^N\right)$.

III) 1-mean Approximation by Stochastic general sigmoid activation function based multivariate Kantorovich type neural network operator

Let $g\in C_{\mathcal{R}}^{U_1}\left(\mathbb{R}^N\right)$, $0<\beta<1$, $\overrightarrow{x}\in\mathbb{R}^N$, $n,N\in\mathbb{N}$, with $\left\|g\right\|_{\infty,\mathbb{R}^N,X}<\infty$, $(X,\mathcal{B},P)$ probability space, $s\in X$.

We define

$$C_n^{(\mathcal{R})}\left(g\right)\left(\overrightarrow{x},s\right):=\sum_{\overrightarrow{k}=-\infty}^{\infty}\left(n^N\int_{\frac{\overrightarrow{k}}{n}}^{\frac{\overrightarrow{k}+1}{n}}g\left(\overrightarrow{t},s\right)d\overrightarrow{t}\right)Z\left(n\overrightarrow{x}-\overrightarrow{k}\right),\quad(61)$$

(see also (28).

We present

Theorem 3.3. *Let* $g\in C_{\mathcal{R}}^{U_1}\left(\mathbb{R}^N\right)$, $0<\beta<1$, $\overrightarrow{x}\in\mathbb{R}^N$, $n,N\in\mathbb{N}$, *with* $n^{1-\beta}>2$, $\left\|g\right\|_{\infty,\mathbb{R}^N,X}<\infty$. *Then*

1)

$$\int_X\left|\left(C_n^{(\mathcal{R})}\left(g\right)\right)\left(\overrightarrow{x},s\right)-g\left(\overrightarrow{x},s\right)\right|P\left(ds\right)\leq$$

$$\left[\Omega_1\left(g,\frac{1}{n}+\frac{1}{n^\beta}\right)_{L^1}+2c\left(\beta,n\right)\left\|g\right\|_{\infty,\mathbb{R}^N,X}\right]=:\gamma_1^{(\mathcal{R})},\quad(62)$$

2)

$$\left\|\int_X\left|\left(C_n^{(\mathcal{R})}\left(g\right)\right)\left(\overrightarrow{x},s\right)-g\left(\overrightarrow{x},s\right)\right|P\left(ds\right)\right\|_{\infty,\mathbb{R}^N}\leq\gamma_1^{(\mathcal{R})}.\quad(63)$$

Proof. Since $\left\|g\right\|_{\infty,\mathbb{R}^N,X}<\infty$, then

$$\left|n^N\int_{\frac{\overrightarrow{k}}{n}}^{\frac{\overrightarrow{k}+1}{n}}g\left(\overrightarrow{t},s\right)d\overrightarrow{t}-g\left(\overrightarrow{x},s\right)\right|=\left|n^N\int_{\frac{\overrightarrow{k}}{n}}^{\frac{\overrightarrow{k}+1}{n}}\left(g\left(\overrightarrow{t},s\right)-g\left(\overrightarrow{x},s\right)\right)d\overrightarrow{t}\right|\leq$$

$$n^N \int_{\frac{\overrightarrow{k}}{n}}^{\frac{\overrightarrow{k}+1}{n}} \left| g\left(\overrightarrow{t}, s\right) - g\left(\overrightarrow{x}, s\right) \right| d\overrightarrow{t} \leq 2 \left\| g \right\|_{\infty, \mathbb{R}^N, X} < \infty. \tag{64}$$

Hence

$$\int_X \left| n^N \int_{\frac{\overrightarrow{k}}{n}}^{\frac{\overrightarrow{k}+1}{n}} g\left(\overrightarrow{t}, s\right) d\overrightarrow{t} - g\left(\overrightarrow{x}, s\right) \right| P\left(ds\right) \leq 2 \left\| g \right\|_{\infty, \mathbb{R}^N, X} < \infty. \tag{65}$$

We observe that

$$\left(C_n^{(\mathcal{R})}\left(g\right)\right)\left(\overrightarrow{x}, s\right) - g\left(\overrightarrow{x}, s\right) =$$

$$\sum_{\overrightarrow{k}=-\infty}^{\infty} \left(n^N \int_{\frac{\overrightarrow{k}}{n}}^{\frac{\overrightarrow{k}+1}{n}} g\left(\overrightarrow{t}, s\right) d\overrightarrow{t} \right) Z\left(n\overrightarrow{x} - \overrightarrow{k}\right) - g\left(\overrightarrow{x}, s\right) =$$

$$\sum_{\overrightarrow{k}=-\infty}^{\infty} \left(n^N \int_{\frac{\overrightarrow{k}}{n}}^{\frac{\overrightarrow{k}+1}{n}} g\left(\overrightarrow{t}, s\right) d\overrightarrow{t} \right) Z\left(n\overrightarrow{x} - \overrightarrow{k}\right) - g\left(\overrightarrow{x}, s\right) \sum_{\overrightarrow{k}=-\infty}^{\infty} Z\left(n\overrightarrow{x} - \overrightarrow{k}\right) = \tag{66}$$

$$\sum_{\overrightarrow{k}=-\infty}^{\infty} \left[\left(n^N \int_{\frac{\overrightarrow{k}}{n}}^{\frac{\overrightarrow{k}+1}{n}} g\left(\overrightarrow{t}, s\right) d\overrightarrow{t} \right) - g\left(\overrightarrow{x}, s\right) \right] Z\left(n\overrightarrow{x} - \overrightarrow{k}\right) =$$

$$\sum_{\overrightarrow{k}=-\infty}^{\infty} \left[n^N \int_{\frac{\overrightarrow{k}}{n}}^{\frac{\overrightarrow{k}+1}{n}} \left(g\left(\overrightarrow{t}, s\right) - g\left(\overrightarrow{x}, s\right) \right) d\overrightarrow{t} \right] Z\left(n\overrightarrow{x} - \overrightarrow{k}\right).$$

However it holds

$$\sum_{\overrightarrow{k}=-\infty}^{\infty} \left[n^N \int_{\frac{\overrightarrow{k}}{n}}^{\frac{\overrightarrow{k}+1}{n}} \left| g\left(\overrightarrow{t}, s\right) - g\left(\overrightarrow{x}, s\right) \right| d\overrightarrow{t} \right] Z\left(n\overrightarrow{x} - \overrightarrow{k}\right) \leq 2 \left\| g \right\|_{\infty, \mathbb{R}^N, X} < \infty. \tag{67}$$

Hence

$$\left| \left(C_n^{(\mathcal{R})}\left(g\right)\right)\left(\overrightarrow{x}, s\right) - g\left(\overrightarrow{x}, s\right) \right| \leq$$

$$\sum_{\overrightarrow{k}=-\infty}^{\infty} \left[n^N \int_{\frac{\overrightarrow{k}}{n}}^{\frac{\overrightarrow{k}+1}{n}} \left| g\left(\overrightarrow{t}, s\right) - g\left(\overrightarrow{x}, s\right) \right| d\overrightarrow{t} \right] Z\left(n\overrightarrow{x} - \overrightarrow{k}\right) = \tag{68}$$

$$\sum_{\substack{\overrightarrow{k}=-\infty \\ \left\| \frac{\overrightarrow{k}}{n} - \overrightarrow{x} \right\|_\infty \leq \frac{1}{n^\beta}}}^{\infty} \left[n^N \int_{\frac{\overrightarrow{k}}{n}}^{\frac{\overrightarrow{k}+1}{n}} \left| g\left(\overrightarrow{t}, s\right) - g\left(\overrightarrow{x}, s\right) \right| d\overrightarrow{t} \right] Z\left(n\overrightarrow{x} - \overrightarrow{k}\right) + \tag{69}$$

$$\sum_{\substack{\overrightarrow{k}=-\infty \\ \left\|\frac{\overrightarrow{k}}{n}-\overrightarrow{x}\right\|_\infty>\frac{1}{n^\beta}}}^{\infty}\left[n^N\int_{\frac{\overrightarrow{k}}{n}}^{\frac{\overrightarrow{k}+1}{n}}\left|g\left(\overrightarrow{t},s\right)-g\left(\overrightarrow{x},s\right)\right|d\overrightarrow{t}\right]Z\left(n\overrightarrow{x}-\overrightarrow{k}\right)=$$

$$\sum_{\substack{\overrightarrow{k}=-\infty \\ \left\|\frac{\overrightarrow{k}}{n}-\overrightarrow{x}\right\|_\infty\leq\frac{1}{n^\beta}}}^{\infty}\left[n^N\int_0^{\frac{1}{n}}\left|g\left(\overrightarrow{t}+\frac{\overrightarrow{k}}{n},s\right)-g\left(\overrightarrow{x},s\right)\right|d\overrightarrow{t}\right]Z\left(n\overrightarrow{x}-\overrightarrow{k}\right)+ \quad (70)$$

$$\sum_{\substack{\overrightarrow{k}=-\infty \\ \left\|\frac{\overrightarrow{k}}{n}-\overrightarrow{x}\right\|_\infty>\frac{1}{n^\beta}}}^{\infty}\left[n^N\int_0^{\frac{1}{n}}\left|g\left(\overrightarrow{t}+\frac{\overrightarrow{k}}{n},s\right)-g\left(\overrightarrow{x},s\right)\right|d\overrightarrow{t}\right]Z\left(n\overrightarrow{x}-\overrightarrow{k}\right).$$

Furthermore it holds

$$\left(\int_X\left|\left(C_n^{(\mathcal{R})}\left(g\right)\right)\left(\overrightarrow{x},s\right)-g\left(\overrightarrow{x},s\right)\right|P\left(ds\right)\right)\underset{\text{(by Fubini's theorem)}}{\leq}$$

$$\sum_{\substack{\overrightarrow{k}=-\infty \\ \left\|\frac{\overrightarrow{k}}{n}-\overrightarrow{x}\right\|_\infty\leq\frac{1}{n^\beta}}}^{\infty}\left[n^N\int_0^{\frac{1}{n}}\left(\int_X\left|g\left(\overrightarrow{t}+\frac{\overrightarrow{k}}{n},s\right)-g\left(\overrightarrow{x},s\right)\right|P\left(ds\right)\right)d\overrightarrow{t}\right]Z\left(n\overrightarrow{x}-\overrightarrow{k}\right)+ \quad (71)$$

$$\sum_{\substack{\overrightarrow{k}=-\infty \\ \left\|\frac{\overrightarrow{k}}{n}-\overrightarrow{x}\right\|_\infty>\frac{1}{n^\beta}}}^{\infty}\left[n^N\int_0^{\frac{1}{n}}\left(\int_X\left|g\left(\overrightarrow{t}+\frac{\overrightarrow{k}}{n},s\right)-g\left(\overrightarrow{x},s\right)\right|P\left(ds\right)\right)d\overrightarrow{t}\right]Z\left(n\overrightarrow{x}-\overrightarrow{k}\right)\leq$$

$$\Omega_1\left(g,\frac{1}{n}+\frac{1}{n^\beta}\right)_{L^1}+2\left\|g\right\|_{\infty,\mathbb{R}^N,X}\sum_{\substack{\overrightarrow{k}=-\infty \\ \left\|\frac{\overrightarrow{k}}{n}-\overrightarrow{x}\right\|_\infty>\frac{1}{n^\beta}}}^{\infty}Z\left(n\overrightarrow{x}-\overrightarrow{k}\right)\leq$$

$$\Omega_1\left(g,\frac{1}{n}+\frac{1}{n^\beta}\right)_{L^1}+2c\left(\beta,n\right)\left\|g\right\|_{\infty,\mathbb{R}^N,X}, \quad (72)$$

proving the claim. ∎

Conclusion 3. *By Theorem 3.3 we obtain pointwise and uniform convergences with rates in the* 1*-mean of random operators* $C_n^{(\mathcal{R})}$ *to the unit operator for* $g\in C_{\mathcal{R}}^{U_1}\left(\mathbb{R}^N\right)$.

IV) 1-mean Approximation by Stochastic general sigmoid activation function based multivariate quadrature type neural network operator

Let $g \in C_{\mathcal{R}}^{U_1}\left(\mathbb{R}^N\right)$, $0 < \beta < 1$, $\overrightarrow{x} \in \mathbb{R}^N$, $n, N \in \mathbb{N}$, with $\|g\|_{\infty,\mathbb{R}^N,X} < \infty$, $(X, \mathcal{B}, P)$ probability space, $s \in X$.

We define

$$D_n^{(\mathcal{R})}\left(g\right)\left(\overrightarrow{x}, s\right) := \sum_{\overrightarrow{k}=-\infty}^{\infty} \left(\delta_{n\overrightarrow{k}}\left(g\right)\right)(s)\, Z\left(n\overrightarrow{x} - \overrightarrow{k}\right), \tag{73}$$

where

$$\left(\delta_{n\overrightarrow{k}}\left(g\right)\right)(s) := \sum_{\overrightarrow{r}=0}^{\overrightarrow{\theta}} w_{\overrightarrow{r}}\, g\left(\frac{\overrightarrow{k}}{n} + \frac{\overrightarrow{r}}{n\overrightarrow{\theta}}, s\right), \tag{74}$$

(see also (29), (30)).

We finally give

Theorem 3.4. *Let $g \in C_{\mathcal{R}}^{U_1}\left(\mathbb{R}^N\right)$, $0 < \beta < 1$, $\overrightarrow{x} \in \mathbb{R}^N$, $n, N \in \mathbb{N}$, with $n^{1-\beta} > 2$, $\|g\|_{\infty,\mathbb{R}^N,X} < \infty$. Then*

1)

$$\int_X \left|\left(D_n^{(\mathcal{R})}\left(g\right)\right)\left(\overrightarrow{x}, s\right) - g\left(\overrightarrow{x}, s\right)\right| P\left(ds\right) \leq$$

$$\left\{\Omega_1\left(g, \frac{1}{n} + \frac{1}{n^\beta}\right)_{L^1} + 2c\left(\beta, n\right)\|g\|_{\infty,\mathbb{R}^N,X}\right\} =: \gamma_1^{(\mathcal{R})}, \tag{75}$$

2)

$$\left\|\int_X \left|\left(D_n^{(\mathcal{R})}\left(g\right)\right)\left(\overrightarrow{x}, s\right) - g\left(\overrightarrow{x}, s\right)\right| P\left(ds\right)\right\|_{\infty,\mathbb{R}^N} \leq \gamma_1^{(\mathcal{R})}. \tag{76}$$

Proof. Notice that

$$\left|\left(\delta_{n\overrightarrow{k}}\left(g\right)\right)(s) - g\left(\overrightarrow{x}, s\right)\right| =$$

$$\left|\sum_{\overrightarrow{r}=0}^{\overrightarrow{\theta}} w_{\overrightarrow{r}}\left(g\left(\frac{\overrightarrow{k}}{n} + \frac{\overrightarrow{r}}{n\overrightarrow{\theta}}, s\right) - g\left(\overrightarrow{x}, s\right)\right)\right| \leq$$

$$\sum_{\overrightarrow{r}=0}^{\overrightarrow{\theta}} w_{\overrightarrow{r}}\left|g\left(\frac{\overrightarrow{k}}{n} + \frac{\overrightarrow{r}}{n\overrightarrow{\theta}}, s\right) - g\left(\overrightarrow{x}, s\right)\right| \leq 2\|g\|_{\infty,\mathbb{R}^N,X} < \infty. \tag{77}$$

Hence

$$\int_X \left|\left(\delta_{n\overrightarrow{k}}\left(g\right)\right)(s) - g\left(\overrightarrow{x}, s\right)\right| P\left(ds\right) \leq 2\|g\|_{\infty,\mathbb{R}^N,X} < \infty. \tag{78}$$

We observe that

$$\left(D_n^{(\mathcal{R})}\left(g\right)\right)\left(\overrightarrow{x},s\right)-g\left(\overrightarrow{x},s\right)=$$

$$\sum_{\overrightarrow{k}=-\infty}^{\infty}\left(\delta_{n\overrightarrow{k}}\left(g\right)\right)\left(s\right)Z\left(n\overrightarrow{x}-\overrightarrow{k}\right)-g\left(\overrightarrow{x},s\right)=$$

$$\sum_{\overrightarrow{k}=-\infty}^{\infty}\left(\left(\delta_{n\overrightarrow{k}}\left(g\right)\right)\left(s\right)-g\left(\overrightarrow{x},s\right)\right)Z\left(n\overrightarrow{x}-\overrightarrow{k}\right). \tag{79}$$

Thus

$$\left|D_n^{(\mathcal{R})}\left(g\right)\left(\overrightarrow{x},s\right)-g\left(\overrightarrow{x},s\right)\right|\leq$$

$$\sum_{\overrightarrow{k}=-\infty}^{\infty}\left|\left(\delta_{n\overrightarrow{k}}\left(g\right)\right)\left(s\right)-g\left(\overrightarrow{x},s\right)\right|Z\left(n\overrightarrow{x}-\overrightarrow{k}\right)\leq 2\left\|g\right\|_{\infty,\mathbb{R}^N,X}<\infty. \tag{80}$$

Hence it holds

$$\left|\left(D_n^{(\mathcal{R})}\left(g\right)\right)\left(\overrightarrow{x},s\right)-g\left(\overrightarrow{x},s\right)\right|\leq$$

$$\sum_{\overrightarrow{k}=-\infty}^{\infty}\left|\left(\delta_{n\overrightarrow{k}}\left(g\right)\right)\left(s\right)-g\left(\overrightarrow{x},s\right)\right|Z\left(n\overrightarrow{x}-\overrightarrow{k}\right)=$$

$$\sum_{\substack{\overrightarrow{k}=-\infty\\ \left\|\frac{\overrightarrow{k}}{n}-\overrightarrow{x}\right\|_\infty\leq\frac{1}{n^\beta}}}^{\infty}\left|\left(\delta_{n\overrightarrow{k}}\left(g\right)\right)\left(s\right)-g\left(\overrightarrow{x},s\right)\right|Z\left(n\overrightarrow{x}-\overrightarrow{k}\right)+$$

$$\sum_{\substack{\overrightarrow{k}=-\infty\\ \left\|\frac{\overrightarrow{k}}{n}-\overrightarrow{x}\right\|_\infty>\frac{1}{n^\beta}}}^{\infty}\left|\left(\delta_{n\overrightarrow{k}}\left(g\right)\right)\left(s\right)-g\left(\overrightarrow{x},s\right)\right|Z\left(n\overrightarrow{x}-\overrightarrow{k}\right). \tag{81}$$

Furthermore we derive

$$\left(\int_X\left|\left(D_n^{(\mathcal{R})}\left(g\right)\right)\left(\overrightarrow{x},s\right)-g\left(\overrightarrow{x},s\right)\right|P\left(ds\right)\right)\leq$$

$$\sum_{\substack{\overrightarrow{k}=-\infty\\ \left\|\frac{\overrightarrow{k}}{n}-\overrightarrow{x}\right\|_\infty\leq\frac{1}{n^\beta}}}^{\infty}\sum_{\overrightarrow{r}=0}^{\overrightarrow{\theta}}w_{\overrightarrow{r}}\left(\int_X\left|g\left(\frac{\overrightarrow{k}}{n}+\frac{\overrightarrow{r}}{n\overrightarrow{\theta}},s\right)-g\left(\overrightarrow{x},s\right)\right|P\left(ds\right)\right)Z\left(n\overrightarrow{x}-\overrightarrow{k}\right) \tag{82}$$

$$+\left(\sum_{\substack{\overrightarrow{k}=-\infty \\ \left\|\frac{\overrightarrow{k}}{n}-\overrightarrow{x}\right\|_\infty>\frac{1}{n^\beta}}}^{\infty} Z\left(n\overrightarrow{x}-\overrightarrow{k}\right)\right) 2\left\|g\right\|_{\infty,\mathbb{R}^N,X} \leq$$

$$\Omega_1\left(g,\frac{1}{n}+\frac{1}{n^\beta}\right)_{L^1}+2c\left(\beta,n\right)\left\|g\right\|_{\infty,\mathbb{R}^N,X}, \tag{83}$$

proving the claim. ∎

Conclusion 4. *From Theorem 3.4 we obtain pointwise and uniform convergences with rates in the* 1*-mean of random operators* $D_n^{(\mathcal{R})}$ *to the unit operator for* $g \in C_{\mathcal{R}}^{U_1}\left(\mathbb{R}^N\right)$.

References

[1] G.A. Anastassiou, *Rate of convergence of Fuzzy neural network operators, univariate case*, The Journal of Fuzzy Mathematics, 10, No. 3 (2002), 755-780.

[2] G.A. Anastassiou, *Higher order Fuzzy Approximation by Fuzzy Wavelet type and Neural Network Operators*, Computers and Mathematics, 48(2004), 1387-1401.

[3] G.A. Anastassiou, *Univariate fuzzy-random neural network approximation operators*, Computers and Mathematics with Applications, Special issue/ Proceedings edited by G. Anastassiou of special session "Computational Methods in Analysis", AMS meeting in Orlando. Florida, November 2002, Vol. 48 (2004), 1263-1283.

[4] G.A. Anastassiou, *Higher order Fuzzy Korovkin Theory via inequalities*, Communications in Applied Analysis, 10(2006), No. 2, 359-392.

[5] G.A. Anastassiou, *Fuzzy Korovkin Theorems and Inequalities*, Journal of Fuzzy Mathematics, 15(2007), No. 1, 169-205.

[6] G.A. Anastassiou, *Multivariate Stochastic Korovkin Theory given quantitatively*, Mathematics and Computer Modeling, 48 (2008), 558-580.

[7] G.A. Anastassiou, *Fuzzy Mathematics: Approximation Theory*, Springer, Heidelberg, New York, 2010.

[8] G.A. Anastassiou, *Inteligent Systems: Approximation by Artificial Neural Networks*, Springer, Heidelberg, 2011.

[9] G.A. Anastassiou, *Univariate hyperbolic tangent neural network approximation*, Mathematics and Computer Modelling, 53(2011), 1111-1132.

[10] G.A. Anastassiou, *Multivariate hyperbolic tangent neural network approximation*, Computers and Mathematics 61(2011), 809-821.

[11] G.A. Anastassiou, *Multivariate sigmoidal neural network approximation*, Neural Networks 24(2011), 378-386.

[12] G.A. Anastassiou, *Higher order multivariate fuzzy approximation by multivariate fuzzy wavelet type and neural network operators*, J. of Fuzzy Mathematics, 19(2011), no. 3, 601-618.

[13] G.A. Anastassiou, *Univariate sigmoidal neural network approximation*, J. of Computational Analysis and Applications, Vol. 14(4), 2012, 659-690.

[14] G.A. Anastassiou, *Rate of convergence of some multivariate neural network operators to the unit,revisited*, J. of Computational Analysis and Application, Vol. 15, No. 7, 2013, 1300-1309.

[15] G.A. Anastassiou, *Higher order multivariate fuzzy approximation by basic neural network operators*, CUBO, 16(3) 2014, 21-35.

[16] G.A. Anastassiou, *Multivariate Fuzzy-Random Quasi-interpolation neural network approximation operators*, J. Fuzzy Mathematics, Vol. 22, No. 1, 2014, 167-184.

[17] G. Anastassiou, *Multivariate Fuzzy-Random error function based Neural Network Approximation*, J. Fuzzy Mathematics, 23(4) (2015), 917-935.

[18] G.A. Anastassiou, *Intelligent Systems II: Complete Approximation by Neural Network Operators*, Springer, Heidelberg, New York, 2016.

[19] G.A. Anastassiou, *Intelligent Computations: Abstract Fractional Calculus, Inequalities, Approximations*, Springer, Heidelberg, New York, 2018.

[20] G.A. Anastassiou, *Banach Space Valued Neural Network*, Springer, Heidelberg, New York, 2023.

[21] G.A. Anastassiou, *General sigmoid based Banach space valued neural network approximation*, J. Computational Analysis and Applications, 31 (4) (2023), 520-534.

[22] Z. Chen and F. Cao, *The approximation operators with sigmoidal functions*, Computers and Mathematics with Applications, 58 (2009), 758-765.

[23] R.M. Dudley, *Real Analysis and Probability*, Wadsworth & Brooks / Cole Mathematics Series, Pacific Grove, California, 1989.

[24] S. Gal, *Approximation Theory in Fuzzy Setting*, Chapter 13 in Handbook of Analytic-Computational Methods in Applied Mathematics, pp. 617-666, edited by G. Anastassiou, Chapman & Hall/CRC, 2000, Boca Raton, New York.

[25] S. Haykin, *Neural Networks: A Comprehensive Foundation* (2 ed.), Prentice Hall, New York, 1998.

[26] T.M. Mitchell, *Machine Learning*, WCB-McGraw-Hill, New York, 1997.

[27] W. McCulloch and W. Pitts, *A logical calculus of the ideas immanent in nervous activity*, Bulletin of Mathematical Biophysics, 7 (1943), 115-133.

[28] Wu Congxin, Gong Zengtai, *On Henstock integral of interval-valued functions and fuzzy valued functions*, Fuzzy Sets and Systems, Vol. 115, No. 3, 2000, 377-391.

[29] C. Wu, Z. Gong, *On Henstock integral of fuzzy-number-valued functions (I)*, Fuzzy Sets and Systems, 120, No. 3, (2001), 523-532.

[30] C. Wu, M. Ma, *On embedding problem of fuzzy number space: Part 1*, Fuzzy Sets and Systems, 44 (1991), 33-38.

ROMAI J., v.19, no.1(2023), 25–34

UPDATED RADIAL OSTROWSKI INEQUALITIES OVER A BALL

George A. Anastassiou

Department of Mathematical Sciences, University of Memphis, Memphis, U.S.A.

ganastss@memphis.edu

Abstract Here we present general multivariate radial mixed Ostrowski type inequalities over balls. The proofs derive by implementation of some essential estimates out of some new trigonometric and hyperbolic Taylor's formulae ([2]) and reducing the multivariate problem to a univariate one via general polar coordinates.

Keywords: Ostrowski inequality, radial function, polar coordinates.
2020 MSC: 26A24, 26D10, 26D15.

1. INTRODUCTION

We are motivated by the following:

In 1938, A. Ostrwoski [5] proved the following famous inequality.

Theorem 1.1. *Let $f : [a,b] \to \mathbb{R}$ be continuous on $[a,b]$ and differentiable on (a,b) whose derivative $f' : (a,b) \to \mathbb{R}$ is bounded on (a,b), i.e., $\|f'\|_\infty = \sup_{t\in(a,b)} |f'(t)| < +\infty$. Then*

$$\left|\frac{1}{b-a}\int_a^b f(t)\,dt - f(x)\right| \leq \left[\frac{1}{4} + \frac{\left(x - \frac{a+b}{2}\right)^2}{(b-a)^2}\right](b-a)\left\|f'\right\|_\infty, \qquad (1)$$

for any $x \in [a,b]$. The constant $\frac{1}{4}$ is the best.

Ostrowski type inequalities have great applications to numerical analysis and probability and their literature is enormous.

Here $K = \mathbb{R}$ or $\mathbb{C}$.

Recently the author proved:

Theorem 1.2. *([2]) Let $f \in C_K^3([c,d])$, $a \in [c,d]$, such that $f'(a) = f''(a) = 0$. Then*

i)

$$\left|\frac{1}{d-c}\int_c^d f(x)\,dx - f(a)\right| \leq \left\|f''' + f'\right\|_\infty \frac{\left[(d-a)^3 + (a-c)^3\right]}{6(d-c)}, \qquad (2)$$

ii) when $f'\left(\frac{c+d}{2}\right) = f''\left(\frac{c+d}{2}\right) = 0$, *and* $a = \frac{c+d}{2}$, *we get*

$$\left|\frac{1}{d-c}\int_c^d f(x)\,dx - f\left(\frac{c+d}{2}\right)\right| \leq \left\|f' + f'''\right\|_\infty \frac{(d-c)^2}{24}. \tag{3}$$

We are also motivated by author's monograph, see chapters 5,6.

This work is based on author's recent article [2], where we developed some new trigonometric and hyperbolic type Taylor's formulae.

We prove here a collection of multivariate Ostrowski type inequalities related to radial functions over a ball in $\mathbb{R}^N$, with respect to all norms $\|\cdot\|_p$, $1 \leq p \leq \infty$, and we give also their generalizations.

2. MAIN RESULTS

We make

Remark 1. *We define the ball*

$$B(0,R) := \left\{x \in \mathbb{R}^N : |x| < R\right\} \subseteq \mathbb{R}^N, \quad N \geq 2,\ R > 0,$$

and the sphere

$$S^{N-1} := \left\{x \in \mathbb{R}^N : |x| = 1\right\},$$

where $|\cdot|$ *is the Euclidean norm.*

Let $d\omega$ *be the element of surface measure on* $\mathbb{S}^{N-1}$ *and let*

$$\omega_N = \int_{S^{N-1}} d\omega = \frac{2\pi^{\frac{N}{2}}}{\Gamma\left(\frac{N}{2}\right)}. \tag{4}$$

For $x \in \mathbb{R}^N - \{0\}$ *we can write uniquely* $x = r\omega$, *where* $r = |x| > 0$ *and* $\omega = \frac{x}{r} \in S^{N-1}$, $|\omega| = 1$.

Note that

$$\int_{B(0,R)} dy = \frac{\omega_N R^N}{N} \tag{5}$$

is the Lebesgue measure of the ball.

Following [3, pp. 149-150, exercise 6] and [4, pp. 87-88, Theorem 5.2.2] we can write for $F : \overline{B(0,R)} \to \mathbb{R}$ *a Lebesgue integrable function that*

$$\int_{B(0,R)} F(x)\,dx = \int_{S^{N-1}} \left(\int_0^R F(r\omega)\, r^{N-1} dr\right) d\omega; \tag{6}$$

a formula to be used next.

We present the following multivariate radial Ostrowski type inequality.

Theorem 2.1. *Let the function $f : \overline{B(0,R)} \to \mathbb{R}$ be radial, that is, there exists a function g such that $f(x) = g(r)$, where $r = |x|$, $r \in [0,R]$, $\forall\ x \in \overline{B(0,R)}$. We further assume that $g \in C^3([0,R])$, and $g^{(k)}(r_0) = 0$, $k = 1,2$, where $r_0 \in [0,R]$ is fixed. Then ($\forall\ \omega \in S^{N-1}$)*

$$\left| f(r_0\omega) - \frac{\int_{B(0,R)} f(y)\,dy}{Vol(B(0,R))} \right| = \left| g(r_0) - \frac{N}{R^N} \int_0^R g(s)\, s^{N-1} ds \right| \leq \tag{7}$$

$$\frac{N!}{R^N} \left[\left\| g''' + g' \right\|_{\infty,[0,r_0]} \frac{r_0^{3+N}}{(3+N)!} + \right.$$

$$\left. \left\| g''' + g' \right\|_{\infty,[r_0,R]} \sum_{k=0}^{N-1} \frac{(-1)^{N+k-1}}{k!\,(N-k+3)!} R^k (R-r_0)^{N-k+3} \right].$$

Proof. As in [2], we get that

$$|g(r) - g(r_0)| \leq \left\| g''' + g' \right\|_{\infty,[r_0,R]} \frac{(r-r_0)^3}{3!}, \tag{8}$$

$\forall\ r \in [r_0, R]$,
and

$$|g(r) - g(r_0)| \leq \left\| g''' + g' \right\|_{\infty,[0,r_0]} \frac{(r_0-r)^3}{3!}, \tag{9}$$

$\forall\ r \in [0, r_0]$.
Next we observe

$$\left| f(r_0\omega) - \frac{\int_{B(0,R)} f(y)\,dy}{Vol(B(0,R))} \right| =$$

$$\left| g(r_0) - \frac{\int_{S^{N-1}} \left(\int_0^R g(s)\, s^{N-1} ds \right) d\omega}{\int_{S^{N-1}} \left(\int_0^R s^{N-1} ds \right) d\omega} \right| =$$

$$\left| g(r_0) - \frac{N}{R^N} \int_0^R g(s)\, s^{N-1} ds \right| = \frac{N}{R^N} \left| \int_0^R s^{N-1} (g(r_0) - g(s))\, ds \right| \leq$$

$$\frac{N}{R^N} \int_0^R s^{N-1} |g(r_0) - g(s)|\, ds = \tag{10}$$

$$\frac{N}{R^N} \left[\int_0^{r_0} s^{N-1} |g(r_0) - g(s)|\, ds + \int_{r_0}^R s^{N-1} |g(r_0) - g(s)|\, ds \right] \leq$$

$$\frac{N}{6R^N} \left[\left\| g''' + g' \right\|_{\infty,[0,r_0]} \int_0^{r_0} s^{N-1} (r_0 - s)^3\, ds + \right.$$

$$\left\|g'''+g'\right\|_{\infty,[r_0,R]}\int_{r_0}^{R}s^{N-1}(s-r_0)^3\,ds\Bigg]=$$

$$\frac{N}{6R^N}\left[\left\|g'''+g'\right\|_{\infty,[0,r_0]}\int_0^{r_0}(r_0-s)^{4-1}(s-0)^{N-1}\,ds+\right. \tag{11}$$

$$\left.\left\|g'''+g'\right\|_{\infty,[r_0,R]}(-1)^{N-1}\int_{r_0}^{R}((R-s)-R)^{N-1}(s-r_0)^3\,ds\right]=$$

$$\frac{N}{6R^N}\left[\left\|g'''+g'\right\|_{\infty,[0,r_0]}\frac{\Gamma(4)\Gamma(N)}{\Gamma(4+N)}r_0^{3+N}+\right.$$

$$\left.\left\|g'''+g'\right\|_{\infty,[r_0,R]}(-1)^{N-1}\sum_{k=0}^{N-1}(-1)^k R^k\binom{N-1}{k}\int_{r_0}^{R}(R-s)^{N-k-1}(s-r_0)^{4-1}\,ds\right]=$$

$$\frac{N}{6R^N}\left[\left\|g'''+g'\right\|_{\infty,[0,r_0]}\frac{3!\,(N-1)!}{(3+N)!}r_0^{3+N}+\right. \tag{12}$$

$$\left.\left\|g'''+g'\right\|_{\infty,[r_0,R]}(-1)^{N-1}\sum_{k=0}^{N-1}(-1)^k R^k\binom{N-1}{k}\frac{(N-k-1)!3!}{(N-k+3)!}(R-r_0)^{N-k+3}\right]=$$

$$\frac{N}{R^N}\left[\left\|g'''+g'\right\|_{\infty,[0,r_0]}\frac{(N-1)!}{(3+N)!}r_0^{3+N}+\right.$$

$$\left.\left\|g'''+g'\right\|_{\infty,[r_0,R]}\sum_{k=0}^{N-1}(-1)^{k+N-1}R^k\binom{N-1}{k}\frac{(N-k-1)!}{(N-k+3)!}(R-r_0)^{N-k+3}\right]=$$

$$\frac{N!}{R^N}\left[\left\|g'''+g'\right\|_{\infty,[0,r_0]}\frac{r_0^{3+N}}{(3+N)!}+\right.$$

$$\left.\left\|g'''+g'\right\|_{\infty,[r_0,R]}\sum_{k=0}^{N-1}(-1)^{k+N-1}\frac{R^k}{k!\,(N-k-1)!}\frac{(N-k-1)!}{(N-k+3)!}(R-r_0)^{N-k+3}\right]=$$

$$\frac{N!}{R^N}\left[\left\|g'''+g'\right\|_{\infty,[0,r_0]}\frac{r_0^{3+N}}{(3+N)!}+\right. \tag{13}$$

$$\left.\left\|g'''+g'\right\|_{\infty,[r_0,R]}\sum_{k=0}^{N-1}\frac{(-1)^{N+k-1}}{k!\,(N-k+3)!}R^k(R-r_0)^{N-k+3}\right].$$

∎

We continue with a more general multivariate radial Ostrowski inequality.

Theorem 2.2. *Let the function $f:\overline{B(0,R)}\to\mathbb{R}$ be radial, that is there exists a function g such that $f(x)=g(r)$, where $r=|x|$, $r\in[0,R]$, $\forall\ x\in\overline{B(0,R)}$.*

We further assume that $g \in C^5([0,R])$, *and* $g^{(k)}(r_0) = 0$, $k = 1,2,3,4$, *where* $r_0 \in [0,R]$ *is fixed. Here* $\alpha, \beta \in \mathbb{R} : \alpha\beta\left(\alpha^2 - \beta^2\right) \neq 0$. *Then* $(\forall\ \omega \in S^{N-1})$

$$\left| f(r_0\omega) - \frac{\int_{B(0,R)} f(y)\,dy}{Vol\left(B(0,R)\right)} \right| = \left| g(r_0) - \frac{N}{R^N}\int_0^R g(s)\, s^{N-1} ds \right| \leq \tag{14}$$

$$\frac{2N!}{R^N\left|\beta^2-\alpha^2\right|}\left[\left\|g^{(5)} + \left(\alpha^2+\beta^2\right)g^{(3)} + \alpha^2\beta^2 g'\right\|_{\infty,[0,r_0]} \frac{r_0^{3+N}}{(3+N)!}\right.$$

$$\left.\left\|g^{(5)} + \left(\alpha^2+\beta^2\right)g^{(3)} + \alpha^2\beta^2 g'\right\|_{\infty,[r_0,R]} \sum_{k=0}^{N-1} \frac{(-1)^{N+k-1}}{k!\,(N-k+3)!} R^k (R-r_0)^{N-k+3}\right]. \tag{15}$$

Proof. As in [2], we get that

$$|g(r) - g(r_0)| \leq \frac{1}{3\left|\beta^2-\alpha^2\right|}\left\|g^{(5)} + \left(\alpha^2+\beta^2\right)g^{(3)} + \alpha^2\beta^2 g'\right\|_{\infty,[r_0,R]} (r-r_0)^3$$

$$=: A(r-r_0)^3, \quad \forall\ r \in [r_0,R], \tag{16}$$

and

$$|g(r) - g(r_0)| \leq \frac{1}{3\left|\beta^2-\alpha^2\right|}\left\|g^{(5)} + \left(\alpha^2+\beta^2\right)g^{(3)} + \alpha^2\beta^2 g'\right\|_{\infty,[0,r_0]} (r_0-r)^3$$

$$=: B(r_0-r)^3, \quad \forall\ r \in [0,r_0]. \tag{17}$$

Next we observe

$$\left| f(r_0\omega) - \frac{\int_{B(0,R)} f(y)\,dy}{Vol\left(B(0,R)\right)} \right| \leq$$

(as in the proof of Theorem 1.1)

$$\frac{N}{R^N}\left[\int_0^{r_0} s^{N-1}\left|g(r_0)-g(s)\right| ds + \int_{r_0}^R s^{N-1}\left|g(r_0)-g(s)\right| ds\right] \leq$$

$$\frac{N}{R^N}\left[B\int_0^{r_0} s^{N-1}(r_0-s)^3\,ds + A\int_{r_0}^R s^{N-1}(s-r_0)^3\,ds\right] = \tag{18}$$

(as earlier)

$$\frac{N}{R^N}\left[B\frac{3!\,(N-1)!}{(3+N)!} r_0^{3+N} + \right.$$

$$\left. A(-1)^{N-1}\sum_{k=0}^{N-1}(-1)^k R^k \binom{N-1}{k} \frac{(N-k-1)!3!}{(N-k+3)!}(R-r_0)^{N-k+3}\right] =$$

$$\frac{6N!}{R^N}\left[B\frac{r_0^{3+N}}{(3+N)!}+A\sum_{k=0}^{N-1}\frac{(-1)^{N+k-1}}{k!\,(N-k+3)!}R^k\,(R-r_0)^{N-k+3}\right].$$

∎

It follows an L_1 Ostrowski inequality.

Theorem 2.3. *All as in Theorem 2.1, except now $g\in C^2([0,R])$. Then ($\forall\ \omega\in S^{N-1}$)*

$$\left|f(r_0\omega)-\frac{\int_{B(0,R)}f(y)\,dy}{Vol\,(B(0,R))}\right|=\left|g(r_0)-\frac{N}{R^N}\int_0^R g(s)\,s^{N-1}ds\right|\leq$$

$$\frac{1}{R^N}\left[\left\|g''+g-g(r_0)\right\|_{L_1([0,r_0])}\frac{r_0^{N+1}}{(N+1)}+\right.$$

$$\left.\left\|g''+g-g(r_0)\right\|_{L_1([r_0,R])}\left[\left(\frac{N}{N+1}\right)\left(R^{N+1}-r_0^{N+1}\right)-r_0\left(R^N-r_0^N\right)\right]\right]. \tag{19}$$

Proof. As in [2], we get that

$$|g(r)-g(r_0)|\leq\left\|g''+g-g(r_0)\right\|_{L_1([0,r_0])}(r_0-r), \tag{20}$$

$\forall\ r\in[0,r_0]$,

and

$$|g(r)-g(r_0)|\leq\left\|g''+g-g(r_0)\right\|_{L_1([r_0,R])}(r-r_0), \tag{21}$$

$\forall\ r\in[r_0,R]$.

Next we observe

$$\left|f(r_0\omega)-\frac{\int_{B(0,R)}f(y)\,dy}{Vol\,(B(0,R))}\right|=\left|g(r_0)-\frac{N}{R^N}\int_0^R g(s)\,s^{N-1}ds\right|\leq$$

$$\frac{N}{R^N}\left[\int_0^{r_0}s^{N-1}\left|g(r_0)-g(s)\right|ds+\int_{r_0}^R s^{N-1}\left|g(r_0)-g(s)\right|ds\right]\leq$$

$$\frac{N}{R^N}\left[\left\|g''+g-g(r_0)\right\|_{L_1([0,r_0])}\int_0^{r_0}s^{N-1}(r_0-s)^{2-1}\,ds+\right. \tag{22}$$

$$\left.\left\|g''+g-g(r_0)\right\|_{L_1([r_0,R])}\int_{r_0}^R s^{N-1}(s-r_0)\,ds\right]=$$

$$\frac{N}{R^N}\left[\left\|g''+g-g(r_0)\right\|_{L_1([0,r_0])}\frac{r_0^{N+1}}{N(N+1)}+\right.$$

$$\left\|g''+g-g\left(r_0\right)\right\|_{L_1([r_0,R])}\left[\left(\frac{R^{N+1}-r_0^{N+1}}{N+1}\right)-r_0\left(\frac{R^N-r_0^N}{N}\right)\right]=$$

$$\frac{1}{R^N}\left[\left\|g''+g-g\left(r_0\right)\right\|_{L_1([0,r_0])}\frac{r_0^{N+1}}{(N+1)}+\right.$$

$$\left.\left\|g''+g-g\left(r_0\right)\right\|_{L_1([r_0,R])}\left[\left(\frac{N}{N+1}\right)\left(R^{N+1}-r_0^{N+1}\right)-r_0\left(R^N-r_0^N\right)\right]\right]. \tag{23}$$

∎

Next comes an Ostrowski multivariate radial inequality for $\|\cdot\|_p$, $p>1$.

Theorem 2.4. *Let $p,q>1:\frac{1}{p}+\frac{1}{q}=1$. Let all as in Theorem 2.3. Then ($\forall$ $\omega\in S^{N-1}$)*

$$\left|f\left(r_0\omega\right)-\frac{\int_{B(0,R)}f\left(y\right)dy}{Vol\left(B\left(0,R\right)\right)}\right|=\left|g\left(r_0\right)-\frac{N}{R^N}\int_0^R g\left(s\right)s^{N-1}ds\right|\leq \tag{24}$$

$$\frac{N!\Gamma\left(2+\frac{1}{q}\right)}{R^N\left(q+1\right)^{\frac{1}{q}}}\left[\left\|g''+g-g\left(r_0\right)\right\|_{L_p([0,r_0])}\frac{r_0^{N+1+\frac{1}{q}}}{\Gamma\left(N+2+\frac{1}{q}\right)}+\right.$$

$$\left.\left\|g''+g-g\left(r_0\right)\right\|_{L_p([r_0,R])}\sum_{k=0}^{N-1}\frac{(-1)^{N+k-1}R^k\left(R-r_0\right)^{N-k+1+\frac{1}{q}}}{k!\Gamma\left(N-k+2+\frac{1}{q}\right)}\right].$$

Proof. As in [2], we get that

$$\left|g\left(r\right)-g\left(r_0\right)\right|\leq\left\|g''+g-g\left(r_0\right)\right\|_{L_p([r_0,R])}\frac{\left(r-r_0\right)^{\frac{q+1}{1}}}{\left(q+1\right)^{\frac{1}{q}}}, \tag{25}$$

$\forall\ r\in[r_0,R]$,

and

$$\left|g\left(r\right)-g\left(r_0\right)\right|\leq\left\|g''+g-g\left(r_0\right)\right\|_{L_p([0,r_0])}\frac{\left(r_0-r\right)^{\frac{q+1}{q}}}{\left(q+1\right)^{\frac{1}{q}}}, \tag{26}$$

$\forall\ r\in[0,r_0]$.

Next we observe

$$\left|f\left(r_0\omega\right)-\frac{\int_{B(0,R)}f\left(y\right)dy}{Vol\left(B\left(0,R\right)\right)}\right|=$$

(as earlier)

$$\left| g(r_0) - \frac{N}{R^N} \int_0^R g(s)\, s^{N-1} ds \right| \leq$$

$$\frac{N}{R^N} \left[\int_0^{r_0} s^{N-1} |g(r_0) - g(s)|\, ds + \int_{r_0}^R s^{N-1} |g(r_0) - g(s)|\, ds \right] \leq$$

$$\frac{N}{R^N (q+1)^{\frac{1}{q}}} \left[\left\| g'' + g - g(r_0) \right\|_{L_p([0,r_0])} \int_0^{r_0} s^{N-1} (r_0 - s)^{\left(2+\frac{1}{q}\right)-1} ds + \right. \quad (27)$$

$$\left. \left\| g'' + g - g(r_0) \right\|_{L_p([r_0,R])} \int_{r_0}^R s^{N-1} (s - r_0)^{1+\frac{1}{q}} ds \right] =$$

$$\frac{N}{R^N (q+1)^{\frac{1}{q}}} \left[\left\| g'' + g - g(r_0) \right\|_{L_p([0,r_0])} \frac{(N-1)! \Gamma\left(2+\frac{1}{q}\right)}{\Gamma\left(N+2+\frac{1}{q}\right)} r_0^{N+1+\frac{1}{q}} + \right.$$

$$\left. \left\| g'' + g - g(r_0) \right\|_{L_p([r_0,R])} (-1)^{N-1} \int_{r_0}^R ((R-s) - R)^{N-1} (s - r_0)^{1+\frac{1}{q}} ds \right] = \quad (28)$$

$$\frac{N}{R^N (q+1)^{\frac{1}{q}}} \left[\left\| g'' + g - g(r_0) \right\|_{L_p([0,r_0])} \frac{(N-1)! \Gamma\left(2+\frac{1}{q}\right)}{\Gamma\left(N+2+\frac{1}{q}\right)} r_0^{N+1+\frac{1}{q}} + \right.$$

$$\left. \left\| g'' + g - g(r_0) \right\|_{L_p([r_0,R])} \sum_{k=0}^{N-1} \frac{(N-1)!}{k!\,(N-k-1)!} (-1)^{N+k-1} R^k \frac{(N-k-1)! \Gamma\left(2+\frac{1}{q}\right)}{\Gamma\left(N-k+2+\frac{1}{q}\right)} (R - r_0)^{N-k+1+\frac{1}{q}} \right] = \quad (29)$$

$$\frac{N! \Gamma\left(2+\frac{1}{q}\right)}{R^N (q+1)^{\frac{1}{q}}} \left[\left\| g'' + g - g(r_0) \right\|_{L_p([0,r_0])} \frac{r_0^{N+1+\frac{1}{q}}}{\Gamma\left(N+2+\frac{1}{q}\right)} + \right.$$

$$\left. \left\| g'' + g - g(r_0) \right\|_{L_p([r_0,R])} \sum_{k=0}^{N-1} (-1)^{N+k-1} R^k \frac{(R - r_0)^{N-k+1+\frac{1}{q}}}{k! \Gamma\left(N-k+2+\frac{1}{q}\right)} \right].$$

∎

It follows a general L_1 estimate.

Theorem 2.5. *Let the function $f : \overline{B(0,R)} \to \mathbb{R}$ be radial, that is, there exists a function g such that $f(x) = g(r)$, where $r = |x|$, $r \in [0,R]$, $\forall\ x \in \overline{B(0,R)}$.*

We further assume that $g \in C^4([0,R])$, *and* $g^{(k)}(r_0) = 0$, $k = 1,2,3,4$, *where* $r_0 \in [0,R]$ *is fixed. Let also* $\alpha, \beta \in \mathbb{R} : \alpha\beta\left(\alpha^2 - \beta^2\right) \neq 0$. *Then* ($\forall\ \omega \in S^{N-1}$)

$$\left| f(r_0\omega) - \frac{\int_{B(0,R)} f(y)\,dy}{Vol\left(B(0,R)\right)} \right| = \left| g(r_0) - \frac{N}{R^N}\int_0^R g(s)\,s^{N-1}ds \right| \leq$$

$$\frac{2}{\left|\beta^2 - \alpha^2\right| R^N}\left[\left\| g'''' + \left(\alpha^2+\beta^2\right) g'' + \alpha^2\beta^2 g - \alpha^2\beta^2 g(r_0) \right\|_{L_1([0,r_0])} \frac{r_0^{N+1}}{(N+1)} + \right.$$

$$\left\| g'''' + \left(\alpha^2+\beta^2\right) g'' + \alpha^2\beta^2 g - \alpha^2\beta^2 g(r_0) \right\|_{L_1([r_0,R])}$$

$$\left.\left[\left(\frac{N}{N+1}\right)\left(R^{N+1} - r_0^{N+1}\right) - r_0\left(R^N - r_0^N\right) \right] \right]. \tag{30}$$

Proof. As in [2], we get that

$$|g(r) - g(r_0)| \leq$$

$$\frac{2}{\left|\beta^2 - \alpha^2\right|} \left\| g'''' + \left(\alpha^2+\beta^2\right) g'' + \alpha^2\beta^2 g - \alpha^2\beta^2 g(r_0) \right\|_{L_1([0,r_0])} (r_0 - r), \tag{31}$$

$\forall\ r \in [0,r_0]$,

and

$$|g(r) - g(r_0)| \leq$$

$$\frac{2}{\left|\beta^2 - \alpha^2\right|} \left\| g'''' + \left(\alpha^2+\beta^2\right) g'' + \alpha^2\beta^2 g - \alpha^2\beta^2 g(r_0) \right\|_{L_1([r_0,R])} (r - r_0), \tag{32}$$

$\forall\ r \in [r_0,R]$.

The rest of the proof goes as in Theorem 2.3. ∎

Next comes a general L_p, $p > 1$, estimate.

Theorem 2.6. *All as in Theorem 2.5 and let* $p, q > 1 : \frac{1}{p} + \frac{1}{q} = 1$. *Then* ($\forall$ $\omega \in S^{N-1}$)

$$\left| f(r_0\omega) - \frac{\int_{B(0,R)} f(y)\,dy}{Vol\left(B(0,R)\right)} \right| = \left| g(r_0) - \frac{N}{R^N}\int_0^R g(s)\,s^{N-1}ds \right| \leq$$

$$\frac{2N!\Gamma\left(2+\frac{1}{q}\right)}{\left|\beta^2 - \alpha^2\right| R^N (q+1)^{\frac{1}{q}}}$$

$$\left[\left\| g'''' + \left(\alpha^2+\beta^2\right) g'' + \alpha^2\beta^2 g - \alpha^2\beta^2 g(r_0) \right\|_{L_p([0,r_0])} \frac{r_0^{N+1+\frac{1}{q}}}{\Gamma\left(N+2+\frac{1}{q}\right)} + \right. \tag{33}$$

$$\left\| g'''' + \left(\alpha^2+\beta^2\right) g'' + \alpha^2\beta^2 g - \alpha^2\beta^2 g\left(r_0\right) \right\|_{L_p([r_0,R])}$$

$$\left. \sum_{k=0}^{N-1} \frac{(-1)^{N+k-1} R^k \left(R-r_0\right)^{N-k+1+\frac{1}{q}}}{k!\Gamma\left(N-k+2+\frac{1}{q}\right)} \right].$$

Proof. As in [2], we have that

$$\left|g\left(r\right) - g\left(r_0\right)\right| \leq \frac{2}{\left|\beta^2-\alpha^2\right|}$$

$$\left\| g'''' + \left(\alpha^2+\beta^2\right) g'' + \alpha^2\beta^2 g - \alpha^2\beta^2 g\left(r_0\right) \right\|_{L_p([0,r_0])} \frac{\left(r_0-r\right)^{\frac{q+1}{1}}}{\left(q+1\right)^{\frac{1}{q}}}, \tag{34}$$

$\forall\ r \in [0, r_0]$,

and

$$\left|g\left(r\right) - g\left(r_0\right)\right| \leq \frac{2}{\left|\beta^2-\alpha^2\right|}$$

$$\left\| g'''' + \left(\alpha^2+\beta^2\right) g'' + \alpha^2\beta^2 g - \alpha^2\beta^2 g\left(r_0\right) \right\|_{L_p([r_0,R])} \frac{\left(r-r_0\right)^{\frac{q+1}{1}}}{\left(q+1\right)^{\frac{1}{q}}}, \tag{35}$$

$\forall\ r \in [r_0, R]$.

The rest of the proof goes as in Theorem 2.4. ∎

References

[1] G.A. Anastassiou, *Advances on Fractional Inequalities*, Springer, Heidelberg, New York, 2011.

[2] G.A. Anastassiou, *Opial and Ostrowski type inequalities based on trigonometric and hyperbolic Taylor formulae*, submitted, 2023.

[3] W. Rudin, *Real and Complex Analysis*, International student edition, Mc Graw Hill, London, New York, 1970.

[4] D. Stroock, *A Concise Introduction in the Theory of Integration*, Third Edition, Birkhaüser, Boston, Basel, Berlin, 1999.

[5] A. Ostrowski, *Über die Absolutabweichung einer differentiebaren Funktion von ihrem Integralmittelwert*, Comment. Math. Helv. 10, (1938), 226-227.

ROMAI J., v.19, no.1(2023), 35–51

MOVING OBJECT DETECTION AND TRACKING USING NONLINEAR PDE-BASED AND ENERGY-BASED SCHEMES

Tudor Barbu
Institute of Computer Science of the Romanian Academy,
Iasi Branch
The Academy of Romanian Scientists
tudor.barbu@iit.academiaromana-is.ro

Abstract This work approaches an important computer vision area that is video object detection and tracking. Variational and non-variational partial differential equation (PDE)-based models for image and video object detection and tracking are surveyed here. Detection and tracking techniques based on Geometric Active Contour models, representing energy-based segmentation schemes, are presented first. The PDE-based detection and tracking geometric models using level-sets are then disscused. Moving object tracking approaches based on the optical flow estimated using PDEs are described next. Histogram-based PDE models for video tracking are then presented. Object detection techniques using PDE-based edge and contour extraction are also discussed. Our own contributions in this field, representing diffusion-based detection and tracking methods for certain object classes, are briefly presented.

Keywords: object detection and tracking, geometric active contour, level-sets, optical flow, variational scheme, nonlinear diffusion.
2020 MSC: 97U99.

1. INTRODUCTION

The object detection and tracking represents the process of locating the objects of interest in a video sequence and tracking them across that entire movie. It is a still challenging computer vision sub-domain that has a variety of important application fields, such as the video surveillance, security systems, human—computer interaction, law enforcement, biometric authentication, video indexing and retrieval, human action recognition, robotic vision, augmented reality and medical imaging. Many object detection and tracking techniques have been developed in the last decades.

Thus, video object detection could be performed applying algorithms based on template matching [1], frame differencing [2], dictionary-based models [3], deformable part-based models [4], active contours [5], boosted cascade classifiers [6], SIFT, SURF and HOG descriptors with SVM [7, 8, 9], neural networks

[10] and deep learning models [11]. The object tracking solutions are based on mean-shift schemes [12], Kalman filters [13], optical flow [14], object instance matching [15], Hidden Markov Models (HMM) [16], Particle Swarm Optimization (PSO) [17], fragment-based models [18] and convolutional neural networks (CNN) [19].

The most detection and tracking approaches are related to several classes of image objects: faces [20], people [21], body components (skin, eyes, hands) [22], vehicles [23], animals [24] and road signs. We have also proposed some skin [25, 26], face [26], person [25, 27] and generic object [9, 28] detection and tracking techniques in the last 15 years. In this work we survey some geometric and PDE-based models for moving object detection and tracking. Our own contributions in this computer vision domain are also described here.

2. GEOMETRIC ACTIVE CONTOUR MODELS FOR DETECTION AND TRACKING

Active Contour models (*snakes*), which were introduced by Michael Kass, Andrew Witkin and Demetri Terzopoulos in 1988 [29], are based on PDE variational schemes and their principle is to evolve an initial curve towards the object of interest. They can be used to detect the image objects in each frame of a video sequence. Then, a video tracking process could be performed by determining the correspondences between the object instances detected in succesive frames.

Since these active contours have some weaknesses, some improved versions have been developed. Thus, the Geometric (Geodesic) Active Contours, introduced by Caselles, V., et al. in 1993 [30], represent an improvement of classical active contour methods. This technique, where the final contour does not depend on initialization, allows the simultaneous detection of external and internal borders of several objects.

An approach based on the next geodesic active contour was proposed by M. Chihaoui et al. in 2016 [31]:

$$\frac{\partial \psi}{\partial t} = g(I)|\nabla \psi| \text{div}\left(\frac{\nabla \psi}{|\nabla \psi|}\right) + \nabla g(I) \cdot \nabla \psi + v g(I)|\nabla \psi| \tag{1}$$

where g represents a decreasing function. Their moving object detection and tracking scheme is described in Fig. 1.

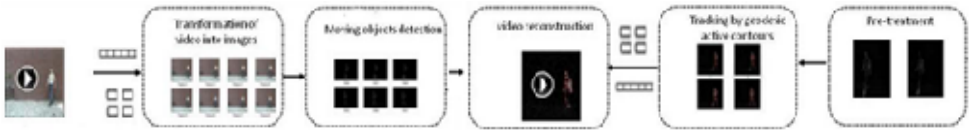

Figure 1. Moving object detection and tracking scheme

The moving object detection component is based on a combination of the frame difference method and the adaptive technique of background subtraction. The process of tracking by the geodesic active contour is performed as following:

- It starts with the first image of that video sequence.
- An initialization is carried by a rectangle parallel to the image contours.
- The geodesic active contour is obtained by the points marked inside and outside the rectangle to detect all the moving objects even if they are outside it.
- Next, the contour is deformed and fixed around the object following the closest point.

A geometric active contour-based object detection and tracking example is displayed in Fig. 2 [31]. This geometric active contour – based framework has some clear advantages. So, compared to conventional methods and geometric methods (rectangle, ellipse ...), it can make detection and monitoring less sensitive to noise and ensure a closed contour without the link between the detected objects, even if they are close or if the background contains regions of high gradient, such as the white lines.

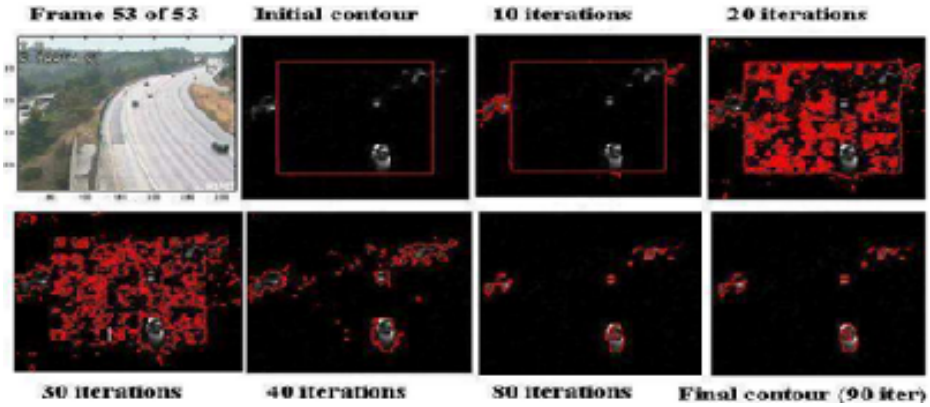

Figure 2. Geometric Active Contour based detection and tracking example

Another category of PDE-based geometric models are those based on level sets. An effective PDE-based level-set approach for moving object detection and tracking was introduced by N. Paragios in 1997 [32]. In the detection stage they define for each pixel the following measurement:

$$I_{detection}(x,y) = \max_{(v,w)\in n_{g_{(x,y)}}} \left\{ \frac{E_{trans}((x,y),(v,w))}{E_{smooth}((x,y),(v,w))} \right\} \tag{2}$$

where

$$\begin{array}{rcl} E_{trans}((x,y),(v,w)) & = & p(d(x,y)|\textbf{static}) \cdot p(d(v,w)|\textbf{mobile}) \\ & + & p(d(x,y)|\textbf{mobile}) \cdot p(d(v,w)|\textbf{static}) \\ E_{smooth}((x,y),(v,w)) & = & p(d(x,y)|\textbf{static}) \cdot p(d(v,w)|\textbf{static}) \\ & + & p(d(x,y)|\textbf{mobile}) \cdot p(d(v,w)|\textbf{mobile}) \end{array} \tag{3}$$

and

$$p(d) = \frac{\lambda}{2}\, e^{-\lambda|d|}, \quad p(d) = \frac{1}{2\sigma\sqrt{\pi}}\, e^{-\frac{d^2}{2\sigma^2}} \tag{4}$$

They find the curve $C(p,t)$ that minimizes the following energy:

$$E(C(p)) = \underbrace{(1-\lambda)\int_0^1 |C'(p)|^2 dp}_{E_{internal}(C)} + \underbrace{\lambda \int_0^1 g^2(|\nabla I_{detection}(C(p))|)dp}_{Eimage(C)} \tag{5}$$

The moving objects are detected if $I(detection)$ has large gradient values only close to the borders of the moving regions [32].

In the object tracking stage, the moving estimated area between two succesive frames is determined as the union of the moving object locations. A modified snake model is proposed for the tracking of these objects. It has the following form:

$$\begin{array}{rcl} E(C(p)) & = & (1-\lambda)\underbrace{\int_0^1 |C'(p)|^2 dp}_{E_{internal}(C)} \\ & + & \lambda \underbrace{\int^1 0(\overbrace{\gamma(|\nabla I_{detection}(C(p))|)}^{detectionterm} + (1-\gamma)\overbrace{g(|\nabla I_t(C(p))|)^2}^{tracking\ term} dp}_{E_{image}(C)} \end{array} \tag{6}$$

While the detection term of this functional forces the curve to fit the moving area, avoiding the edges or static objects, the tracking term is used for curve evolution until the curve reaches the exact location of the moving object. The associated Euler–Lagrange PDE is then solved by applying the level-set scheme of Osher and Sethian. An object detection and tracking example based on the

described model is displayed in Fig. 3.

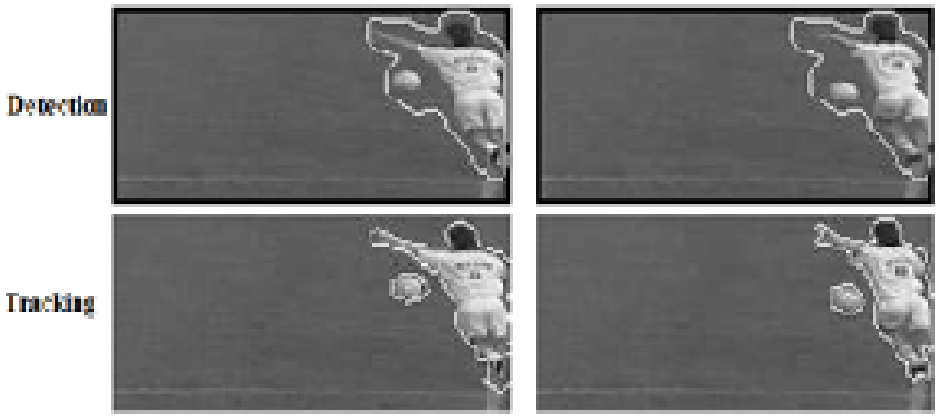

Figure 3. Object detection and tracking example

3. HISTOGRAM-BASED PARTIAL DIFFERENTIAL EQUATIONS FOR OBJECT TRACKING

A histogram-based PDE model for tracking video objects with complex shapes and / or with high nonlinear motion was introduced by P. Li and L. Xiao in 2009 [33]. They formulate histogram-based tracking as a functional optimization problem using Jesson–Shannon divergence that is bounded, symmetric and a true metric. Optimization of the functional consists in searching for a candidate region of very complex shape, whose color distribution is most similar to the known, target distribution. If the target density $p(u)$ is given in the form of color histogram, then the candidate histogram is represented as:

$$q(\mathbf{u},\Omega) = \frac{G_1(\mathbf{u},\Omega)}{G_2(\Omega)} = \frac{\int_\Omega \delta(\mathbf{I}(x)-\mathbf{u})d\mathbf{x}}{\int_\Omega d\mathbf{x}} \tag{7}$$

The tracking problem is formulated as seeking a candidate image region which minimizes the energy functional:

$$\underset{\Omega}{\operatorname{argmin}}\, E(\Omega) = \int_{R^m} f(\mathbf{u},\Omega)d\mathbf{u} \tag{8}$$

where

$$f(\mathbf{u},\Omega) = -p(\mathbf{u})\ln\frac{2p(\mathbf{u})}{p(\mathbf{u})+q(\mathbf{u},\Omega)} - q(\mathbf{u},\Omega)\ln\frac{2q(\mathbf{u},\Omega)}{p(\mathbf{u})+q(\mathbf{u},\Omega)} \tag{9}$$

One derives the partial differential equation (PDE) that describes the evolution of the object contour:

$$\partial\Omega_t = F\mathbf{N} \tag{10}$$

where $N(x)$ is the unit inward normal to the boundary and

$$F = -\frac{1}{G_2(\Omega)}\left(\ln\frac{2q(\mathbf{I}(\mathbf{x}),\Omega)}{p(\mathbf{I}(\mathbf{x}))+q(\mathbf{I}(\mathbf{x}),\Omega)} - \int_{R^m} q(\mathbf{u},\Omega)\ln\frac{2q(\mathbf{u},\Omega)}{p(\mathbf{u})+q(\mathbf{u},\Omega)}\,d\mathbf{u}\right) \tag{11}$$

A level-set algorithm is then applied to compute the solution of this PDE. Its idea is that at any time the contour is implicitly represented by a zero level set of a higher-dimensional function. So, we have:

$$\phi(\tau, \partial\Omega(\mathbf{x},\tau)) = 0, \quad \text{given } \partial\Omega(\mathbf{x},\tau=0) \tag{12}$$

A PDE is obtained as $\phi_\tau = F|\nabla\phi|$ and it is numerically discretized on a fixed discrete grid. This level-set technique can deal succesfully with topological change of the object's shape. It is effective in following objects with complex shapes or with highly non-rigid motion. It is also global convergent, independent of the initial position. Its main disadvantage is the high computational cost, given its high complexity [33].

An example of object tracking performed using the histogram-based PDE model is depicted in Fig. 4. The process at the frames 5, 35, 70 and 90 of a movie sequence is described in that figure.

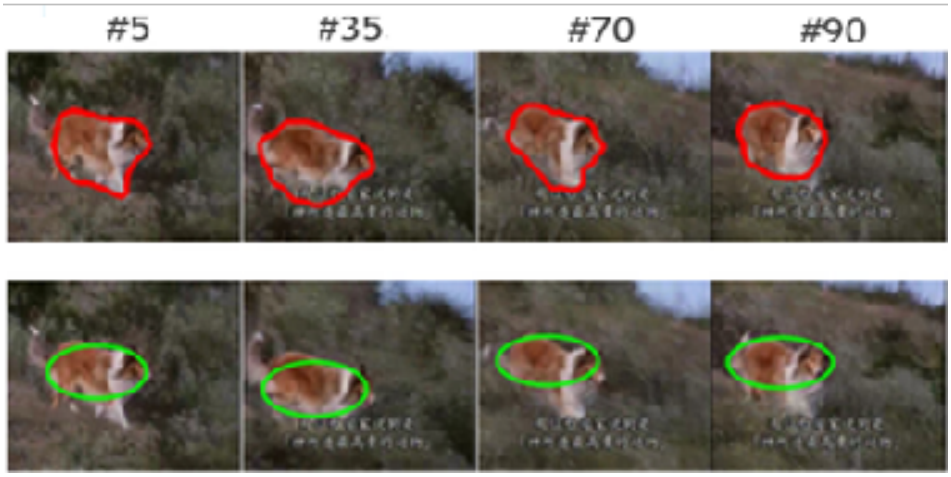

Figure 4. Object tracking: frames #5, #35, #70 and #90

4. OPTICAL FLOW-BASED MOVING OBJECT TRACKING

Optical flow represents the pattern of apparent motion of objects, surfaces, and edges in a visual scene caused by the relative motion between an observer and a scene. Optical flow is an effective approach to track the movement of

the objects. It studies the relative motion of objects across different frame sequences based on the velocity of the movement and illumination changes [34]. There are various methods of determination of the optical flow, which can be grouped in the following categories:

- Block-based methods: based on the minimizing sum of squared differences or sum of absolute differences
- Phase correlation based approaches
- Differential techniques: Lucas–Kanade, Horn–Schunck, Buxton–Buxton and Black–Jepson methods

Here one describes PDE variational optical flow computation schemes, like the Horn-Schunck model and its extensions [34]. They formulate the flow as a global energy functional to be minimized:

$$E = \iint [(I_x u + I_y v + I_t)^2 + \alpha^2(\|\nabla u\|^2 + \|\nabla v\|^2)]dxdy \tag{13}$$

where $\vec{V} = [u(x,y), v(x,y)]^\top$. It is solved by using two Euler–Lagrange partial differential equations:

$$\begin{aligned} \frac{\partial L}{\partial u} - \frac{\partial}{\partial x}\frac{\partial L}{\partial u_x} - \frac{\partial}{\partial y}\frac{\partial L}{\partial u_y} = 0 \\ \frac{\partial L}{\partial v} - \frac{\partial}{\partial x}\frac{\partial L}{\partial v_x} - \frac{\partial}{\partial y}\frac{\partial L}{\partial v_y} = 0 \end{aligned} \tag{14}$$

where L is the integrand of E. One obtains the next system:

$$\begin{aligned} I_x(I_x u + I_y v + I_t) - \alpha^2 \Delta u = 0 \\ I_y(I_x u + I_y v + I_t) - \alpha^2 \Delta v = 0 \end{aligned} \tag{15}$$

It is solved by using the following iterative schemes:

$$u^{k+1} = \bar{u}^k - \frac{I_x(I_x\bar{u}^k + I_y\bar{v}^k + I_t)}{4\alpha^2 + I_x^2 + I_y^2}, \quad v^{k+1} = \bar{v}^k - \frac{I_y(I_x\bar{u}^k + I_y\bar{v}^k + I_t)}{4\alpha^2 + I_x^2 + I_y^2} \tag{16}$$

The Horn–Schunck model is sensitive to noise and applicable to tracking objects with high speed movement [34]. Other variational models, representing improved versions of it, use other data terms and other smoothness components.

Many moving object detection and tracking techniques have been developed using these optical flow models. Their general scheme is the following one:

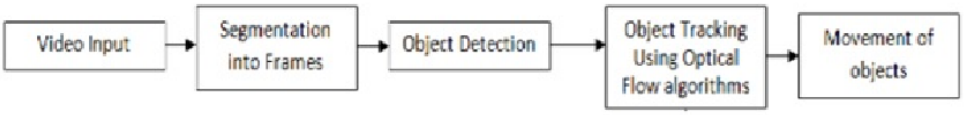

Figure 5. Object detection and tracking based on optical flow

In the next figure there is described an example of optical flow motion tracking in a traffic scene.

Figure 6. Object detection and tracking based on optical flow

5. CONTOUR-BASED MOVING OBJECT DETECTION AND TRACKING

The edges and contours of the images are successfully used for moving object detection and tracking. Such a contour-based detection and tracking technique was proposed by M. Yokoyama and T. Poggio in 2014 [35].

Their approach detects the moving edges by using a gradient-based optical flow technique and an edge detector. Canny edge detector is used to extract those edges having strong magnitudes of the gradients, but some PDE – based edge detectors could be used as well. The extracted edges are restored as lines, and background lines of the previous frame are subtracted. A line clustering process is then performed: a NN-based clustering with respect to the distance and velocity is applied for this task [35].

It labels two lines as the same, if they satisfy the following constraints:

$$\begin{aligned} \min_{\substack{i\in\{1,\ldots,m\}\\ j\in\{1,\ldots,n\}}} \{|x_{p_i} - x_{q_j}| + |y_{p_i} - y_{q_j}|\} &\leq \alpha_d, \min_{\substack{i\in\{1,\ldots,m\}\\ j\in\{1,\ldots,n\}}} \{|u_{p_i} - u_{q_j}|\} \\ &\leq \alpha_u, \min_{\substack{i\in\{1,\ldots,m\}\\ j\in\{1,\ldots,n\}}} \{|v_{p_i} - v_{q_j}|\} \leq \alpha_v \end{aligned} \tag{17}$$

where (u_p, v_p) represents the velocity.

Then, the contours of the clustered lines are obtained by using active contours. The discrete energy function of a snake of the contour $\{p_1, ..., p_N\}$ is

$$E = \sum_{i=1}^{N} (\alpha_i E_{cont} + \beta_i E_{curv} + \gamma_i E_{image}), \tag{18}$$

where

$$E_{cont} = \|\mathbf{p}_i - \mathbf{p}_{i-1}\|^2, \; E_{curv} = \|\mathbf{p}_{i-1} - 2\mathbf{p}_i + \mathbf{p}_{i+1}\|^2, \; E_{image} = -\|\nabla I\| \tag{19}$$

Then, the object tracking process consists in solving the correspondence problem for the detected objects. The similarity between an object of the previous frame, $\{\hat{S}_1, ..., \hat{S}_{N_m}\} \in \hat{R}_{prev}(m)$, and an object of the current frame, $\{\hat{\mathbf{p}}_1, ..., \hat{\mathbf{p}}_n\} \in \hat{S}$, is defined as:

$$p(m, m') = \frac{\sum_{j=1}^{N_m} \sum_{i=1}^{n_j} l_{ij}}{\sum_{j=1}^{N_m} |S_j|}, \quad l_{ij} = \begin{cases} 1 & \text{if } \hat{\mathbf{p}}_i \in R_{curv}(m') \text{ where } \hat{\mathbf{p}}_i \in \hat{S}_j \\ 0 & \text{otherwise.} \end{cases} \tag{20}$$

Effective moving object detection and tracking results have been obtained. A contour-based moving object detection example is described in Fig. 7.

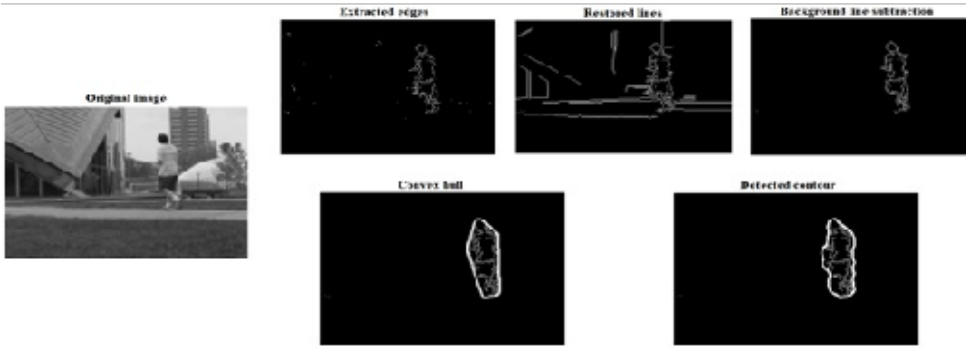

Figure 7. Contour-based video object detection

6. PDE-BASED AUTOMATIC DETECTION AND TRACKING TECHNIQUES FOR CERTAIN OBJECT CLASSES

Our own contributions in the moving object detection and tracking domain are described in this section. We proposed some novel video detection and tracking techniques that use the nonlinear PDE models, which have been widely approached by us in the last years [36, 37, 38], to perform a multi-scale analysis of the detected objects in order to solve the correspondence problem.

The first one is a vehicle detection and tracking technique that was disseminated in a high impact journal [39]. It detects the moving vehicles in the frames of the video sequence by combining some deep and machine learning-based detection techniques: Gaussian Mixture Models (GMM), Aggregated Channels Network (ACF), YOLO-V2 and Faster R-CNN.

Then, the correspondence between the video objects detected in successive frames is determined using a multi-scale analysis of those objects. A scale-space representation is created by applying the numerical approximation algorithm that solves a nonlinear fourth-order reaction-diffusion based model whose mathematical validity is rigorously investigated here [39]. A color image feature extraction is then performed at each scale using SURF and HOG-based features and the feature vectors determined at multiple scales are next concatenated into a final descriptor. An instance matching-based vehicle tracking technique using the distances between these feature vectors is then proposed in [39]. We developed some proper metrics for feature vector distance computing [41, 42, 43]. The proposed approach outperforms other techniques, as shown by the method comparison results in Table 1.

Table 1. Vehicle detection and tracking method comparison results

Detection technique	*Precision*	*Recall*	*Tracking approach*	*Precision*	*Recall*
The proposed approach	0.8423	0.8257	The proposed technique	0.8401	0.8216
Aggregated Channels Network (ACF)	0.6741	0.6824	GMM+Mean-shift tracking	0.7148	0.7332
Gaussian Mixture Models (GMM)	0.6843	0.6722	GMM+ Kalman filter	0.7643	0.7527
Fastert R-CNN	0.8192	0.8046	EB+IoU tracker	0.8576	0.8615
R-CNN	0.6581	0.6625	SIFT tracking	0.6233	0.6181
YOLO-v2	0.7632	0.7811	SIFT+ Kalman filtering	0.7486	0.7391
Frame differencing (FD)	0.5826	0.5972	Frame differencing (FD)+object matching	0.5801	0.5879
HOG+SVM	0.6149	0.6349	HOG+SVM +feature matching	0.6102	0.6213

A moving vehicle detection and tracking example is described in Fig. 8.

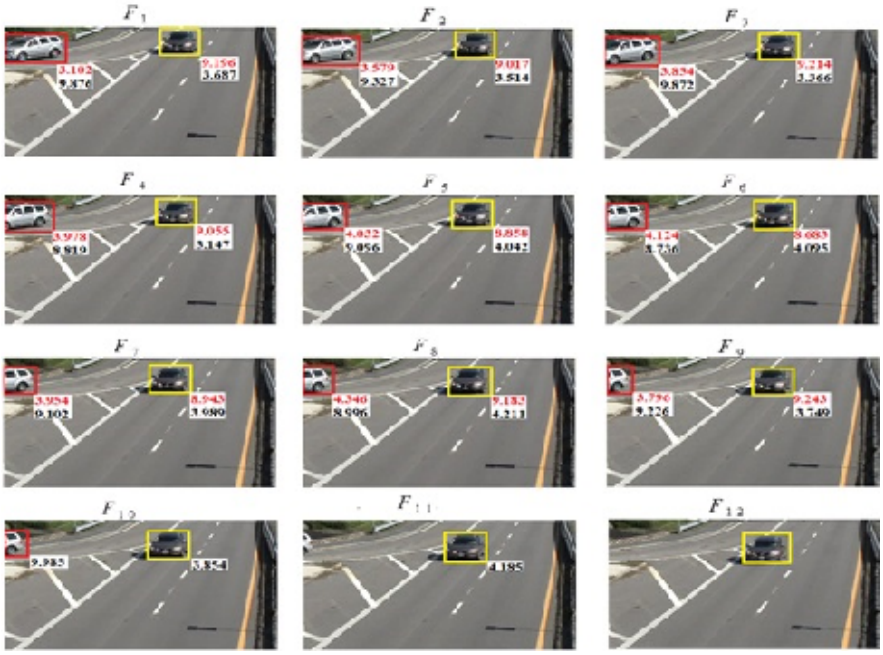

Figure 8. Moving vehicle detection and tracking example (feature vector distances are attached to bboxes)

Here we describe only the reaction-diffusion based scale-space representation that uses the following well-posed nonlinear anisotropic diffusion-based filtering model proposed by us [36]:

$$\begin{cases} \dfrac{\partial u}{\partial t} + \lambda\xi(\|\nabla^2 u\|)\Delta(\psi(\|\nabla u_\sigma\|)\nabla^2 u) + \alpha(u - u_0) = 0, \quad \text{in } (0,T)\times\Omega \\ u(0,x,y) = u_0(x,y), \ \forall (x,y) \in \Omega \\ u(t,x,y) = 0, \ \forall (x,y) \in \partial\Omega, \ \text{in } (0,t)\times\Omega \\ \dfrac{\partial}{\partial \vec{n}}(t,x,y) = 0, \ \forall (x,y) \in \partial\Omega, \ \text{in } (0,t)\times\Omega \end{cases} \tag{21}$$

where the diffusivity function is

$$\psi : [0,\infty) \to [0,\infty) : \psi(s) = \beta \sqrt[3]{\frac{\delta}{|\zeta + \gamma s^2|}} \tag{22}$$

and

$$\xi : [0,\infty) \to [0,\infty) : \xi(s) = \zeta(\eta s^{\varepsilon} + \nu)^{\frac{1}{\varepsilon+1}}, \ \nu,\eta \in [1,5), \ \zeta \in (0,1), \ \varepsilon \in (0,1). \tag{23}$$

This PDE model is solved by applying the finite difference method and the following explicit iterative numerical approximation scheme is obtained for it:

$$u_{i,j}^{n+1} = u_{i,j}^{n}(\alpha+1) - \lambda\xi(\|\Delta u_{i,j}^{n}\|)(\psi_{i+1,j}^{n} + \psi_{i-1,j}^{n} + \psi_{i,j+1}^{n} + \psi_{i,j-1}^{n} - 4\psi_{i,j}^{n}) - u_{i,j}^{0}\alpha \tag{24}$$

This numerical algorithm, which is stable and consistent to the PDE in (6.1), is then used to create the scale-space representation for the detected RGB color objects. We consider the next solution to this issue, since applying it on each of the 3 color channels is not a good one since R, G and B have high correlation levels. One converts the RGB object Veh to the decorrelated color space CIE L* a^* b^* and its luminance channel $L(Veh)$ is filtered by applying the numerical scheme. We obtain the following multi-scale representation of K scales for the vehicle object:

$$\begin{aligned} S(Veh) = \{&Veh, RGB([(L(Veh))^{\tau}, a(Veh), b(Veh)]), ..., \\ &RGB([(L(Veh))^{\tau(K-1)}, a(Veh), b(Veh)])\} \end{aligned} \tag{25}$$

Another contribution represents a multiple pedestrian tracking framework that was disseminated in a IEEE conference volume [40]. The moving person detection process is performed by applying a combination of advanced computer vision and machine learning solutions, such as GMM, HOG, SVM, ACF [40]. An instance matching-based tracking technique that uses a deep learning-based multiscale analysis of the subimages of the detected pedestrians is then proposed.

Its scale-space is created by applying the numerical approximation algorithm of a well-posed nonlinear second-order anisotropic diffusion-based model that is introduced here [40]. It has the following form:

$$\begin{cases} \dfrac{\partial u}{\partial t} - \alpha\psi(|\nabla^2 u|)\nabla \cdot (\delta(\|\nabla u\|)\nabla u) + \beta(u - u_0) = 0, \ (x,y) \in \Omega \\ u(0,x,y) = u_0(x,y), \ \forall (x,y) \in \Omega \\ u(t,x,y) = 0, \ \forall (x,y) \in \partial\Omega; \end{cases} \tag{26}$$

where its functions are the following:

$$\begin{aligned} &\delta : [0,\infty) \to [0,\infty) : \delta(s) = \lambda\left(\frac{\xi}{|\gamma s^3 + \eta \log_{10}\xi|}\right) \\ &\psi : [0,\infty) \to [0,\infty) : \psi(s) = \zeta\sqrt[r]{\varphi s^r + \nu} \end{aligned} \tag{27}$$

where $\alpha \in [1,2)$, $\beta \in (0,0.4)$, $\eta \in (0,1]$, $\gamma \geq 3$, $\xi \geq 4$, $\varphi, \nu \in [1,5)$, $\zeta \in (0,0.5,1)$ and $\lambda \geq 1$.

The explicit iterative numerical approximation scheme that solves this parabolic PDE model, by applying the finite difference method, is obtained in the following form:

$$u_{i,j}^{n+1} = u_{i,j}^{n}(1-\beta) + u_{i,j}^{0}\beta + \alpha\psi(u_{i+h,j}^{n} + u_{i-h,j}^{n} + u_{i,j+h}^{n} + u_{i,j-h}^{n} - 4u_{i,j}) \cdot \\ \cdot \left(\delta_{i+\frac{1}{2}j}(u_{i+1,j}^{n} - u_{i,j}^{n}) - \delta_{i-\frac{h}{2}j}(u_{i,j}^{n} - u_{i-1,j}^{n}) \right. \\ \left. + \delta_{i,j+\frac{1}{2}}(u_{i,j+1}^{n} - u_{i,j}^{n}) - \delta_{i,j-\frac{1}{2}}(u_{i,j}^{n} - u_{i,j-1}^{n})\right).$$

The obtained scale-space has the form $S(p) = \{p, RGB([(L(p))^{\rho}, a(p), b(p)]), ..., RGB([(L(p))^{\rho(K-1)}, a(p), b(p)])\}$ where $\rho \in [3.10]$ and $K \geq 3$. A feature extraction process involving two pre-trained CNNs (Inception-V3 and ResNet-101) is applied at each scale, powerful 2D feature vectors being obtained [40]. Then, a video object instance matching technique that is based on the feature vector distances is next applied to determine the correspondences between the pedestrians detected in consecutive frames. Thus, the moving person trajectories are identified succesfully [40]. A multiple pedestrian tracking example is displayed in Fig. 9.

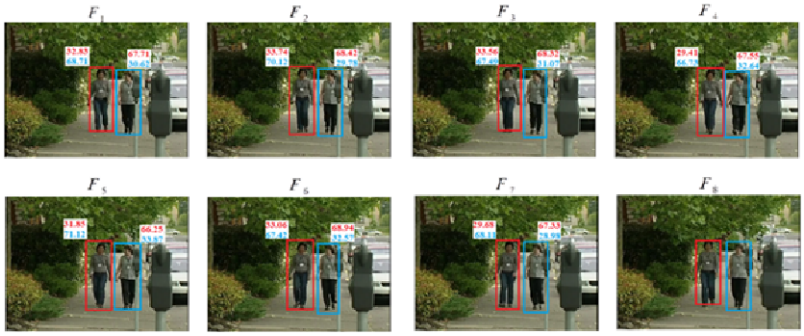

Figure 9. Multiple pedestrian tracking example

This approach outperforms many other pedestrians detectors and trackers, as illustrated by the method comparison results in Table 2 [40].

Table 2. Method comparison results

Technique	*Precision*	Recall
The proposed framework	0.8467	0.8351
AdaBoost+Blcok matching	0.8312	0.8221
Faster R-CNN+color feature matching	0.7839	0.7693
HOG+SVM+Kalman filtering	0.7362	0.7285
Temporal differencing+object mathcing	0.7137	0.7214
HOG+SVM+feature matching	0.7423	0.6372

7. CONCLUSIONS

An overview of geometric and PDE-based models for moving object detection and tracking has been presented here. The PDE-based models can be used in the detection stage (see Active Contours), tracking stage (see optical flow) or both processes. They provide effective detection and tracking results but may lead to higher computational costs, due to their complexity.

Our contributions in this computer vision field, representing detection and tracking models for special classes of objects (vehicles, pedestrians), have been also disscused. While the most PDE models for detection and tracking have variational characters, the PDE-based schemes proposed by us are non-variational, since they cannot be achieved by minimizing some energy functionals.

Also, our nonlinear diffusion models are used only for the multi-scale analysis that facilitates the correspondence-based tracking processes. We have also developed some PDE-based edge detection techniques that could lead to some object detection and tracking models which will represent the focus of our future research work.

8. ACKNOWLEDGEMENTS

This research work was supported by a grant of the Ministry of Research, Innovation and Digitization, CNCS - UEFISCDI, project number PN-III-P4-PCE-2021-0006, within PNCDI III.

References

[1] A. Banharnsakun, S. Tanathong, *Object detection based on template matching through use of best-so-far ABC*, Computational intelligence and neuroscience, 2014.

[2] S.S. Sengar, S. Mukhopadhyay, *A novel method for moving object detection based on block based frame differencing*, 2016 3^{rd} International Conference on Recent Advances in Information Technology (RAIT), March 2016. IEEE, 467-472.

[3] A. Wu, S. Zhao, C. Deng, W. Liu, *Generalized and Discriminative Few-Shot Object Detection via SVD-Dictionary Enhancement*, Advances in Neural Information Processing Systems 34, 2021.

[4] P.F. Felzenszwalb, R.B. Girshick, D. McAllester, D. Ramanan, *Object detection with discriminatively trained part-based models*, IEEE Transactions on pattern analysis and machine intelligence, 32 (9) (2009), 1627-1645.

[5] T. F. Chan, L. A. Vese, *Active contours without edges*, IEEE Transactions on Image Processing, 10 (2) (2001) 266-277.

[6] P. Viola, M. Jones, *Rapid object detection using a boosted cascade of simple features*, Proceedings of the 2001 IEEE computer society conference on computer vision and pattern recognition, CVPR 2001, Vol. 1, pp. I-I, Dec. 2001.

[7] T. Nguyen, E. Park, J. Han, D.C. Park. S.Y. Min, *Object detection using scale invariant feature transform*, Genetic and evolutionary computing, Springer, Cham, 2014, 65-72.

[8] J. Farooq, *Object detection and identification using SURF and BoW model*, 2016 International Conference on Computing, Electronic and Electrical Engineering (ICE Cube), April 2016, 318-323.

[9] T. Barbu, *SVM-based Human Cell Detection Technique using Histograms of Oriented Gradients*, Mathematical Methods for Information Science & Economics: Proc. of AMATHI '12, Montreux, Switzerland, Dec. 29-31, 2012, 156-160.

[10] M. Zhang, V. Ciesielski, *Using back propagation algorithm and genetic algorithm to train and refine neural networks for object detection*, International Conference on Database and Expert Systems Applications, Springer, Berlin, Heidelberg, August 1999, 626-635.

[11] L. Liu, W. Ouyang, X. Wang, P. Fieguth, J. Chen, X. Liu, M. Pietikäinen, *Deep learning for generic object detection: A survey*, International Journal of Computer Vision 128 (2) (2020), 261-318.

[12] C. Yang, R. Duraiswami, L. Davis, *Efficient mean-shift tracking via a new similarity measure*, 2005 IEEE Computer Society Conference on Computer Vision and Pattern Recognition (CVPR'05) 1 (2005), IEEE, 176-183.

[13] H.A. Patel, D.G. Thakore, *Moving object tracking using kalman filter*, International Journal of Computer Science and Mobile Computing 2 (4) (2013), 326-332.

[14] K. Kale, S. Pawar, P. Dhulekar, *Moving object tracking using optical flow and motion vector estimation*, 2015 4^{th} International conference on reliability, infocom technologies and optimization (ICRITO)(trends and future directions), September 2015. IEEE, 1-6.

[15] W. Chantara, J. H. Mun, D. W. Shin, Y. S. Ho, *Object tracking using adaptive template matching*, IEIE Transactions on Smart Processing and Computing 4 (1) (2015), 1-9.

[16] Y. Yuan, H. Yang, Y. Fang, W. Lin, *Visual object tracking by structure complexity coefficients*, IEEE Transactions on Multimedia, 17 (8) (2015), 1125-1136.

[17] C.C. Hsu and G. T. Dai, *Multiple object tracking using particle swarm optimization*, International Journal of Electronics and Communication Engineering 6 (8) (2012), 744-747.

[18] V. Srikrishnan, T. Nagaraj, S. Chaudhuri, *Fragment based tracking for scale and orientation adaptation*, 6^{th} Indian Conf. on Computer Vision, Graphics & Image Processing, dec. 2008. IEEE, 328-335.

[19] G. Ciaparrone, F. L. Sánchez, S. Tabik, L. Troiano, R. Tagliaferri, F. Herrera, *Deep learning in video multi-object tracking: A survey*, Neurocomputing 381 (2020), 61-88.

[20] C. Küblbeck, A. Ernst, *Face detection and tracking in video sequences using the modified census transformation*, Image and Vision Computing 24 (6) (2006), 564-572.

[21] J. Zhou, J. Hoang, *Real time robust human detection and tracking system*, 2005 IEEE Computer Society Conf. on Computer Vision and Pattern Recognition (CVPR'05)-Workshops, 2005. IEEE, 149-149.

[22] A. Nadeem, A. Jalal, K. Kim, *Human actions tracking and recognition based on body parts detection via Artificial neural network*, 2020 3^{rd} International conference on advancements in computational sciences (ICACS), February 2020. IEEE, 1-6.

[23] M. Betke, E. Haritaoglu, L. S. Davis, *Real-time multiple vehicle detection and tracking from a moving vehicle*, Machine vision and applications 12 (2) (2000), 69-83.

[24] T. Burghardt, J. Calic, *Real-time face detection and tracking of animals*, Seminar on neural network applications in electrical engineering, (2006), IEEE, 27-32.

[25] T. Barbu, *Pedestrian detection and tracking using temporal differencing and HOG features*, Computers & Electrical Engineering 40 (4) (2014), 1072—1079.

[26] T. Barbu, *An Automatic Face Detection System for RGB Images*, International Journal of Computers, Communications & Control 6 (1) (2011), 21-32.

[27] T. Barbu, *Novel Approach for Moving Human Detection and Tracking in Static Camera Video Sequences*, Proceedings of the Romanian Academy Series A, 13 (3) (2012), 269-277.

[28] T. Barbu, *Multiple object detection and tracking in sonar movies using an improved temporal differencing approach and texture analysis*, U.P.B. Scientific Bulletin Series A 74 (2012), 27—40.

[29] M. Kass, A., Witkin, D. Terzopoulos, Snakes: *Active contour models*, International journal of computer vision 1 (4) (1988), 321-331.

[30] V. Caselles, R. Kimmel, G. Sapiro, *Geodesic active contours*, International Journal of Computer Vision 22 (1) (1997), 61-79.

[31] M. Chihaoui, A. Elkefi, W. Bellil, C. Amar, *Detection and tracking of the moving objects in a video sequence by geodesic active contour*, 2016 13^{th} International Conference on Computer Graphics, Imaging and Visualization (CGiV March 2016. IEEE, 212-215.

[32] N. Paragios, R. Deriche, *Geodesic active contours and level sets for the detection and tracking of moving objects*, IEEE Transactions on pattern analysis and machine intelligence 22 (3) (2000), 266-280.

[33] P. Li, L. Xiao, *Histogram-based partial differential equation for object tracking*, In 2009 Seventh International Conference on Advances in Pattern Recognition, 2009. IEEE, 286-289.

[34] K. Horn, G. Schunck, *Determining optical flow*, Artificial Intelligence 17 (1–3) (1981), 185–203.

[35] M. Yokoyama, T. Poggio, *A contour-based moving object detection and tracking*, 2005 IEEE international workshop on visual surveillance and performance evaluation of tracking and surveillance, 2005, 271-276.

[36] T. Barbu, *Novel Diffusion-based Models for Image Restoration and Interpolation*, Book Series: Signals and Communication Technology, Springer International Publishing, 2019.

[37] T. Barbu *Robust contour tracking model using a variational level-set algorithm*, Numerical Functional Analysis and Optimization 35 (3) (2014), 263-274.

[38] T. Barbu, *A PDE based Model for Sonar Image and Video Denoising*, Analele Stiintifice ale Universitatii "Ovidius" Constanta, Seria Matematică, 19 (3), (2011), 51-58.

[39] T. Barbu, *Deep Learning-based Multiple Moving Vehicle Detection and Tracking using a Nonlinear Fourth-order Reaction-Diffusion based Multi-scale Video Object Analysis*, Discrete & Continuous Dynamical Systems - Series S, AIMS Journals, Volume 16, Issue 1, (2023), 6-32.

[40] T. Barbu, *Multiple Pedestrian Tracking Framework using Deep Learning-based Multi-scale Image Analysis for Stationary-camera Video Surveillance*, 8^{th} IEEE International Smart Cities Conference 2022, ISC2 2022, Paphos, Cyprus, 26-29 september (2022). IEEE.

[41] T. Barbu, *Comparing Various Voice Recognition Techniques*, Proceedings of the 5^{th} International Conference on Speech Technology and Human-Computer Dialogue, SPED 2009, Constanta, Romania, June 18-21, (2009), 1-6. IEEE.

[42] T. Barbu, *A supervised text-independent speaker recognition approach*, International Journal of Computer, Information, Systems and Control Engineering, Vol. 1, No. 9, World Acad. Sci. Eng. Technol., (2007), 2710-2714.

[43] T. Barbu, *Unsupervised SIFT-based face recognition using an automatic hierarchical agglomerative clustering solution*, Procedia Computer Science, Elsevier, Vol. 35, September (2014), 522-530.

ROMAI J., v.19, no.1(2023), 53–62

GEOMETRIC SUBPROGRESSION STABILIZER IN COMMON METRIC

Semeon A. Bogatyy

M. V. Lomonosov Moscow State University, Moscow, Russia

bogatyi@inbox.ru

Abstract A series of such metric spaces is constructed (subgeometric sequences of real numbers), for which the multiplication of the metric by any positive number not equal to one, gives a space at an infinite Gromov–Hausdorff distance from the original space.

Keywords: metric space, Gromov–Hausdorff distance, group action.
2020 MSC: 51F99.

1. INTRODUCTION

The work is devoted to the geometry of the Gromov–Hausdorff distance [1, 2, 3, 4] defined on the class of all non-empty metric spaces and is closely related to the works [7, 9], the concepts and results of which we use without detailed explanation.

M. Gromov in his "Metric structures for Riemannian and non-Riemannian spaces" [3] made a short remark: "One can also make a moduli space of isometry classes of non-compact spaces X lying within a finite Hausdorff distance from a given X_0, e.g. $X_0 = \mathbb{R}^n$. Such moduli spaces are also complete and contractible."

This observation was not proved in [3] because it probably seemed obvious. In [7, Theorem 4] the completeness of moduli spaces (clouds) is proved and it is stated, that a natural attempt to prove the contractibility of a cloud poses the problem of describing the stabilizer and the center of the cloud. Let us give the basic definitions.

Let (X, ϱ) be an arbitrary metric space and $0 < r \leq \infty$ be a real number. As is customary in metric geometry, instead of $\varrho(x, y)$ we write $|xy|$ as a rule. If A and B are non-empty subsets of X, then we put

$$|AB| = |BA| = \inf\big\{|ab| : a \in A,\, b \in B\big\}.$$

Next, we define the closed r-neighborhood of the set A by setting $B_r(A) = \big\{x \in X : |xA| \leq r\big\}$.
Finally, the *Hausdorff distance* between A and B is the value

$$d_H(A, B) = \inf\big\{r : A \subset B_r(B), \quad B \subset B_r(A)\big\}.$$

The Hausdorff distance is a generalized pseudometric. The word "generalized" means that the distance may take infinite value, as in the case of the straight line $\mathbb{R}$ and any of its points. The prefix "pseudo" means that the distance may take zero value between different subsets, as in the case of a set and its dense subset. It is obvious that the Hausdorff distance satisfies all the axioms of generalized pseudometrics: it is non-negative, symmetric and satisfies the triangle inequality. Nevertheless, on the set consisting of all non-empty bounded closed subsets of a metric space X, the Hausdorff distance is a metric.

The *Gromov–Hausdorff distance* between non-empty metric spaces X and Y is the value

$$d_{GH}(X,Y) = \inf\bigl\{d_H(X',Y')\colon X',Y' \subset Z,\, X' \approx X,\, Y' \approx Y\bigr\},$$

where for the metric spaces X and X' the expression $X \approx X'$ means that these spaces are isometric. *The Gromov–Hausdorff distance is a generalized pseudometric vanishing on each pair of isometric spaces* [4]. There are a countable discrete complete bounded metric space X and a countable locally compact complete bounded metric space with exactly one non-isolated point Y such that $d_{GH}(X,Y) = 0$.

Compact metric spaces form the set $\mathcal{G}H_c$, on which the Gromov–Hausdorff distance is a metric. The class $\mathcal{G}H_b$ of all bounded metric spaces no longer forms a set. But within the framework of von Neumann–Bernays–Gödel set theory we can say that the Gromov–Hausdorff distance is a pseudometric on $\mathcal{G}H_b$. We will denote the class of all metric spaces by $\mathcal{G}H$, and the class of all metric spaces located at a finite distance from of a given metric space X will be called *the cloud of the space* X and denoted by $[X]$. By Δ_1 we denote a one-point metric space. It is clear that $[\Delta_1] = \mathcal{G}H_b$. For a metric space (X,ϱ) and a positive number $\lambda > 0$, λX means the "similar space" $(X,\lambda\varrho)$, i.e. the set X, the distances on which are multiplied by λ.

The transformation $H_\lambda\colon \mathcal{G}H \to \mathcal{G}H$, $H_\lambda : X \mapsto \lambda X$ for $\lambda > 0$ we call *similarity with the coefficient* λ.

The diameter of a metric space is defined as

$$\operatorname{diam} X = \sup\{|xy|\colon x,y \in X\}.$$

Theorem 1.1 ([4])**.** *For any metric spaces X and Y,*

(1) $2d_{GH}(\Delta_1, X) = \operatorname{diam} X$*;*

(2) $2d_{GH}(X,Y) \le \max\{\operatorname{diam} X, \operatorname{diam} Y\}$*;*

(3) if the diameter of X or Y is finite, then $\bigl|\operatorname{diam} X - \operatorname{diam} Y\bigr| \le 2d_{GH}(X,Y)$.

(4) if the diameter of X is finite, then for any $\lambda > 0$ and $\mu > 0$ we have $d_{GH}(\lambda X, \mu X) = \frac{1}{2}|\lambda - \mu| \operatorname{diam} X$*, whence it immediately follows that the curve* $\gamma(t) := t\,X$ *is shortest between any of its points, and the length of such a segment of the curve is equal to the distance between its ends.*

(5) for any $\lambda > 0$, we have $d_{GH}(\lambda X, \lambda Y) = \lambda\, d_{GH}(X, Y)$.

Property (5) implies that similarities are well defined on the classes $\mathcal{G}H_c$, $\mathcal{G}H_b$, and $\mathcal{G}H$.

Returning to the contractibility of the cloud, we note that formulas (4) and (5) illustrate the existence of a canonical contraction of the Gromov–Hausdorff space of all compact metric spaces to the one-point space Δ_1. It is also possible to give a strict meaning to the statement that similarity carries out contraction of the cloud of all bounded metric spaces to the one-point space Δ_1.

Formula (5) means that the similarity is continuous in space, but formula (4) in all other clouds does not guarantee continuity with respect to the contraction parameter λ.

There are constructed [5, Corollary 5.9], [10] examples of spaces X such that the spaces X and λX lie in the same cloud if and only if $\lambda = 1$. This means that, in the general case, the similarity cannot contract the cloud by itself. Therefore, the author believes that the statement about the contractibility of any cloud (even in the case of cloud $[\mathbb{R}^n]$, mentioned by Gromov) is currently a hypothesis. Recently the author proved that the cloud of any space "with large metric gaps" (the spaces considered in this work are as follows) is contractible [11, Theorem 1.2].

Since for an unbounded metric space (X, ϱ) the "similar" space $\lambda X = (X, \lambda\varrho)$ can be at infinite Gromov–Hausdorff distance from the original space X [5, 6, 7, 8, 9, 10], then the cloud stabilizer becomes important:

$$\mathrm{St}[X] = \big\{\lambda \in \mathbb{R}_+ : d_{GH}(X, \lambda X) < \infty\big\} = \Big\{\lambda \in \mathbb{R}_+ : [\lambda X] = [X]\Big\}.$$

The cloud stabilizer does not depend on the representative X taken from the cloud and is a subgroup in the multiplicative group of positive numbers $(\mathbb{R}_+, \times)$.

In this plan, already subsets of the half-line (of non-negative numbers with the standard metric of the modulus of the difference) give many interesting and varied examples.

For example, in [5] it is shown that in the case of a countable subset X whose points go to infinity very quickly (for example, for geometric hyperprogression $X = \big\{p^{n^\alpha}\big\}_{n=1}^{\infty}$, $p > 1$, $\alpha > 1$) and the standard line metric, $\mathrm{St}[X] = \{1\}$. In [10] a similar result is proved for an arbitrary normalized metric on a geometric hyperprogression, i.e. for a metric for which only distances to the zero point are induced from the straight line.

In [5, 6, 8] it is shown that for a geometric progression $X_p = \big\{p^n\big\}_{n=1}^{\infty}$, $p > 1$, and the standard line metric, $\mathrm{St}[X_p] = G_p = \big\{p^n\big\}_{n=-\infty}^{\infty}$. In [9] it is shown that for an arbitrary normalized metric on a geometric progression any subgroup of the group G_p can be the stabilizer. One could get the feeling that the value $\alpha = 1$ is some kind of watershed in the nature of the stabilizer.

In this work, we show that for a geometric subprogression $X = \{p^{n^\alpha}\}_{n=1}^{\infty}$, $p > 1$, $0 < \alpha < 1$, and an arbitrary normalized metric, the equality $\mathrm{St}[X] = \{1\}$ holds. Thus, we can say that for $\alpha = 1$ there is not a "water divide", but "an archipelago of islands in a sea of trivial stabilizer".

The normed vector spaces form the "Himalayas" with maximum stabilizer – the whole multiplicative group of positive numbers. We especially note that for every nontrivial proper subgroup $H \subset (\mathbb{R}_+, \times)$, one of the following is valid:

a) H is closed - in which case, $H = G_p$ for some $p > 1$;

b) H is not closed - in which case, H is everywhere dense.

There are exactly $2^{\mathfrak{c}} = 2^{2^{\aleph_0}}$ of proper dense subgroups, but the author does not know of any example of a cloud with such a stabilizer.

2. BASIC CONCEPTS

Let X and Y be arbitrary sets. A multi-valued mapping $R\colon X \to Y$ is uniquely determined by its graph, for which we keep the notation

$$R = \big\{(x, y)\colon\ y \in R(x)\big\}.$$

It is clear that the graphs of set-valued mappings are exactly subsets of $R \subset X \times Y$ such that for any point $x \in X$ there exists a point $y \in Y$ such that $(x, y) \in R$. Such a set $R \subset X \times Y$ will also be called a *complete relation*. To simplify the notation for a point from $R(x)$, we will also use the notation y_x. In metric geometry, a surjective set-valued mapping is called a *correspondence*. For a R correspondence, the R^{-1} inverse plot is a subset of the product $Y \times X$, so we will denote it by R^*. The set of all correspondences X in Y is denoted by $\mathcal{R}(X, Y)$. To avoid confusion, we always denote the points of the second space as y even though it is also denoted by X.

For a correspondence $R \subset X \times Y$ of metric spaces (X, ϱ_X) and (Y, ϱ_Y), define its *distortion* as

$$\operatorname{dis} R = \sup\Big\{\big|\varrho_X(x, x') - \varrho_Y(y, y')\big| : (x, y),\ (x', y') \in R\Big\}. \tag{1}$$

It is convenient to estimate the Gromov–Hausdorff distance in terms of distortion of correspondences [4]

Theorem 2.1. *For any metric spaces X and Y the following equality holds:*

$$d_{GH}(X, Y) = \frac{1}{2}\inf\big\{\operatorname{dis} R : R \in \mathcal{R}(X, Y)\big\}.$$

In what follows, we will assume that $X, Y \subset [0, \infty)$ and $0 \in X$, $0 \in Y$. The point 0 in the set X will be denoted by 0_X. Since we will consider different metrics on these sets, then, if necessary, we will use the notation $\operatorname{dis}_{\varrho_X, \varrho_Y} R$.

We are interested in *normalized* metrics, i.e. such metrics ϱ on the set X that

$$\varrho(x, 0_X) = x \text{ for any point } x \in X. \tag{2}$$

It follows from the triangle inequality that for any two points $x, x' \in X$ we have:

$$x - x' = \varrho(x, 0_X) - \varrho(x', 0_X) \le \varrho(x, x') \le \varrho(x, 0_X) + \varrho(0_X, x') = x + x'. \tag{3}$$

Both extreme cases provide interesting examples. The case of left equality (for all $x > x'$) corresponds to the fact that the metric is taken from the line on the set X. The case of right equality (for all $x \ne x'$) corresponds to the discrete hedgehog $\hat{X}$ [7]. Intermediate "linear" metrics also provide important examples. For any $-1 \le \alpha \le 1$ we define on the set of non-negative numbers, and hence on any set X we consider, the metric

$$\varrho_\alpha(x, x') = x + \alpha x' = \frac{1-\alpha}{2}|x - x'| + \frac{1+\alpha}{2}(x + x') \text{ when } x' < x. \tag{4}$$

It is clear that the formula (4) defines a metric on the set of non-negative real numbers. The inequalities (3) can be formulated as the assertion that for any normalized metric ϱ the inequalities $\varrho_{-1} \le \varrho \le \varrho_1$ are valid.

Let $\varphi\colon \{0\} \cup \mathbb{N} \to [0, \infty)$, $\varphi(0) = 0$, be a strictly increasing function. Consider on the number line the subset

$$X_\varphi = \big\{x_n = \varphi(n)\colon n \in \{0\} \cup \mathbb{N}\} \subset [0, \infty)\big\}. \tag{5}$$

The set of all normalized metrics on X_φ denoted by $\mathcal{M}_\varphi$ or $\mathcal{M}$ for a fixed function φ.

The function φ will be called *sparse*, if the difference

$$\Delta_\varphi(n) = \varphi(n) - \varphi(n-1), n \ge 1,$$

monotonically (from some rank n_0) increases to infinity, i.e.

$$\Delta_\varphi(n+1) \ge \Delta_\varphi(n) \quad \text{for} \quad n \ge n_0 \quad \text{and} \quad \Delta_\varphi(n) \overset{n\to\infty}{\longrightarrow} \infty. \tag{6}$$

Sparse functions are remarkable in that their correspondences with finite distortion have a simple structure.

Theorem 2.2. *Let φ and ψ be sparse functions and $R \in \mathcal{R}(X_{\varphi,\varrho}, X_{\psi,\rho})$ is a correspondence such that* $\operatorname{dis} R < M$. *Then for some n_0 and an integer k for all $n \ge n_0$ the equality $R(x_n) = \{y_{n+k}\}$ holds.*

This is where our main result comes from.

Theorem 2.3. *For numbers $p > 1$, $0 < \alpha < 1$ and any normalized metric $\varrho \in \mathcal{M}_\varphi$ on a sparse set X_φ, where $\varphi(n) = p^{n^\alpha}$, we have the equality*

$$\mathrm{St}\big[(X_\varphi, \varrho)\big] = \{1\}.$$

On the one hand, the theorem 2.2 gives a strong necessary condition for the correspondence of a finite distortion. On the other hand, this necessary condition is based only on comparing the distances to the zero point, therefore, it cannot be sufficient for the finiteness of the distortion of this correspondence. Sufficiency holds for metrics with some condition of "translation invariance". For a geometric progression, invariant normalized metrics are important. In our case, the analog is the class of the following metrics. Let's say that the metric $\varrho \in \mathcal{M}_\varphi$ is *invariant* ($\varrho \in \mathcal{IM}_\varphi$), if there exists a function $\alpha\colon \mathbb{N} \to [-1, 1]$ such that

$$\varrho(x_m, x_n) = x_m + \alpha(m-n)x_n \quad \text{for} \quad n < m. \tag{7}$$

In [9, Proposition 3.5], there is a description of such functions α that define a metric on X_φ by the formula (7). The following result [9, Theorem 2.14] contains all linear metrics of (4).

Theorem 2.4. *Any function $\alpha\colon \mathbb{N} \to [a, b]$, where $-1 \le a \le b \le 1$ and $b \le 1 + 2a$, by the formula (7) defines an invariant normalized metric $\varrho_\alpha \in \mathcal{IM}_\varphi$.*

Theorem 2.5. *Let φ and ψ be strictly increasing functions such that $|\psi(n+k) - \varphi(n)| < K$ for some fixed $k \in \mathbb{Z}$, $K > 0$ and all sufficiently large n ($n \ge n_0$). Then*

$$d_{GH}\big((X_\varphi, \varrho_\alpha), (X_\psi, \varrho_\alpha)\big) < \infty$$

for any function α from theorem 2.4.

Corollary 2.1. *Let φ and ψ be sparse functions, and α and β be the functions from theorem 2.4. Then the following conditions are equivalent:*

1) $d_{GH}\big((X_\varphi, \varrho_\alpha), (X_\psi, \varrho_\beta)\big) < \infty$;

2) $\alpha = \beta$ and $d_{GH}\big((X_\varphi, \varrho_{-1}), (X_\psi, \varrho_{-1})\big) < \infty$;

3) $\alpha = \beta$ and $|\psi(n+k) - \varphi(n)| < K$ for some fixed $k \in \mathbb{Z}$, $K > 0$ and all sufficiently large n ($n \ge n_0$).

Example 2.1. *For any strictly increasing functions φ and ψ the implications 3) $\Longrightarrow$ 1), 2) are valid for any number $-1 \le \alpha \le 1$. For the functions $\varphi(n) = 3^{\left[\frac{n+1}{2}\right]} + (-1)^n$ and $\psi(n) = 3^n$ condition 2) is satisfied, but for $\alpha > -1$ conditions 1) and 3) are not true.*

However, the reason lies not so much in the non-sparseness of the functions φ and ψ, but in the fact that that the case $\alpha = -1$ is exceptional and different

from the general function $\alpha\colon \mathbb{N} \to [-1+\varepsilon, 1]$*, whose values are separated from the number* -1*.*

3. PROOFS

In [9, Proposition 1.1] the assertion is proved, which we present in full for the convenience of the reader.

Proposition 3.1. *If for the complete relation* R *of the spaces* X_{ϱ_X} *and* Y_{ϱ_Y} *the inequality* $\operatorname{dis} R < M$ *is true, then for every point* $x \in X$ *and every point* $y_x \in R(x)$ *the inequality* $|x - y_x| < K$ *is true, where* $K = M + y_0$*.*

For any sparse function φ, for any number $M > 0$, there exists a number $n > 1$, such that

$$\varphi(n) - \varphi(n-1) \geq M.$$

We denote the smallest such number by $n_\varphi(M)$.

Proposition 3.2. *If for a sparse function* $\psi\colon \mathbb{N} \to \mathbb{R}_+$ *and a complete relation* R *of the spaces* X_{ϱ_X} *and* $X_{\psi,\rho}$ *the inequality* $\operatorname{dis} R < M$ *is true, then for any point* $x \in X$ *from* $y \in R(x)$ *and* $y \geq y_{n_\psi(M)} = \psi(n_\psi(M))$ *the equality* $R(x) = \{y\}$ *follows.*

Proof. Let $y' \in R(x)$. Then

$$|y' - y| \leq \rho(y', y) = \rho(y', y) - \varrho(x, x) \leq \operatorname{dis} R < M.$$

The condition $y \geq \psi(n_\psi(M))$ and the definition of the number $n_\psi(M)$ imply the equality $y' = y$. ∎

Proposition 3.3. *If for a sparse function* $\varphi\colon \mathbb{N} \to \mathbb{R}_+$ *and a complete relation* R *of the spaces* X_{φ,ϱ_X} *and* X_ρ *the inequality* $\operatorname{dis} R < M$ *is true, then for any point* $x \in X$ *from* $x \geq x_{n_\varphi(M)} = \varphi(n_\varphi(M))$ *and* $R(x) \cap R(x') \neq \emptyset$ *follows* $x = x'$*.*

Proof. Let $y \in R(x) \cap R(x')$. Then

$$|x' - x| \leq \varrho(x', x) = \varrho(x', x) - \rho(y, y) \leq \operatorname{dis} R < M.$$

The condition $x \geq \varphi(n_\varphi(M))$ and the definition of the number $n_\varphi(M)$ imply the equality $x' = x$. ∎

Proof of the theorem 2.2. Since the metric spaces $X_{\varphi,\varrho}$ and $X_{\psi,\rho}$ are unbounded, then there are numbers $n_0 \geq n_\varphi(2M + 2y_0) \geq n_\varphi(M)$ and $m_0 \geq n_\psi(2M + 2x_0) \geq n_\psi(M)$ such that $y_{m_0} \in R(x_{n_0})$. Here $y_0 \in R(0)$ and $x_0 \in R^*(0)$, i.e. $0 \in R(x_0)$.

Since $m_0 \geq n_\psi(M)$, then according to the proposition 3.2 $R(x_{n_0}) = \{y_{m_0}\}$; from $n_0 \geq n_\varphi(M)$ according to the proposition 3.3 it follows $R^*(y_{m_0}) = \{x_{n_0}\}$.

According to Proposition 3.1 $|x_{n_0} - y_{m_0}| < M + y_0$, so $y_{m_0} < x_{n_0} + M + y_0$. Similarly $|x_{n_0+1} - y_{x_{n_0+1}}| < M + y_0$, so $x_{n_0+1} - M - y_0 < y_{x_{n_0+1}}$.

It follows from the inequality $n_0 \geq n(2M + 2y_0)$ that

$$x_{n_0+1} - x_{n_0} > x_{n_0} - x_{n_0-1} \geq 2M + 2y_0.$$

So $y_{x_{n_0+1}} > x_{n_0+1} - M - y_0 > x_{n_0} + M + y_0$. Therefore, $y_{x_{n_0+1}} > y_{m_0} = y_{x_{n_0}}$.

Thus, we have proved that $y_{x_{n_2}} > y_{x_{n_1}} \geq y_{m_0}$ follows from $n_2 > n_1 \geq n_0$.

A similar property is also true for the inverse (symmetric) correspondence R^*. $m_2 > m_1 \geq m_0$ implies $x_{y_{m_2}} > x_{y_{m_1}} \geq x_{n_0}$.

If $y_{x_{n_0+1}} > y_{m_0+1}$, then for the point $x_{y_{m_0+1}}$ from the proven monotonicity property the inequality $x_{n_0} < x_{y_{m_0+1}} < x_{n_0+1}$.

The resulting contradiction shows that $y_{x_{n_0+1}} = y_{m_0+1}$. We prove by induction that $y_{x_{n_0+i}} = y_{m_0+i}$ for every $i \geq 1$. It is clear that $k = m_0 - n_0$ is the desired one. □

Proposition 3.4. *For $p > 1$ and $0 < \alpha < 1$, the following properties hold for the function $\varphi(x) = p^{x^\alpha}$:*

1) The function $\varphi(n)$ is sparse.

2) For any integer k the equality $\lim_{x\to\infty} \frac{\varphi(x+k)}{\varphi(x)} = 1$ is true.

Proof. Consider the function $\varphi(x) = p^{x^\alpha}$, $x > 0$. It is easy to calculate that $\varphi'(x) = \alpha x^{\alpha-1}\varphi(x)\ln p = \alpha \ln p \frac{p^{x^\alpha}}{x^{1-\alpha}} > 0$.

1) Therefore, the sequence $\{\varphi(n) = p^{n^\alpha}\}$ is strictly increasing. An increase of the sequence $\Delta_\varphi(n)$ is equivalent to the convexity of the sequence $\{\varphi(n)\}$, i.e. to the condition

$$\varphi(n+1) \leq \frac{\varphi(n+2) + \varphi(n)}{2} \text{ for each } n. \tag{8}$$

It is easy to calculate that $\varphi''(x) = \alpha x^{\alpha-2}\big(\alpha x^\alpha \ln p + \alpha - 1\big)\varphi(x)\ln p$. For sufficiently large x the second derivative is positive $\varphi''(x) > 0$, therefore the inequality (8) is true for all sufficiently large n.

Let us show that $\varphi'(x) \to \infty$ as $x \to \infty$. This will be done via L'Hopital's rule applied to the related exponent, by means of the substitution $x^\alpha = t$:

$$\lim_{x\to\infty} \frac{p^{x^\alpha}}{x^{1-\alpha}} = \lim_{t\to\infty} \frac{p^t}{t^{\frac{1-\alpha}{\alpha}}} = \lim_{t\to\infty} \frac{\alpha \ln p}{1-\alpha} \cdot \frac{p^t}{t^{\frac{1-2\alpha}{\alpha}}} = \ldots =$$

$$= \lim_{t\to\infty} \frac{\alpha^k \ln p}{\Pi_{i=1}^k (1 - i\alpha)} \cdot \frac{p^t}{t^{\frac{1-(k+1)\alpha}{\alpha}}} = \infty,$$

where k is a number such that $1-k\alpha > 0$ and $1-(k+1)\alpha \le 0$. By Lagrange's theorem, $\Delta_\varphi(n+1) = \varphi(n+1)-\varphi(n) = \varphi'(n+\theta_n) \xrightarrow{n\to\infty} \infty$, where $0 < \theta_n < 1$.

2) Consider the function $f(x) = x^\alpha$. It is easy to calculate that $f'(x) = \alpha x^{\alpha-1} = \frac{\alpha}{x^{1-\alpha}} \xrightarrow{x\to\infty} 0$. By Lagrange's theorem,

$$\Delta_f(n+k) = f(n+k) - f(n) = f'(n+k\theta_n)k \xrightarrow{n\to\infty} 0,$$

where $0 < \theta_n < 1$.
Hence $\lim_{n\to\infty} \frac{\varphi(n+k)}{\varphi(n)} = \lim_{n\to\infty} p^{(n+k)^\alpha - n^\alpha} = p^{\lim_{n\to\infty}\Delta_f(n+k)} = p^0 = 1$. ∎

Proof of Theorem 2.3. The sparseness of the φ function is proved in the Proposition 3.4.

Let $\varrho \in \mathcal{M}_{X_\varphi}$ and $\lambda \in \mathrm{St}\big[(X_\varphi, \varrho)\big]$. According to [9, Proposition 1.4], the $\lambda\varrho$ metric on X_φ can be identified with the normalized metric on the sparse set $X_{\lambda\varphi}$ given by the function $\lambda\varphi$. Let R be a correspondence between sets X_φ and $X_{\lambda\varphi}$ such that $\operatorname{dis} R < \infty$. According to the theorem 2.2 there exist natural n_0 and integer k such that that $R(x_n) = \{y_{n+k}\}$ for all $n \ge n_0$. According to the proposition 3.1 there exists a number $K > 0$, that $|y_{n+k} - x_n| < K$ for all $n \ge n_0$. The latter means that

$$|\lambda p^{(n+k)^\alpha} - p^{n^\alpha}| < K \text{ for all } n \ge n_0.$$

The inequality can be written as

$$|\lambda - p^{n^\alpha-(n+k)^\alpha}| < \frac{K}{p^{(n+k)^\alpha}} \text{ for all } n \ge n_0.$$

The left and right sides of the last inequality have limits as $n \to \infty$. Obviously, the limit of the right-hand side is the number 0. According to the proposition 3.4 the limit of the left side is equal to $|\lambda - 1|$. From the limit inequality $|\lambda-1| \le 0$ the required equality $\lambda = 1$ follows.

Proof of Theorem 2.5. The correspondence $R \in \mathcal{R}(X_\varphi, X_\psi)$ is given by the formula $R(x_n) = \{y_{n+k}\}$ for $n \ge n_0$ and $R(x_n) = \{0_Y, y_1, \dots, y_{n+k-1}\}$ for $n < n_0$. Let us estimate $\operatorname{dis} R$.

For numbers $m > n \ge n_0$, the following estimate is true

$$\big||x_m x_n| - |y_{m+k}y_{n+k}|\big| = \big|x_m + \alpha(m-n)x_n - y_{m+k} - \alpha(m+k-n-k)y_{n+k}\big| \le \big|x_m - y_{m+k}\big| + \big|\alpha(m-n)(x_n - y$$

For numbers $m \ge n_0 > n$, the estimate is true $\big||x_m x_n| - |y_{m+k}y_{n+k}|\big| = \big|x_m + a_n x_n - y_{m+k} - a_{n+k}y_{n+k}\big| \le \big|x_m - y_{m+k}\big| + x_n + y_{n+k} \le K + \varphi(n_0 - 1) + \varphi(n_0 + k - 1)$, where a_n, a_{n+k} are some numbers between -1 and 1.

For numbers $n_0 > m, n$, the estimate is true $\big||x_m x_n| - |y_{m+k}y_{n+k}|\big| \le x_m + x_n + y_{m+k} + y_{n+k} \le 2\varphi(n_0-1) + 2\varphi(n_0+k-1)$. □

Proof of the theorem 2.1. 1) $\Longrightarrow$ 3). Let $R \in \mathcal{R}(X_\varphi, X_\psi)$ be a correspondence such that $\operatorname{dis} R < M$. According to the theorem 2.2 for some n_0 and an integer k for all $n \geq n_0$ $R(x_n) = \{y_{n+k}\}$. According to the proposition 3.1 there are integers n_0 and $K > 0$ such that for every $n \geq n_0$ the inequality $|x_n - y_{n+k}| < K$ is true.

Let r be an arbitrary natural number. For every $n \geq 1$, the following inequality holds: $|\beta(r)-\alpha(r)|x_n \leq |\beta(r)-\alpha(r)|x_n+K-|\beta(r)||y_{n+k}-x_n|+K-|y_{n+r+k}-x_{n+r}| \leq 2K+\big|(\beta(r)-\alpha(r))x_n+\beta(r)(y_{n+k}-x_n)+(y_{n+r+k}-x_{n+r})\big| = 2K+\big|(y_{n+r+k}+\beta(r)y_{n+k})-(x_{n+r}+\alpha(r))x_n)\big| \leq 3K$. Since the numbers x_n tend to infinity, it follows from the above inequality that $|\beta(r) - \alpha(r)| = 1$. The latter means that α and β functions coincide.

The implications 3) $\Longrightarrow$ 1), 2) are contained in Theorem 2.5.

The implication 2) $\Longrightarrow$ 3) is contained in Theorem 2.2. □

References

[1] Edwards D., *The Structure of Superspace. In: Studies in Topology*, ed. by Stavrakas N.M. and Allen K.R., New York, London, San Francisco, Academic Press, Inc., 1975.

[2] Gromov M., *Structures métriques pour les variétés riemanniennes*, edited by Lafontaine and Pierre Pansu, 1981.

[3] Gromov M., *Metric structures for Riemannian and non-Riemannian spaces*, Birkhäuser (1999). ISBN 0-8176-3898-9 (translation with additional content).

[4] Burago D., Burago Yu., Ivanov S., *A Course in Metric Geometry*, AMS GSM 33, 2001.

[5] Bogatyy S.A., Tuzhilin A.A., *Gromov–Hausdorff class: its completeness and cloud geometry*, 2021, ArXiv e-prints, arXiv:2110.06101 [math.MG].

[6] Bogatyy S.A., Tuzhilin A.A., *Action of similarity transformation on families of metric spaces*, Modern mathematics. Fundamental Directions, 2023, v. 69.

[7] Bogataya S.I., Bogatyy S.A., Redkozubov V.V., Tuzhilin A.A., *Clouds in Gromov–Hausdorff Class: their completeness and centers*, Topology and its Applications, 2024,

[8] Bogataya S.I., Bogatyy S.A., *Isometric Cloud Stabilizer*, Topology and its Applications, 2024,

[9] Bogatyy S.A., *Geometric progression stabilizer in a general metric*, Sbornik Mathematics, 2023, v. 214, no. 3, 363–382 pp. DOI: 10.4213/sm9782e

[10] Bogataya S.I., Bogatyy S.A., Redkozubov V.V., Tuzhilin A.A., *Clouds with a trivial stabilizer*, Vestnik Moskov. Univ. Ser. I Mat. Mekh., 2024.

[11] Bogatyy S.A., *Contractibility of a sparse cloud*, Mathematical Notes, 2024.

ROMAI J., v.19, no.1(2023), 63–71

LA CATÉGORIE DES ESPACES $\mathcal{B}$-INDUCTIFS SEMI-RÉFLEXIFS

Dumitru Botnaru

L'Université d'Etat de Tiraspol, Chisinau, Moldova, Department of Mathematics

dumitru.botnaru@gmail.com

Abstract It is demonstrated that the $\mathcal{B}$-inductive semi-reflexive spaces forms a S-semi-reflexive subcategory.

Mots clés: sous-catégories réflectives, coréflectives, $\mathcal{L}$-semi-réflexives sous-catégories, espaces inductifs semi-réflexifs.

2020 MSC: 18F60, 18G99.

1. INTRODUCTION

Notons avec $\mathcal{C}_2\mathcal{V}$ la catégorie des espaces localement convexes topologiques vectoriels Hausdorff (voir [6]). Nous utiliserons les notations suivantes.

Structures de factorisation:
$(\mathcal{E}pi, \mathcal{M}_f)$ = (la classe des épimorphismes, la classe des noyaux) = (la classe des morphismes à image dense, les inclusions topologiques à image fermée);
$(\mathcal{E}_u, \mathcal{M}_p)$ = (la classe des épimorphismes universels, la classe des monomorphismes précis)=(la classe des morphismes surjectifs, la classe des inclusions topologiques);
$(\mathcal{E}_p, \mathcal{M}_u)$ = (la classe des épimorphismes précis, la classe des monomorphismes universels) (voir [2]);

Sous-catégories coréflectives, réflectives et leurs foncteurs:
$\widetilde{\mathcal{M}}$ = des espaces avec la topologie Mackey, $m : \mathcal{C}_2\mathcal{V} \to \widetilde{\mathcal{M}}$;
$\mathcal{S}$ = des espaces avec la topologie faible, $s : \mathcal{C}_2\mathcal{V} \to \mathcal{S}$;
$\mathcal{S}h$ = des espaces Schwartz, $s_h : \mathcal{C}_2\mathcal{V} \to \mathcal{S}h$;
$i\mathcal{R}$ = des espaces inductifs semi-réflexifs [1], $i_r : \mathcal{C}_2\mathcal{V} \to i\mathcal{R}$;
$s\mathcal{R}$ = des espaces semi-réflexifs, $r_s : \mathcal{C}_2\mathcal{V} \to s\mathcal{R}$;
Γ_0 = des espaces complets, $g_0 : \mathcal{C}_2\mathcal{V} \to \Gamma_0$;
$l\Gamma_0$ = des espaces localement complets [5];
$q\Gamma_0$ = des espaces quasicomplets.

1.1. Soit $\mathcal{A}$ et $\mathcal{B}$ deux classes de morphismes. Alors:
1. $\mathcal{A} \circ \mathcal{B} = \{a \cdot b | a \in \mathcal{A}, b \in \mathcal{B}$ et la composition $a \cdot b$ existe$\}$.
2. La classe $\mathcal{A}$ se nomme $\mathcal{B}$-héréditaire, si $f \cdot g \in \mathcal{A}$ et $f \in \mathcal{B}$, alors $g \in \mathcal{A}$.

LEMME ([2], Lemme 2.6). *La classe $\mathcal{E}pi$ est $\mathcal{M}_u$-héréditaire.*

2^0. La classe $\mathcal{A}$ se nomme $\mathcal{B}$-cohéréditaire, si $f \cdot g \in \mathcal{A}$ et $g \in \mathcal{B}$, alors $f \in \mathcal{A}$.

3. $\mathcal{A}^\top$ est la classe de tous les morphismes orthogonaux du dessus pour tout morphisme de $\mathcal{A}$, et $\mathcal{A}^\urcorner = \mathcal{A}^\top \cap \mathcal{E}pi$ (voir [2]).

3^0. $\mathcal{A}^\perp$ est la classe de tous les morphismes orthogonaux du bas pour tout morphisme de $\mathcal{A}$, et $\mathcal{A}^\llcorner = \mathcal{A}^\perp \cap \mathcal{M}ono$.

1.2. Pour $\mathcal{M}$, classe de monomorphismes, et $\mathcal{A}$, classe d'objets (une sous-catégorie), notons par $\mathbf{S}_{\mathcal{M}}(\mathcal{A})$ la sous-catégorie pleine de tous les $\mathcal{M}$-sous-objets des objets de $\mathcal{A}$, et par $P(\mathcal{A})$ la sous-catégorie pleine de tout produit des objets de $\mathcal{A}$.

Notation duale: $\mathbf{Q}_{\mathcal{E}}(\mathcal{A})$, où $\mathcal{E} \subset \mathcal{E}pi$.

1.3. Couples de sous-catégories conjuguées, sous-catégories c-coréflectives et c-réflectives (voir [3]).

Soit $k : \mathcal{C}_2\mathcal{V} \to \mathcal{K}$ et $l : \mathcal{C}_2\mathcal{V} \to \mathcal{L}$ un foncteur coréflecteur et un foncteur réflecteur.

Notons $\mu\mathcal{K} = \{m \in \mathcal{M}ono |\ k(m) \in \mathcal{I}so\}$, $\varepsilon\mathcal{L} = \{e \in \mathcal{E}pi |\ l(e) \in \mathcal{I}so\}$.

Définition (voir [3]). $(\mathcal{K}, \mathcal{L})$ se nomme un couple de sous-catégories conjuguées de la catégorie $\mathcal{C}_2\mathcal{V}$, si $\mu\mathcal{K} = \varepsilon\mathcal{L}$.

Soit $\mathbb{P}_c$ la classe de couples des sous-catégories conjuguées. Chaque composente d'un couple de sous-catégories conjuguées est unique déterminée. $(\tilde{\mathcal{M}}, \mathcal{S})$ est le plus petit élément, et $(\mathcal{C}_2\mathcal{V}, \mathcal{C}_2\mathcal{V})$ le plus grand élément de la classe $\mathbb{P}_c$.

Si $(\mathcal{K}, \mathcal{L}) \in \mathbb{P}_c$, alors $\mathcal{K}$ se nomme la sous-catégorie c-coréflective, et $\mathcal{L}$ - la sous-catégorie c-réflective. Soit $\mathbb{K}_c$ (respectivement: $\mathbb{R}_c$) la classe des sous-catégories c-coréflectives (respectivement: sous-catégories c-réflectives), et $\mathcal{B}ic = \{\varepsilon\mathcal{L} | \mathcal{L} \in \mathbb{R}_c\}$.

1.4. La sous-catégorie $\mathcal{S}h$ des espaces Schwartz et la sous-catégorie $u\mathcal{N}$ des espaces ultranucléaires sont des sous-catégories c-réflectives (voir [3]).

1.5. Pour $\mathcal{A}$, une classe d'objets injectifs ($\mathcal{M}_p$-injectifs), la sous-catégorie $\mathcal{S}_{\mathcal{M}_p}P(\mathcal{A})$ est c-réflective . Ces sous-catégories forment une classe propre de sous-catégories (voir [3]).

1.6. *L'opération* $\lambda_{\mathcal{R}}$ (voir [4]). Soit $\mathcal{A}$ une classe d'épimorphismes de la catégorie $\mathcal{C}_2\mathcal{V}$. Notons avec $\lambda(\mathcal{A})$ la sous-catégorie pleine de tous les objets Z à propriété:

Pour tout $p : X \to Y \in \mathcal{A}$, tout morphisme $f : X \to Z$ s'exteint par p:

$$f = g \cdot p,$$

pour un g. Si $\mathcal{L}$ est une classe d'objets ou une sous-catégorie de la catégorie $\mathcal{C}_2\mathcal{V}$ et $\mathcal{R} \in \mathbb{R}$, alors notons $\lambda_{\mathcal{R}}(\mathcal{L}) = \lambda(\mathcal{A})$, où $\mathcal{A} = \{r^X | X \in |\mathcal{L}|\}$.

L'opération λ^* est définie duale et $\lambda^*(\mathcal{A})$, où $\mathcal{A} \subset \mathcal{M}ono$, et $\mathcal{A}$ est une sous-catégorie de la catégorie $\mathcal{C}_2\mathcal{V}$.

1.7. Proposition. *1. Pour toute classe d'épimorphismes $\mathcal{A}$, la sous-catégorie $\lambda(\mathcal{A})$ est épiréflective.*
2. Soit $(\mathcal{K}, \mathcal{L}) \in \mathbb{P}_c$, et $\mathcal{B} = \mu\mathcal{K}$. Alors $\lambda(\mathcal{B}) = \mathcal{L}$, et $\lambda^*(\mathcal{B}) = \mathcal{K}$.

1.8. Foncteurs commutatifs. On examinera deux foncteurs t_1, t_2, tous les deux coréflecteurs, tous les deux réflecteurs, ou l'un coréflecteur et l'autre réflecteur. Dans la catégorie $\mathcal{C}_2\mathcal{V}$ si $t_1t_2A \sim t_2t_1A$ pour tout $A \in |\mathcal{C}_2\mathcal{V}|$, alors on peut facilement vérifier que les foncteurs $t_1 \cdot t_2$ et $t_2 \cdot t_1$ sont isomorphes.

1.9. Sous-catégories semi-réflexives.
Définition (voir [4]). 1. *Soit $\mathcal{A}$ une sous-catégorie et $\mathcal{L}$ une sous-catégorie réflective de la catégorie $\mathcal{C}_2\mathcal{V}$. L'objet X se nomme $(\mathcal{L}, \mathcal{A})$-semi-réflexif, si sa $\mathcal{L}$-réplique appartient à la sous-catégorie $\mathcal{A}$. La sous-catégorie pleine de tous les objets $(\mathcal{L}, \mathcal{A})$-semi-réflexifs se nomme produit semi-réflexif des sous-catégories $\mathcal{L}$ et $\mathcal{A}$, notée*

$$\mathcal{R} = \mathcal{L} *_{sr} \mathcal{A}.$$

2. *Soit $\mathcal{L}$ et $\mathcal{R}$ deux sous-catégories réflectives de la catégorie $\mathcal{C}_2\mathcal{V}$. $\mathcal{R}$ se nomme une sous-catégorie $\mathcal{L}$-semi-réflexive, si elle est fermée par rapport à $(\varepsilon\mathcal{L})$-sous-objets et $(\varepsilon\mathcal{L})$-facteur-objets.*

La classe de toutes les sous-catégories $\mathcal{L}$-semi-réflexives est notée $\mathbb{R}^s_f(\varepsilon\mathcal{L})$. Alors $\mathbb{R}^s_f(\varepsilon\mathcal{L}) = \mathbb{R}^s(\varepsilon\mathcal{L}) \cap \mathbb{R}_f(\varepsilon\mathcal{L})$, où $\mathbb{R}^s(\varepsilon\mathcal{L}) = \{\mathcal{R} \in \mathbb{R} | \mathcal{R} = \mathcal{S}_{\varepsilon\mathcal{L}}(\mathcal{R})\}$ et $\mathbb{R}_f(\varepsilon\mathcal{L}) = \{\mathcal{R} \in \mathbb{R} | \mathcal{R} = \mathcal{Q}_{\varepsilon\mathcal{L}}(\mathcal{R})\}$.

Théorème [4]. 1. *Soit $\mathcal{L} \in \mathbb{R}_c$ et $\mathcal{R} \in \mathbb{R}$. Alors: $\mathcal{L} *_{sr} \mathcal{R} \in \mathbb{R}^s_f(\varepsilon\mathcal{L})$.*
2. Soit $\mathcal{R} \in \mathbb{R}^s_f(\varepsilon\mathcal{L})$, $\mathcal{T} \in \mathbb{R}$ et $\mathcal{L} \cap \mathcal{R} \subset \mathcal{T} \subset \lambda_{\mathcal{R}}(\mathcal{L})$. Alors $\mathcal{R} = \mathcal{L} *_{sr} (\mathcal{T})$.

Les résultats principaux de l'ouvrage.

On affirme que $i\mathcal{R} \subset \mathcal{B}$-$i\mathcal{R} \subset s\mathcal{R}$ (Lemme 3.4) et $\mathcal{B}$-$i\mathcal{R}$ est une sous-catégorie $\mathcal{S}$-semi-réflexive (Théorème 3.5). La Théorème 3.7 permete de construire $\mathcal{B}$-$i\mathcal{R}$-replique de tout objet de la catégorie $\mathcal{C}_2\mathcal{V}$.

2. La sous-catégorie des espaces inductifs semi-réflexifs

2.1. Soit (E, t) un espace localement convexe et A un ensemble absolument convexe dans l'espace dual E'. L'espace normé (E'_A, n_A) est défini par l'espace linéaire E'_A de l'ensemble A et le fonctionnnel Minkowski n_A de l'ensemble A.

Définition. *Soit $\mathcal{F}$ une famille d'ensembles absolument convexes de l'espace E'. La topologie inductive $j(\mathcal{F})$ définie par la famille $\mathcal{F}$ sur l'espace E' est*

la plus fine topologie localement convexe pour laquelle les applications $j_A : (E'_A, n_A) \to (E', j(\mathcal{F}))$ *sont continues.*

On a examiné divers cas pour la famille $\mathcal{F}$, famille des ensembles absolument convexes et compacts ou précompacts dans les espaces E'_τ et E'_β (E'_τ est l'espace E' avec la topologie Mackey τ, β est la topologie de la convergeance uniforme sur tous les ensembles bornés de (E,t)).

2.2. Soit $\mathcal{U}$ une base d'ensembles absolument convexes de la topologie t et $\mathcal{F} = \{U^0, U \in \mathcal{U}\}$, où U^0 est polaire à l'ensemble $U : U^0 = \{f \in E' || f(U)| \leq 1\}$.

Définition [1]. *L'espace* (E,t) *est nommé inductif semi-réflexif, si* $(E', j(\mathcal{F}))' = E$.

La sous-catégorie des espaces inductifs semi-réflexifs sera notée par $i\mathcal{R}$.

2.3. Théorème [1]. *Un espace localement convexe est inductif semi-réflectif alors et seulement alors quand sa* $\mathcal{S}h$*-réplique est un espace complet.*

2.4. Remarques. 1. *Tenant compte des notations ci-dessus, le résultat mentionné sera écrit*

$$i\mathcal{R} = \mathcal{S}h *_{sr} \Gamma_0.$$

2. *Ainsi* $i\mathcal{R} \in \mathbb{R}^s_{fg}(\varepsilon\mathcal{S}h)$, *et*

$$i\mathcal{R} = \mathcal{S}h *_{sr} \mathcal{T}$$

pour $\mathcal{T} \in \mathbb{R}$ *et* $\mathcal{S}h \cap i\mathcal{R} \subset \mathcal{T} \subset \lambda_{iR}(\mathcal{S}h)$ ([4], Théorème 4.13).

3. ([4], Théorème 6.4). $i\mathcal{R} = Ch *_d (\mathcal{S}h \cap \Gamma_0)$ où $(Ch, \mathcal{S}h) \in \mathbb{P}_c$.

2.5. Théorèmes. 1. $t^X = u^X \cdot v^X$ *est* $((\varepsilon\mathcal{S}h)^\top, \varepsilon\mathcal{S}h)$*-factorisation de morphisme* t^X.

2. Mentionnons aussi que

$$s\mathcal{R} = \mathcal{S} *_{sr} q\Gamma_0$$

(voir [6]). De plus,

$$s\mathcal{R} = \mathcal{S} *_{sr} \mathcal{T}, s\mathcal{R} = \widetilde{\mathcal{M}} *_d (\mathcal{S} \cap q\Gamma_0)$$

pour $\mathcal{T} \in \mathbb{R}$ et $\mathcal{S} \cap s\mathcal{R} \subset \mathcal{T} \subset \lambda_{sR}(\mathcal{S})$ ([4], Théorème 4.13).

3. La sous-catégorie des espaces $\mathcal{B}$-inductifs semi-réflexifs

3.1.Définition [5]. *Un ensemble* A *absolument convexe dans un espace localement convexe* (E,t) *est nommé sphère Banach, si* (E_A, n_A) *est un espace Banach.*

3.2. Définition [7]). *Soit (E,t) un espace localement convexe et $\mathcal{F}$ la famille de toutes les sphères Banach de $E^{'}$. L'espace (E,t) est nommé $\mathcal{B}$-inductif semi-réflexif si $(E^{'},j(\mathcal{F}))^{'}=E$.*

La sous-catégorie des espaces $\mathcal{B}$-inductifs semi-réflexifs sera notée par $\mathcal{B}$-$i\mathcal{R}$.

3.3. Soit $X\in|\mathcal{C}_2\mathcal{V}|, m^X: mX\to X$ la $\tilde{\mathcal{M}}$-coréplique de X et $s_h^{mX}: mX\to s_hmX$ la Sh-réplique de mX.

Théorème [7]. *L'espace localement convexe X est $\mathcal{B}$-inductif semi-réflexif alors et seulement alors quand s_hmX est complet: $s_hmX\in|\Gamma_0|$.*

3.4. Lemme. 1. $i\mathcal{R}\subset\mathcal{B}$-$i\mathcal{R}\subset s\mathcal{R}$.

2. $\mathcal{B}$-$i\mathcal{R}=\mathcal{Q}_{\varepsilon S}(\widetilde{\mathcal{M}}\cap i\mathcal{R})$.

3. $\mathcal{B}$-$i\mathcal{R}=\mathcal{Q}_{\varepsilon\mathcal{S}}(i\mathcal{R})$.

Démonstration. 1. L'inclusion $i\mathcal{R}\subset\mathcal{B}$-$i\mathcal{R}$ est mentionnée dans [7].

$\mathcal{B}$-$i\mathcal{R}\subset s\mathcal{R}$. Soit $(E,t)\in|\mathcal{B}$-$i\mathcal{R}|$. Alors $E'_\tau=(E',j(\mathcal{F}))$. Donc E'_τ est un espace tonnelé comme limite inductive d'une famille d'espace Banach ([6], cap.II, p.7.1 et 7.2). Alors (E,t) est un espace semi-réflexif ([6], cap.IV, Affirmation 5.5).

2. $\mathcal{B}$-$i\mathcal{R}\subset\mathcal{Q}_{\varepsilon\mathcal{S}}(\tilde{\mathcal{M}}\cap i\mathcal{R})$. Soit $A\in|\mathcal{B}$-$i\mathcal{R}|, m^A: mA\to A$ $\tilde{\mathcal{M}}$-coréplique de A et $s_h^{mA}: mA\to s_hmA$ $\mathcal{S}h$-réplique de mA. En vertu du Théorème 3.3 $s_hmA\in|\Gamma_0|$ et en vertu de p. 2.4 $mA\in|i\mathcal{R}|$. Donc $A\in|\mathcal{Q}_{\varepsilon\mathcal{S}}(\tilde{\mathcal{M}}\cap i\mathcal{R})|$.

$\mathcal{Q}_{\varepsilon\mathcal{S}}(\tilde{\mathcal{M}}\cap i\mathcal{R})\subset\mathcal{B}$-$i\mathcal{R}$. Soit $A\in|\mathcal{Q}_{\varepsilon\mathcal{S}}(\tilde{\mathcal{M}}\cap i\mathcal{R})|$, $m^A: mA\to A$ $\tilde{\mathcal{M}}$-coréplique de A. Alors $mA\in|i\mathcal{R}|$. Donc $s_hmA\in|\Gamma_0|$.

3. $\mathcal{B}$-$i\mathcal{R}\subset\mathcal{Q}_{\varepsilon\mathcal{S}}(i\mathcal{R})$. Soit $X\in|\mathcal{B}$-$i\mathcal{R}|$, et $m^X: mX\to X$ $\widetilde{\mathcal{M}}$-coréplique de l'objet X. Alors $mX\in|i\mathcal{R}|$ et $m^X\in\mu\widetilde{\mathcal{M}}=\varepsilon\mathcal{S}$. Donc $X\in|\mathcal{Q}_{\varepsilon\mathcal{S}}(i\mathcal{R})|$.

$\mathcal{Q}_{\varepsilon\mathcal{S}}(i\mathcal{R})\subset\mathcal{B}$-$i\mathcal{R}$. Soit $A\in|\mathcal{Q}_{\varepsilon\mathcal{R}}(i\mathcal{R})|$. Alors A est un $(\varepsilon\mathcal{S})$-facteur-objet d'un objet $X\in|i\mathcal{R}|$: $b: X\to A\in\varepsilon\mathcal{S}$. Soit $m^X: mX\to X$ $\widetilde{\mathcal{M}}$-coréplique de l'objet X. Alors $b\cdot m^X: mX\to A$ et $\widetilde{\mathcal{M}}$-coréplique de l'objet A.

Soit encore que $s_h^{mX}: mX\to s_hmX$ et $s_h^A: X\to s_hX$ Sh-répliques des l'objets respectifs. Alors

$$s_h^X\cdot m^X=s_h(m^X)\cdot s_h^{mX},\tag{1}$$

où s_h^X, s_h^{mX} et m^X appartiennent à la classe $\varepsilon\mathcal{S}=\mathcal{E}_u\cap\mathcal{M}_u$. Donc $s_h(m^X)\in\varepsilon\mathcal{S}$ aussi.

Puisque $X\in|i\mathcal{R}|$, il résulte que $s_hX\in|\Gamma_0|$. Alors $s_hmX\in|\Gamma_0|$ aussi, puisque $s_h(m^X)\in\varepsilon\mathcal{S}$. Ainsi on a démontré que $s_hmA\in|\Gamma_0|$ et $A\in|\mathcal{B}$-$i\mathcal{R}|$.□

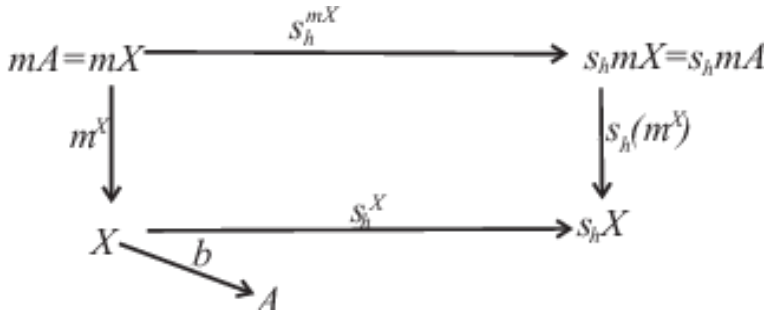

3.5. Théorème. $\mathcal{B}$-$i\mathcal{R} \in \mathbb{R}_f^s(\varepsilon\mathcal{S})$.

Démonstration. Vérifions que $\mathcal{B}$-$i\mathcal{R} \in \mathbb{R}$. Il en suffit de démontrer que la sous-catégorie $\mathcal{B}$-$i\mathcal{R}$ est fermée par rapport avec les produits et les sous-espaces fermés - $\mathcal{M}_f$-sous-objets.

Soit $\{X_i, i \in \mathcal{I}\}$ une famille d'objets de la sous-catégorie $\mathcal{B}$-$i\mathcal{R}$, on a

$$s_h m \Pi X_i = s_h \Pi m X_i$$

puisque le foncteur coréflecteur $m : \mathcal{C}_2\mathcal{V} \to \widetilde{\mathcal{M}}$ commute avec les produits ([6], cap. IV, Théorème 4.3). Puisque $S \subset Sh$, le foncteur $s_h : \mathcal{C}_2\mathcal{V} \to Sh$ commute avec les produits, (voire [3], Exemple 3.9). Donc

$s_h \Pi m X_i = \Pi s_h m X_i$ et $s_h m \Pi X_i \in |\Gamma_0|$.

Vérifions que la sous-catégorie $\mathcal{B}$-$i\mathcal{R}$ est fermée par rapport aux les sous-espaces fermés - $\mathcal{M}_f$-sous-objets. Soit $A \in |\mathcal{B}\text{-}i\mathcal{R}|$ et $i : X \to A \in \mathcal{M}_f$. Examinons le diagramme suivant commutatif formé de $\widetilde{\mathcal{M}}$-coréplique et $\mathcal{S}h$-réplique des objets respectifs.

$$i \cdot m^X = m^A \cdot m(i), \tag{1}$$

$$s_h(i) \cdot s_h^X = s_h^A \cdot i, \tag{2}$$

$$s_h m(i) \cdot s_h^{mX} = s_h^{mA} \cdot m(i), \tag{3}$$

$$s_h^X \cdot m^X = s_h(m^X) \cdot s_h^{mX}, \tag{4}$$

$$s_h^A \cdot m^A = s_h(m^A) \cdot s_h^{mA}, \tag{5}$$

$$s_h(i) \cdot s_h(m^X) = s_h(m^A) \cdot s_h m(i). \tag{6}$$

De plus

$$s_h(i) \cdot b = s_h(m^A) \cdot i_1 \tag{7}$$

est le carré cartésien construit sur les morphismes $s_h(i)$ et $s_h(m^A)$. Alors, de l'égalité (6), on déduit que

$$s_h(m^X) = b \cdot b_1, \tag{8}$$

$$s_h m(i) = i_1 \cdot b_1. \tag{9}$$

pour un morphisme b_1.

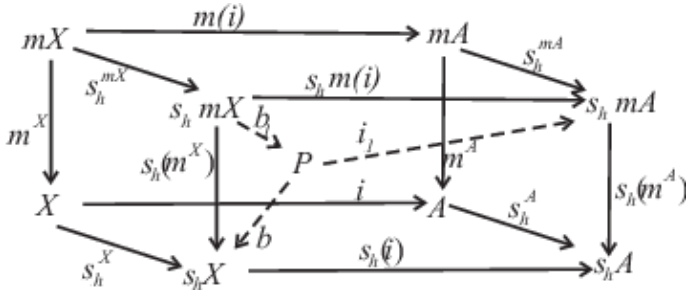

$\widetilde{\mathcal{M}}$ est une sous-catégorie $(\mathcal{E}_u \cap \mathcal{M}_u)$-coréflective et $\mathcal{S}h$ est une sous-catégorie $(\mathcal{E}_u \cap \mathcal{M}_u)$-réflective. De plus, la classe $\mathcal{E}_u \cap \mathcal{M}_u$ est $(\mathcal{E}_u \cap \mathcal{M}_u)$-héréditare et $(\mathcal{E}_u \cap \mathcal{M}_u)$-cohéréditare. Ainsi, dans les égalités (4) et (5), tous les morphismes appartiennent à la classe $\mathcal{E}_u \cap \mathcal{M}_u$. Puisque $s_h(m^A) \in \mathcal{E}_u \cap \mathcal{M}_u$, il résulte que $b \in \mathcal{E}_u \cap \mathcal{M}_u$. De l'égalité (8), on déduit que $b_1 \in \mathcal{E}_u \cap \mathcal{M}_u$ aussi.

La sous-catégorie $\mathcal{S}h$ est c-réflective (voir [3]). Une sous-catégorie $\mathcal{R}$ est c-réflective si et seulement si $\mathcal{R}$ est $\mathcal{E}_u$-réflective et le foncteur $r : \mathcal{C}_2\mathcal{V} \to \mathcal{R}$ est exactement à gauche: $r(\mathcal{M}_f) \subset \mathcal{M}_f$ ([3], Théorème 2.7).

Ainsi $s_h(i) \in \mathcal{M}_f$. Donc $i_1 \in \mathcal{M}_f$ aussi, et P, comme sous-espace fermé de l'espace complet $s_h mA$, est complet. Puisque s_h^{mX} est une application bijective et $b_1 \in \mathcal{M}_u$, les topologies des espaces mX et $s_h mX$ sont compatibles avec la même dualité. Donc $s_h mX \in |\Gamma_0|$.

$\mathcal{B}$-$i\mathcal{R} \in \mathbb{R}_f(\varepsilon\mathcal{S})$. Résulte du Lemme 3.4 p.2.

$\mathcal{B}$-$i\mathcal{R} \in \mathbb{R}^s(\varepsilon\mathcal{S})$. Soit $A \in |\mathcal{B}\text{-}i\mathcal{R}|$, $b : X \to A \in \varepsilon\mathcal{S} = \mu\widetilde{\mathcal{M}}$ et $m^X : mX \to X$ $\widetilde{\mathcal{M}}$-coréplique de X. Donc $b \cdot m^X : mX \to A$ est $\widetilde{\mathcal{M}}$-coréplique de A et $mX \in |i\mathcal{R}|$. Alors $X \in |\mathcal{B}\text{-}i\mathcal{R}|$.□

3.6. Mentionnons que $i\mathcal{R} \in \mathbb{R}_f^s(\varepsilon Sh)$ et $\mathcal{B}$-$i\mathcal{R}$, $s\mathcal{R} \in \mathbb{R}_f^s(\varepsilon\mathcal{S})$. Dans l'ouvrage [7], on affirme que les sous-catégories des espaces inductifs semi-réflexifs et $\mathcal{B}$-inductifs semi-réflexifs ne coïncident pas. Soit (E, t) un espace réflexif normé infinit dimensionnel. On affirme que $(E, \sigma(E, E'))$ est $\mathcal{B}$-inductif semi-réflexif, mais il n'est pas inductif semi-réflexif.

3.7. Théorème. 1. $\mathcal{B}$-$i\mathcal{R} = \mathcal{C}h *_d (\mathcal{S}h \cap \mathcal{U})$, *où* $\mathcal{U} = \mathcal{S}h \vee \mathcal{B}$-$i\mathcal{R}$, $\mathcal{U}$ *est le suprême des sous-catégories* $\mathcal{S}h$ *et* $\mathcal{B}$-$i\mathcal{R}$ *dans la latice* $\mathbb{R}$.

2. $\mathcal{B}$-$i\mathcal{R} = \mathcal{S}h *_{sr} \mathcal{T}$, *pour tout* $\mathcal{T} \in \mathbb{R}$ *et* $\mathcal{S} \cap \mathcal{B}$-$i\mathcal{R} \subset \mathcal{T} \subset \lambda_{\mathcal{B}-i\mathcal{R}}(\mathcal{S}h)$.

3. $\mathcal{B}$-$i\mathcal{R} \subset \mathcal{S}h *_{sr} l\Gamma_0$.

Démonstration. 1.Le Théorème 6.4 [4] indique une méthode qui permet de construire $\mathcal{B}$-$i\mathcal{R}$-réplique de tout objet de la catégorie $\mathcal{C}_2\mathcal{V}$.

2. Voir [4] Théorème 4.19.

3. Soit $A \in |\mathcal{B}$-$i\mathcal{R}|$ et on va démontrer que $\mathcal{S}h$-réplique s_hA appartient à la catégorie $l\Gamma_0$. On a le diagramme commutatif

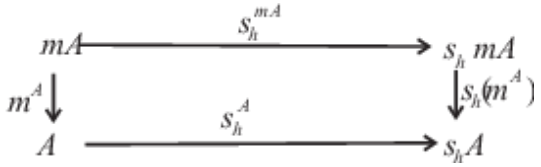

dans lequel tous les morphismes appartiennent à la classe $\mathcal{E}_u \cap \mathcal{M}_u = \varepsilon\mathcal{S}$. De plus, $s_hmA \in |\Gamma_0|$. Ainsi, $s_hA \in |\mathcal{Q}_{\varepsilon\mathcal{S}}(\Gamma_0)| = |l\Gamma_0|$.□

3.8. Soit $\mathcal{C}h$ la conjuguée de la sous-catégorie $\mathcal{S}h : (\mathcal{C}h, \mathcal{S}h) \in \mathbb{P}_c$. Examinons les foncteurs respectifs:

$$c_h : \mathcal{C}_2\mathcal{V} \to \mathcal{C}h, s_h : \mathcal{C}_2\mathcal{V} \to \mathcal{S}h, i_r : \mathcal{C}_2\mathcal{V} \to i\mathcal{R},$$

$$b_r : \mathcal{C}_2\mathcal{V} \to \mathcal{B}\text{-}i\mathcal{R}, m : \mathcal{C}_2\mathcal{V} \to \tilde{\mathcal{M}}, s : \mathcal{C}_2\mathcal{V} \to \mathcal{S}.$$

Théorème. *1. Soit* $\mathcal{T} \in \mathbb{K}_c$ *et* $\mathcal{C}h \subset \mathcal{T}$. *Alors les foncteurs* $t : \mathcal{C}_2\mathcal{V} \to \mathcal{T}$ *et* i_r *commutent:* $t \cdot i_r = i_r \cdot t$.

2. Soit $\mathcal{L} \in \mathbb{R}_c$ *et* $\mathcal{L} \subset \mathcal{S}h$. *Alors les foncteurs* $l : \mathcal{C}_2\mathcal{V} \to \mathcal{L}$ *et* i_r *commutent:* $l \cdot i_r = i_r \cdot l$.

3. Soit $\mathcal{T} \in \mathbb{K}_c$. *Alors les foncteurs* $t : \mathcal{C}_2\mathcal{V} \to \mathcal{T}$ *et* b_r *commutent:* $t \cdot b_r = b_r \cdot t$.

Démonstration. Les affirmations 1 et 3 résultent du Théorème 5.2, et les affirmations 2 et 4 résultent du Corollaire 5.5 [4].□

References

[1] Berezanskii Yu.A., *Inductivno refleksivnye lokal'no vyruklye prostranstva,* Soviet Math.Dokl, 9 (1968), 1080-1082 (en russe).

[2] Botnaru D., *Structures bicatégorielles complémentaires,* Rev. Roumaine Math. Pures Appl., LV(2010), 2, 97-119.

[3] Botnaru D., *Couples des sous-catégories conjuguées,* ROMAI J. 14(2018), 1, 23-41.

[4] Botnaru D., *Noyaux des sous-catégories semi-réflexives,* ROMAI J. 14(2018), 2, 1-32.

[5] Raïcov D.A., *Loi exponentielle pour espaces des applications linéaires continues,* Mat. sb., 7(109), (1965), 2, 279-302 (en russe).

[6] Schaefer H.H., *Topological vector spaces,* Macmillan company, New York, Collier-Macmilian Limited, London, 1966.

[7] Sekevanov V.S., *Espaces localement convexes $\mathcal{B}$-inductifs réflexifs,* Func. an., Meybouzz. sb., Oulianovsk, 14(1980), 128-131 (en russe).

ROMAI J., v.19, no.1(2023), 73–105

FLUID FLOW ON VEGETATED HILLSLOPE: A MATHEMATICAL MODEL

Stelian Ion, Dorin Marinescu, Ştefan-Gicu Cruceanu

"Gheorghe Mihoc-Caius Iacob" Institute of Mathematical Statistics and Applied Mathematics of Romanian Academy, Bucharest, Romania

stelian.ion@ismma.ro, marinescu.dorin@ismma.ro, stefan.cruceanu@ismma.ro

Abstract In this paper, we present a deduction of swallow water equations in the presence of vegetation based on spatial averaging techniques starting from the general principles of conservation of mass and momentum. For this purpose, we worked in the hydrostatic approximation of the pressure field and we considered certain hypotheses of kinematic and topographical nature and assumptions on the structure of the vegetation. Some elements of differential geometry necessary to facilitate the reading of the paper can be found in the Appendix.

Keywords: shallow water equation, numerical approximation.
2020 MSC: 35Q35, 35K55, 35L60, 76S99, 53Z05.

1. INTRODUCTION

The presence of plants on the hill creates a resistance force to the water flow and influences the process of water accumulation on the soil surface. The large diversity of plants growing on a hill makes the elaboration of an unitary model of the water flow over a soil covered by vegetation very difficult. Here, we present a model based on water mass and momentum balance equations that takes into account the presence of certain type of plants.

More precisely, the plants form a dense net of rigid vertical tubes and the water fills the "voided" space up to a level not higher than these plant tubes, see Figure 1. The figure 1 explaines the representative element of the volume P_δ used for mediation. The bottom surface of P_δ has a representative width δ along two orthogonal directions on this surface. The water depth h associated to P_δ is the averaged value of the physical water depth $\widetilde{h}$ inside P_δ.

The article is structured as follows. A full hyperbolic PDE model obtained by averaging the equations for the conservation of mass and momentum is presented in Section 2. Some closure relations for these balance equations can be found in

In the Section 3 we introduce some closure relations conceerning the water-plant and water-soil interaction and we anlyse some mathematical properties of the model. We note that, by suitable assumptions, different simplified models can be obtained from the general model.

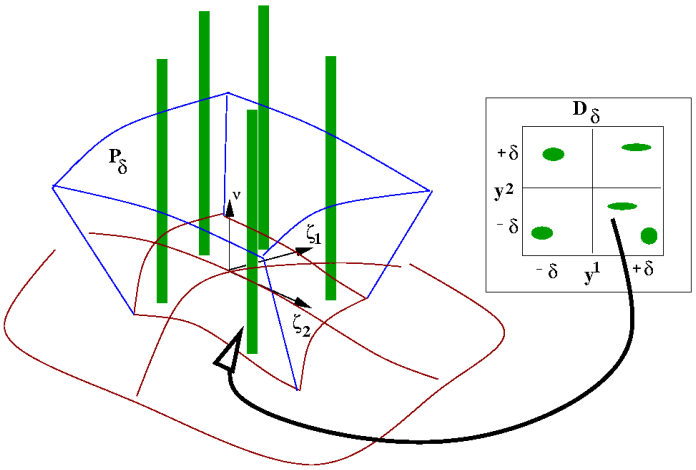

Fig. 1. The representative element of the volume used for mediation

The Appendix is dedicated to some elements of differential geometry used throughout the paper.

2. SPACE AVERAGING MODELS

Space averaging is a method to define a unique continuous model associated to a heterogeneous fluid-solid mechanical system. The method is largely used in porous soil media models [2, 5, 12]. For the fluid-plant physical system, the porous analogy was also used in [1, 6, 8], especially in the case of submerged vegetation.

At a hydrographic basin scale, there are variations in the geometrical properties of the terrain (curvature, orientation, slope) and vegetation density or vegetation type etc. Assume there is a map that models the terrain surface

$$x^i = b^i(\xi^1, \xi^2), \quad (\xi^1, \xi^2) \in D \subset \mathbb{R}^2, \quad i = 1, 2, 3. \tag{1}$$

Denote the tangent vectors to the coordinate curves on this surface by

$$\boldsymbol{\varsigma}_a = \partial_a \boldsymbol{b} := \frac{\partial \boldsymbol{b}}{\partial \xi^a}, \quad a = 1, 2. \tag{2}$$

Using this fixed surface, one introduces a new coordinate y^3 along the normal direction $\boldsymbol{\nu}$ to the surface. A point in the neighborhood of this surface is defined in this new system of coordinates $Y = (\xi^1, \xi^2, y^3)$ by

$$x^i = b^i(\xi^1, \xi^2) + y^3 \nu^i, \quad (\xi^1, \xi^2) \in D \subset \mathbb{R}^2, \quad y^3 \in J \in \mathbb{R}, \quad i = 1, 2, 3, \tag{3}$$

where $\boldsymbol{\nu} = (\nu^1, \nu^2, \nu^3)$ represents the unit normal to the surface.

We introduce the tangent vectors to the coordinate curves defined by Y

$$\boldsymbol{\zeta}_I := \partial_I \boldsymbol{x}, \quad I = 1, 2, 3. \tag{4}$$

One has

$$\boldsymbol{\zeta}_3 = \boldsymbol{\nu}, \quad \boldsymbol{\zeta}_a = (\delta_a^b - y^3 \kappa_a^b)\boldsymbol{\varsigma}_b, \quad a = 1, 2, \tag{5}$$

where $\boldsymbol{\kappa}$ is the curvature tensor of the terrain surface.

In the presence of vegetation on the hill slope, the fluid occupies the free space between plant bodies and the mechanical characteristics of the fluid flow are defined only in the domain occupied by the fluid.

We adopt the following

General convention: *any variable bearing a tilde over it designates a micro-local physical quantity, while the absence of tilde indicates the corresponding averaged quantity. Also, when the micro-local quantity does not differ from the corresponding averaged quantity, we denote the micro-local quantity without tilde.*

Denote by Ω_f and Ω_p the spatial domain occupied by fluid and plants, respectively. Consider $\widetilde{\psi}$ to be some microscopic quantity that refers to the fluid. Let $\boldsymbol{y} = (y^1, y^2)$ be a point in D. One introduces the rectangular domain

$$D_\delta = D_\delta(\boldsymbol{y}) := [y^1 - \delta, y^1 + \delta] \times [y^2 - \delta, y^2 + \delta]. \tag{6}$$

Define the spatial averaging volume

$$P = P(\boldsymbol{y}) = \left\{(x^1, x^2, x^3) \,|\, x^i = b^i(\xi^1, \xi^2) + y^3 \nu^i, \right. \\ \left. 0 < y^3 < \bar{h}(\xi^1, \xi^2),\ (\xi^1, \xi^2) \in D_\delta(\boldsymbol{y}),\ i = 1, 2, 3\right\}.$$

Here, $\bar{h}$ is some extension of $\widetilde{h}$ to the domain D, where $\widetilde{h}$ is the function describing the free water surface outside the domain occupied by plants.

Denote by P^f the fluid domain inside P,

$$P^f := P \cap \Omega^f.$$

The boundary of P^f can be partitioned as

$$\partial P^f = \Sigma^{fp} \cap \Sigma^{ff} \cap \Sigma^{fa} \cap \Sigma^{fs},$$

where Σ^{fp} is the fluid-plant contact surface inside P^f, Σ^{fa} is the free surface of the fluid inside P^f, Σ^{fs} is the fluid-soil contact surface inside P^f, and Σ^{ff} is the boundary surface separating the fluid inside and outside P^f.

The general form of a balance equation, [7] is

$$\partial_t \int\limits_{P^f} \widetilde{\rho}\,\widetilde{\psi} \mathrm{d}V + \int\limits_{\partial P^f} \widetilde{\rho}\,\widetilde{\psi}(\widetilde{\boldsymbol{v}} \cdot \boldsymbol{n} - u_n)\mathrm{d}\sigma = \int\limits_{\partial P^f} \widetilde{\boldsymbol{\Phi}}_\psi \cdot \boldsymbol{n} \mathrm{d}\sigma + \int\limits_{P^f} \widetilde{\rho}\,\widetilde{\boldsymbol{\phi}}_\psi \mathrm{d}V. \tag{7}$$

Here, the significance of the above quantities are:
- $\widetilde{\rho}$ – the micro-local mass density of the fluid;
- $\widetilde{\boldsymbol{v}}$ – the micro-local velocity of the fluid;
- $\boldsymbol{n}$ – the exterior unit normal on ∂P^f;
- $\widetilde{\boldsymbol{\Phi}}_\psi$ – the micro-local flux density of $\widetilde{\psi}$;
- $\widetilde{\boldsymbol{\phi}}_\psi$ – the micro-local mass density of supply $\widetilde{\psi}$;
- u_n – the normal surface velocity;
- $\mathrm{d}V$ – the volume element;
- $\mathrm{d}\sigma$ – the surface element.

To obtain a mathematical treatable model, one needs to make some assumptions concerning the complex fluid-plant-soil system. The first assumption refers to the plant cover.

Assumption 2.1 (Vegetation structure)**.** *The plant cover satisfies:*
A1*. The plants are almost normal to the terrain surface and they behave like rigid sticks.*
A2*. The water depth is smaller than the height of the plants.*

We remark that A1 is often used in the porous model of the vegetation and A2 is proper to the overland flow.

The soil-fluid $\mathcal{I}_{fs}$ and fluid-air $\mathcal{I}_{fa}$ interfaces can be represented as

$$\mathcal{I}_{fs} := \{\boldsymbol{x} \,\big|\, x^i = b^i(\xi^1,\xi^2), \quad (\xi^1,\xi^2) \in D^f,\ i=1,2,3\}$$

and

$$\mathcal{I}_{fa} := \{\boldsymbol{x} \,\big|\, x^i = b^i(\xi^1,\xi^2) + \widetilde{h}(\xi^1,\xi^2)\delta^i_3, \quad (\xi^1,\xi^2) \in D^f,\ i=1,2,3\},$$

respectively, where $D^f := \big\{(\xi^1,\xi^2) \in D \,\big|\, \boldsymbol{b}(\xi^1,\xi^2) \in \Omega^f\big\}$.

Define the averaged water depth by

$$h(y^1,y^2,t) := \frac{1}{\omega_f} \int\limits_{D^f_\delta} \widetilde{h}(\xi^1,\xi^2,t)\beta(\xi^1,\xi^2)\mathrm{d}\xi^1\mathrm{d}\xi^2, \tag{8}$$

where ω_f measures the area of Σ^{fs},

$$\omega_f := \int\limits_{D^f_\delta} \beta(\xi^1,\xi^2)\mathrm{d}\xi^1\mathrm{d}\xi^2. \tag{9}$$

The volume of the fluid inside the elementary domain P is given by

$$\mathrm{vol}(P^f) = \omega_f h. \tag{10}$$

A pure geometrical result which refers to the flux of $\widetilde{\psi}$ through the boundary Σ^{ff} is formulated as:

Lemma 1.

$$\int\limits_{\Sigma^{ff}} \widetilde{\rho}\,\widetilde{\psi}\,\widetilde{\boldsymbol{v}}\cdot\boldsymbol{n}\mathrm{d}\sigma = \partial_a \int\limits_{D^f} \int\limits_{0}^{\widetilde{h}(\xi^1,\xi^2,t)} \widetilde{\rho}\,\widetilde{\psi}\,\widetilde{v}^a \Delta \mathrm{d}y^3 \beta(\xi^1,\xi^2)\mathrm{d}\xi^1\mathrm{d}\xi^2, \tag{11}$$

where $\Delta = 1 - y^3 K_M + (y^3)^2 K_G$, with K_M and K_G the mean and Gauss curvature respectively, and $\beta \mathrm{d}\xi\mathrm{d}\eta$ is the area element of the terrain surface. The quantities $\widetilde{v}^a$, with $a = 1, 2$ stand for the contravariant components of the velocity fields in the local basis $\{\boldsymbol{\zeta}_I\}_{I=\overline{1,3}}$

$$\widetilde{\boldsymbol{v}} = \widetilde{v}^a \boldsymbol{\zeta}_a + \widetilde{v}^3 \boldsymbol{\nu}.$$

In Lemma 1, the partial differentiation ∂_a stands for

$$\partial_a := \frac{\partial}{\partial y^a}.$$

2.1. AVERAGED MASS BALANCE EQUATION

Although the water density is considered to be a constant function, we keep it in the mass balance formulation for emphasizing the physical meaning of the equations. Define the averaged water flux by

$$\rho v^a(\boldsymbol{x},t) := \frac{1}{\mathrm{vol}(P^f)} \int\limits_{D^f_\delta} \int\limits_{0}^{\widetilde{h}(\xi^1,\xi^2,t)} \widetilde{\rho}\,\widetilde{v}^a \Delta \mathrm{d}y^3 \beta \mathrm{d}\xi^1\mathrm{d}\xi^2. \tag{12}$$

The mass balance equation results from (7) by taking $\widetilde{\psi} = 1$, $\widetilde{\boldsymbol{\Phi}}_\psi = 0$ and $\widetilde{\phi}_\psi = 0$. Since the plants are treated as solid bodies and the water does not penetrate the plant bodies, the water flux through the boundary of the elementary volume P^f reduces to

$$\int\limits_{\partial P^f} \widetilde{\rho}(\widetilde{\boldsymbol{v}}\cdot\boldsymbol{n} - u_n)\mathrm{d}\sigma = \int\limits_{\Sigma^{ff}} \widetilde{\rho}\,\widetilde{\boldsymbol{v}}\cdot\boldsymbol{n}\mathrm{d}\sigma + \int\limits_{\Sigma^{fa}} \widetilde{\rho}(\widetilde{\boldsymbol{v}}\cdot\boldsymbol{n} - u_n)\mathrm{d}\sigma + \int\limits_{\Sigma^{fs}} \widetilde{\rho}\,\widetilde{\boldsymbol{v}}\cdot\boldsymbol{n}\mathrm{d}\sigma.$$

The second integral in the r.h.s. of the above relation represents the water flux due to the rain which leads to the water mass gain inside P^f. The third term corresponds to the water flux due to the infiltration which contributes to

the water loss inside P^f. Using Lemma 1 and the definition of the averaged quantities, one can write the mass balance:

$$\frac{\partial}{\partial t}\left(\omega_f h\right) + \partial_a\left(\omega_f h v^a\right) = \omega r - \omega_f i, \tag{13}$$

with

$$\int\limits_{\Sigma^{fa}} \widetilde{\rho}(\widetilde{\boldsymbol{v}}\cdot\boldsymbol{n} - u_n)\mathrm{d}\sigma = -\rho\omega r \quad \text{and} \quad \int\limits_{\Sigma^{fs}} \widetilde{\rho}\,\widetilde{\boldsymbol{v}}\cdot\boldsymbol{n}\mathrm{d}\sigma = \rho\omega_f i \tag{14}$$

representing the rain and the infiltration rates, respectively. Here, as in (9), ω is defined as

$$\omega := \int_{D_\delta} \beta(\xi^1,\xi^2)\mathrm{d}\xi^1\mathrm{d}\xi^2.$$

2.2. AVERAGED MOMENTUM BALANCE EQUATIONS

The momentum balance equation results from (7) with $\widetilde{\psi} = \widetilde{\boldsymbol{v}}$, $\widetilde{\boldsymbol{\Phi}}_\psi = \widetilde{\boldsymbol{T}}$, where $\widetilde{\boldsymbol{T}}$ is the stress tensor and $\widetilde{\phi}_\psi = \widetilde{\boldsymbol{f}}$, with $\widetilde{\boldsymbol{f}}$ denoting the body forces. Here, we only consider the gravitational force.

In contrast to the planar case, there are some difficulties in writing componentwise the space averaging balance momentum equations. These difficulties appear due to the point dependence of the local basis. In the euclidean basis of X, the momentum of the elementary volume P^f is given by

$$\mathcal{H}^i(P^f) = \int\limits_{P^f} \widetilde{\rho}\,\widetilde{v}^i\mathrm{d}V.$$

Using the components of $\widetilde{\boldsymbol{v}}$ in the basis of Y coordinates, we obtain

$$\mathcal{H}^i(P^f) = \int\limits_{\Sigma^{fs}}\int\limits_0^{\widetilde{h}} \widetilde{\rho}\,\zeta^i_a\,\widetilde{v}^a\Delta\mathrm{d}y^3\mathrm{d}\sigma + \int\limits_{\Sigma^{fs}}\int\limits_0^{\widetilde{h}} \widetilde{\rho}\,\nu^i\,\widetilde{v}^3\Delta\mathrm{d}y^3\mathrm{d}\sigma, \tag{15}$$

which can be rewritten as

$$\mathcal{H}^i(P^f) = \varsigma^i_a \int\limits_{\Sigma^{fs}}\int\limits_0^{\widetilde{h}} \widetilde{\rho}\,\widetilde{v}^a\Delta\mathrm{d}y^3\mathrm{d}\sigma + \nu^i \int\limits_{\Sigma^{fs}}\int\limits_0^{\widetilde{h}} \widetilde{\rho}\,\widetilde{v}^3\Delta\mathrm{d}y^3\mathrm{d}\sigma + \mathcal{E}^i_1(\widetilde{\boldsymbol{v}}, P^f). \tag{16}$$

Here and in what follows, we make the following convention: $\boldsymbol{\varsigma}_a = \boldsymbol{\varsigma}_a(\boldsymbol{y})$, where $\boldsymbol{y} = (y^1, y^2)$ is the point defining the domain $D_\delta(\boldsymbol{y})$ from (6). When it appears inside the integral, the unit normal $\boldsymbol{\nu}$ is a variable quantity depending

on the current point from the domain D_δ, but when it appears outside the integral, it is the unit normal defined by the same $\boldsymbol{y}$ as $\boldsymbol{\varsigma}_a$.

The term

$$\mathcal{E}_1^i(\widetilde{\boldsymbol{v}}, P^f) := \int\limits_{\Sigma^{fs}} \int\limits_0^{\widetilde{h}} \widetilde{\rho}(\zeta_a^i - \varsigma_a^i)\widetilde{v}^a \Delta \mathrm{d}y^3 \mathrm{d}\sigma$$

represents an error introduced by neglecting the variation of the basis $\boldsymbol{\zeta}_I$ along the domain P^f.

By averaging, from (16) one has

$$\mathcal{H}(P^f) = \rho h \omega_f v^a \boldsymbol{\varsigma}_a + \rho h \omega_f v^3 \boldsymbol{\nu} + \mathcal{E}_1(\widetilde{\boldsymbol{v}}, P^f). \tag{17}$$

If one neglects the momentum transfer on the fluid-air and fluid-soil interfaces, then the flux of the momentum through the boundary ∂P^f can be reduced to

$$\mathcal{F}(\widetilde{\rho}\,\widetilde{\boldsymbol{v}}, \partial P^f) := \int\limits_{\partial P^f} \widetilde{\rho}\,\widetilde{\boldsymbol{v}}(\widetilde{\boldsymbol{v}} \cdot \boldsymbol{n} - u_n)\mathrm{d}\sigma = \int\limits_{\Sigma^{ff}} \widetilde{\rho}\,\widetilde{\boldsymbol{v}}(\widetilde{\boldsymbol{v}} \cdot \boldsymbol{n})\mathrm{d}\sigma.$$

Using Lemma 1, one has

$$\mathcal{F}(\widetilde{\rho}\,\widetilde{\boldsymbol{v}}, \partial P^f) = \partial_a \int\limits_{D^f} \int\limits_0^{\widetilde{h}(\xi^1,\xi^2,t)} \widetilde{\rho}\,\widetilde{\boldsymbol{v}}\,\widetilde{v}^a \Delta \mathrm{d}y^3 \beta(\xi^1, \xi^2)\mathrm{d}\xi^1\mathrm{d}\xi^2,$$

and then,

$$\begin{aligned}\mathcal{F}(\widetilde{\rho}\,\widetilde{\boldsymbol{v}}, \partial P^f) = \\ &\partial_a(\rho\omega_f h v^b v^a \boldsymbol{\varsigma}_b) + \partial_a(\rho\omega_f h w^{ba}\boldsymbol{\varsigma}_b) + \partial_a(\rho\omega_f h v^3 v^a \boldsymbol{\nu}) + \\ &\mathcal{E}_2(\widetilde{v}^2, P^f),\end{aligned} \tag{18}$$

where the fluctuation

$$\rho w^{ab} := \frac{1}{\omega_f h}\int_{\Sigma^f}\int_0^{\widetilde{h}(\xi^1,\xi^2,t)} \widetilde{\rho}(\widetilde{v}^b - v^b)\widetilde{v}^a y^3 \beta(\xi^1, \xi^2)\mathrm{d}\xi^1\mathrm{d}\xi^2.$$

The quantity $\mathcal{E}_2(\widetilde{v}^2, P^f)$ (as $\mathcal{E}_1(\widetilde{v}, P^f)$ appearing above), represents the error introduced by approximating the variable local basis $(\boldsymbol{\zeta}_1(\xi^1, \xi^2, y^3), \boldsymbol{\zeta}_2(\xi^1, \xi^2, y^3), \boldsymbol{\nu}(\xi^1, \xi^2, 0))$ with the fixed local basis $(\boldsymbol{\varsigma}_1, \boldsymbol{\varsigma}_2, \boldsymbol{\nu})$ at $(y^1, y^2, 0)$. The quantities $\mathcal{E}_3$, $\mathcal{E}_4$ and $\mathcal{E}_5$ introduced in what follows are errors of the same nature.

Rel. (18) can be rewritten as

$$\begin{aligned}
&\mathcal{F}(\widetilde{\rho}\,\widetilde{\boldsymbol{v}}, \partial P^f) = \\
=&\partial_a(\rho\omega_f h v^b v^a)\boldsymbol{\varsigma}_b + \rho\omega_f h v^b v^a \partial_a \boldsymbol{\varsigma}_b + \partial_a(\rho\omega_f h w^{ba})\boldsymbol{\varsigma}_b + \rho\omega_f h w^{ba}\partial_a\boldsymbol{\varsigma}_b + \\
&\partial_a(\rho\omega_f h v^3 v^a)\boldsymbol{\nu} + \rho\omega_f h v^3 v^a \partial_a \boldsymbol{\nu} + \mathcal{E}_2(\widetilde{v}^2, P^f) \\
=&\partial_a(\rho\omega_f h v^b v^a)\boldsymbol{\varsigma}_b + \rho\omega_f (h v^b v^a + w^{ba})(\gamma^c_{ab}\boldsymbol{\varsigma_c} + \kappa_{ab}\boldsymbol{\nu}) + \\
&\partial_a(\rho\omega_f h w^{ba})\boldsymbol{\varsigma}_b + \partial_a(\rho\omega_f h v^3 v^a)\boldsymbol{\nu} - \rho\omega_f h v^3 v^a \kappa^b_a \boldsymbol{\varsigma}_b + \mathcal{E}_2(\widetilde{v}^2, P^f) \\
=&\partial_a(\rho\omega_f h(v^b v^a + w^{ba}))\boldsymbol{\varsigma}_b - \rho\omega_f h v^3 v^a \kappa^b_a \boldsymbol{\varsigma}_b + \rho\omega_f (h v^b v^a + w^{ba})\gamma^c_{ab}\boldsymbol{\varsigma_c} + \\
&\rho\omega_f (h v^b v^a + w^{ba})\kappa_{ab}\boldsymbol{\nu} + \partial_a(\rho\omega_f h v^3 v^a)\boldsymbol{\nu} + \mathcal{E}_2(\widetilde{v}^2, P^f),
\end{aligned} \tag{19}$$

where γ^c_{ab} are the Christoffel symbols.

To express the contribution of the stress forces to the momentum balance, we decompose the stress tensor field $\widetilde{\boldsymbol{T}}$ in two components: the pressure field $\widetilde{p}$ and the viscous part of the stress tensor field $\widetilde{\boldsymbol{\tau}}$

$$\widetilde{\boldsymbol{T}} = -\widetilde{p}\boldsymbol{I} + \widetilde{\boldsymbol{\tau}}.$$

The flux of the stress vector can now be written as

$$\mathcal{F}(\widetilde{\boldsymbol{T}}, \partial P_f) = \mathcal{F}(-p\boldsymbol{I}, \partial P_f) + \mathcal{F}(\widetilde{\boldsymbol{\tau}}, \partial P_f).$$

An elementary calculation show that

$$\mathcal{F}(-p\boldsymbol{I}, \partial P_f) = -\int\limits_{D^f}\int\limits_{0}^{\widetilde{h}(\xi^1,\xi^2,t)} \Big(\partial_a p g^{ab}\boldsymbol{\zeta}_b + \partial_3 p\boldsymbol{\nu}\Big)\,\Delta \mathrm{d}y^3 \beta \mathrm{d}\xi^1 \mathrm{d}\xi^2 \tag{20}$$

The pressure field is determined up to a constant value. If we subtract the atmospheric pressure from the water pressure, on the interface fluid-air the pressure must be zero. We assume the pressure field to be hydrostatically distributed.

Let $\boldsymbol{g} = -g\boldsymbol{i}_3$ be the gravitational force acting on the mass unit. In the local frame of coordinates related to the free surface of the fluid, this force has the representation

$$\boldsymbol{g} = \widetilde{f}^a\boldsymbol{\zeta}_a - \widetilde{f}^3\boldsymbol{\nu}.$$

Assumption 2.2 (Hydrostatic approximation)**.** *One assumes that*
A3. *The hydrostatic pressure field has the form*

$$\widetilde{p}(\xi^1, \xi^2, y^3) = \widetilde{\rho}\,\widetilde{f}^3(\widetilde{h}(\xi^1, \xi^2) - y^3).$$

We neglect the shear forces on the fluid-air interface, i.e.

$$\mathcal{F}(\widetilde{\boldsymbol{\tau}}, \Sigma^{fa}) = 0.$$

On the fluid-soil interface, the stress vector $\widetilde{\boldsymbol{t}} := \widetilde{\boldsymbol{\tau}} \cdot \boldsymbol{n}$ can be written as

$$\widetilde{\boldsymbol{t}} = \widetilde{t}^a \boldsymbol{\zeta}_a + \widetilde{t}^3 \boldsymbol{\nu}.$$

On the soil-water interface, we can write

$$\mathcal{F}(\widetilde{\boldsymbol{\tau}}, \Sigma^{fs}) = \boldsymbol{\varsigma}_a \int\limits_{\Sigma^{fs}} \widetilde{t}^a \mathrm{d}\sigma + \boldsymbol{\nu} \int\limits_{\Sigma^{fs}} \widetilde{t}^3 \mathrm{d}\sigma + \mathcal{E}_3(\widetilde{\boldsymbol{T}}, \Sigma^{fs}). \tag{21}$$

Introducing the shear force at the fluid-soil interface

$$\sigma_s^a = \frac{1}{\rho \omega_f} \int\limits_{\Sigma^{fs}} \widetilde{t}^a \mathrm{d}\sigma,$$

relation (21) takes the form

$$\mathcal{F}(\widetilde{\boldsymbol{\tau}}, \Sigma^{fs}) = \boldsymbol{\varsigma}_a \rho \omega_f \sigma_s^a + \boldsymbol{\nu} \int\limits_{\Sigma^{fs}} \widetilde{t}^3 \mathrm{d}\sigma + \mathcal{E}_3(\widetilde{\boldsymbol{T}}, \Sigma^{fs}). \tag{22}$$

On the fluid-plant interface

$$\mathcal{F}(\widetilde{\boldsymbol{\tau}}, \Sigma^{fp}) = \int\limits_{\Sigma^{fp}} \widetilde{\boldsymbol{\tau}} \cdot \boldsymbol{n} \mathrm{d}\sigma = \sum_l \int\limits_{\Sigma_l^{fp}} \widetilde{\boldsymbol{\tau}} \cdot \boldsymbol{n} \mathrm{d}\sigma, \tag{23}$$

where Σ_l^{fp} is the fluid-plant surface corresponding to the plant l. Obviously, $\bigcup\limits_l \Sigma_l^{fp} = \Sigma^{fp}$. Since the plant stems are supposed to be perpendicular to the ground surface, (23) becomes

$$\mathcal{F}(\widetilde{\boldsymbol{\tau}}, \Sigma^{fp}) = \boldsymbol{\varsigma}_a \sum_l \int\limits_{\Sigma_l^{fp}} \widetilde{t}^a \mathrm{d}\sigma + \mathcal{E}_4(\widetilde{\boldsymbol{\tau}}, \Sigma^{fp}) \tag{24}$$

and introducing the plant resistance force

$$\sigma_p^a = \frac{1}{\rho \omega} \sum_l \int\limits_{\Sigma_l^{fp}} \widetilde{t}^a \mathrm{d}\sigma,$$

relation (24) becomes

$$\mathcal{F}(\widetilde{\boldsymbol{\tau}}, \Sigma^{fp}) = \boldsymbol{\varsigma}_a \rho \omega \sigma_p^a + \mathcal{E}_4(\widetilde{\boldsymbol{\tau}}, \Sigma^{fp}). \tag{25}$$

On the fluid interface of P^f, invoking again Lemma 1, the contribution of the viscous part of the stress tensor on the interface fluid-fluid takes the form

$$\mathcal{F}(\widetilde{\boldsymbol{\tau}}, \Sigma^{ff}) = \partial_a \int\limits_{\Sigma^{fs}} \int\limits_0^{\widetilde{h}} \widetilde{\tau}^{ba} \boldsymbol{\zeta}_b \Delta \mathrm{d}y^3 \mathrm{d}\sigma + \partial_a \int\limits_{\Sigma^{fs}} \int\limits_0^{\widetilde{h}} \widetilde{\tau}^{3a} \boldsymbol{\nu} \Delta \mathrm{d}y^3 \mathrm{d}\sigma.$$

Then, we write the above quantity as,

$$\mathcal{F}(\widetilde{\boldsymbol{\tau}}, \Sigma^{ff}) = \partial_a(\omega_f h \tau^{ba} \boldsymbol{\varsigma}_b) + \partial_a(\omega_f h \tau^{3a} \boldsymbol{\nu}) + \mathcal{E}_5(\widetilde{\boldsymbol{\tau}}_v, P^f). \tag{26}$$

Rel. (26) implies that

$$\begin{aligned}
\mathcal{F}(\widetilde{\boldsymbol{\tau}}, \Sigma^{ff}) = & \\
&= \partial_a(\omega_f h \tau^{ba}) \boldsymbol{\varsigma}_b + \omega_f h \tau^{ba} \partial_a \boldsymbol{\varsigma}_b + \partial_a(\omega_f h \tau^{3a}) \boldsymbol{\nu} + \omega_f h \tau^{3a} \partial_a \boldsymbol{\nu} \\
&+ \mathcal{E}_5(\widetilde{\boldsymbol{\tau}}_v, P^f) \\
&= \partial_a(\omega_f h \tau^{ba}) \boldsymbol{\varsigma}_b + \omega_f h \tau^{ba} (\gamma^c_{ab} \boldsymbol{\varsigma}_c + \kappa_{ab} \boldsymbol{\nu}) + \partial_a(\omega_f h \tau^{3a}) \boldsymbol{\nu} \\
&- \omega_f h \tau^{3a} \kappa^b_a \boldsymbol{\varsigma}_b + \mathcal{E}_5(\widetilde{\boldsymbol{\tau}}_v, P^f) \\
&= \partial_a(\omega_f h \tau^{ba}) \boldsymbol{\varsigma}_b - \omega_f h \tau^{3a} \kappa^b_a \boldsymbol{\varsigma}_b + \omega_f h \tau^{ba} \gamma^c_{ab} \boldsymbol{\varsigma}_c + \omega_f h \tau^{ba} \kappa_{ab} \boldsymbol{\nu} \\
&+ \partial_a(\omega_f h \tau^{3a}) \boldsymbol{\nu} + \mathcal{E}_5(\widetilde{\boldsymbol{\tau}}_v, P^f).
\end{aligned} \tag{27}$$

For the supply $\widetilde{\Phi}_\psi$, we only consider the contribution of the gravitational force. Proceeding by components as in (16), the second term in the r.h.s. of (7) is finally expressed as

$$\int\limits_{P^f} \widetilde{\rho} \widetilde{\boldsymbol{\phi}}_\psi \mathrm{d}V = \int\limits_{D^f} \int\limits_0^{\widetilde{h}(\xi^1, \xi^2, t)} \left(\widetilde{f}^a \boldsymbol{\zeta}_a - \widetilde{f}^3 \boldsymbol{\nu} \right) \Delta \mathrm{d}y^3 \beta \mathrm{d}\xi^1 \mathrm{d}\xi^2 \tag{28}$$

The relations (17, 19, 20, 22, 25, 27) and some order assumptions are the basis for averaged momentum equations.

The porosity θ of the plant cover is defined by

$$\theta = \frac{\omega_f}{\omega}.$$

Let $\beta_0 = \beta(y_1, y_2)$, where $\boldsymbol{y} = (y^1, y^2)$ is the point defining the domain $D_\delta(\boldsymbol{y})$ from (6).

Let ϵ be a small parameter.

Assumption 2.3 (Kinematical and topographical assumptions)**.** *Suppose that the physical processes satisfy the following properties:*

A4. The water depth. $\widetilde{h} = O(\epsilon)$.
A5. The velocity. $v^3 = O(\epsilon)$.
A6. Geometric assumptions:
A6.1. Curvature. *The terrain surface curvatures and the curvature of the coordinate curves are of order of* ϵ. *This means that locally the surface is almost planar.*
A6.2. Metric tensor. $\beta = \beta_0 + O(\epsilon)$.
A7. The averaged dimension δ. $d_p \ll \delta \ll L$ *and* $\delta K_M = O(\epsilon)$.

In what follows, by abuse of notations, we denote β_0 by β.

The shallow water type approximation of the averaged momentum balance for an incompressible fluid results by an asymptotic analysis.

Theorem 2.1 (Averaged momentum equations)**.** *Under assumptions* A1–A7*, the first order approximation for the momentum equations is given by*

$$\partial_t(h\beta\theta v^a) + \partial_b \mathfrak{F}^{ab}(h, \boldsymbol{v}) + h\beta\theta\beta^{ab}\partial_a w = \mathfrak{G}^a(h, \boldsymbol{v}), \quad a = 1, 2, \tag{29}$$

where

$$w = g(b^3 + h\nu^3), \quad (g - \textit{the gravitational acceleration})$$

$$\mathfrak{F}^{ab}(h, \boldsymbol{v}) = h\beta\theta\left(v^a v^b + w^{ab} - \frac{1}{\rho}\tau^{ab}\right),$$

$$\mathfrak{G}^a(h, \boldsymbol{v}) = \beta\theta\sigma_p^a + \beta\theta\sigma_s^a - \gamma_{bc}^a\eta^{bc}$$

and

$$\eta^{ac} = h\beta\theta\left(v^a v^b + w^{ab} - \frac{1}{\rho}\tau^{ab}\right).$$

Sketch of proof. Using Assumption 2.3 and relations (17, 19, 22, 25, 27) one can prove that the terms $\mathcal{E}_1, \ldots, \mathcal{E}_5$ are of order ϵ^2. For $\epsilon \ll 1$ these terms as well as the terms containing the factors $v^3 h$, $h\kappa$ or h^2 (which are of same order ϵ^2) can be neglected.

The equations (29) must be supplemented by empirical laws concerning the *averaged stress tensor* $\boldsymbol{\tau}$, the *averaged vegetation force resistance* $\boldsymbol{\sigma}_p$, the *averaged shear fluid-soil force* $\boldsymbol{\sigma}_s$ and the *averaged fluctuation* w^{ab}. These empirical laws are expressed by functions depending on the averaged velocity $\boldsymbol{v}$, the averaged water depth h and a set of parameters $\boldsymbol{\lambda}$ defined by the

characteristics of the plant cover.

$$\begin{cases} \tau^{ab} = \mathfrak{T}^{ab}(\nabla \boldsymbol{v}, h, \boldsymbol{\lambda}), \\ \sigma_p^b = \mathfrak{S}_p^b(\boldsymbol{v}, h, \boldsymbol{\lambda}), \\ \sigma_s^b = \mathfrak{S}_s^b(\boldsymbol{v}, h, \boldsymbol{\lambda}), \\ w^{ab} = \mathfrak{W}^{ab}(\boldsymbol{v}, h, \boldsymbol{\lambda}). \end{cases} \tag{30}$$

3. SHALOW WATER EQUATIONS WITH VEGETATION (SWE-VEG) MODELS

The averaged models of water flow on a vegetated hillslope consists of mass balance equation (13), momentum balance equations (29) and a set of empirical relations (30). The empirical relations are generaly obtained by experiments or in situ mesurements of hydrodinamic variables.

The models we will present here quantify the interactions water-plant, σ_p^b and water-soil, σ_p^b. One assumes that the viscosity of fluid and the fluctuation of the velocity field have a small effect as compared with the bed friction and plant resistance. We set

$$\boldsymbol{\tau} = 0, \quad \boldsymbol{w} = 0$$

The averaged vegetation force resistance

The most used empirical relations that relate the vegetation resistance and fluid velocity have the form [8, 1]

$$\sigma_p^a = -\frac{1}{2} C_d m h d |\boldsymbol{v}| v^a, \tag{31}$$

where m is the number of stems on the surface ω and d is the averaged diameters of the stems.

The bed shear stress

One uses the experimental relations of Manning or Ch´ezy, or the Darcy–Weisbach formula:

$$\sigma_b^a = -\frac{g}{C_b^2} |\boldsymbol{v}| v^a, \tag{32}$$

$|\boldsymbol{v}|$ being the magnitude of the averaged velocity *i.e.*

$$|\boldsymbol{v}|^2 = \beta_{ab} v^a v^b.$$

Generally, C_b depends on h, see [11], [13]

Therefore the base model is given by

$$\begin{aligned} \frac{\partial}{\partial t}\left(h\beta\theta\right) + \partial_a\left(h\beta\theta v^a\right) =& \beta(\mathfrak{m}_r - \theta\mathfrak{m}_i), \\ \frac{\partial}{\partial t}h\theta\beta v^c + \frac{\partial}{\partial y^a}\theta\beta\, hv^c v^a + h\theta\beta\gamma^c_{ab}v^a v^b + h\beta\theta\beta^{ca}\partial_a w =& -\beta\mathcal{K}(h,\theta)|\boldsymbol{v}|v^c. \end{aligned} \tag{33}$$

The parameter function $\mathcal{K}(h,\theta)$ is given by

$$\mathcal{K}(h,\theta) = \frac{1}{2}C_d m(\boldsymbol{y})hd + \frac{g\theta}{C_b^2}$$

here m stands for the density number of the stems on surface area. In our model, the porosity θ and the density number m are related by

$$\theta = 1 - m\frac{\pi d^2}{4}.$$

such that one can write

$$\mathcal{K}(h,\theta) = \alpha_p h(1-\theta) + \alpha_s\theta,$$

where the new parameters are given by

$$\alpha_p = \frac{2C_d}{\pi d}, \quad \alpha_s = \frac{g}{C_b^2}.$$

Note that the system equations modeling the water flow on an unvegetated hill can be obtained from the model (33) by simply considering the porosity $\theta = 1$.

The full PDE model for the water flow on vegetated hill is given by (33). The system is hyperbolic with source terms and there is an energy function that is a conserved quantity in the absence of plants and water-soil friction. Also, the model preserves the steady state of the lake.

Proposition 2. *The model* (33) *is of hyperbolic type with source terms.*
(a) *The conservative form of the system is given by*

$$\partial_t\mathcal{H}^i(\boldsymbol{y},t,\boldsymbol{u}) + \partial_a\mathcal{F}^{ia}(\boldsymbol{y},t,\boldsymbol{u}) = \mathcal{P}^i(\boldsymbol{y},t,\boldsymbol{u}), \tag{34}$$

where

$$\boldsymbol{u} = \begin{pmatrix} h \\ v^1 \\ v^2 \end{pmatrix}, \quad \mathcal{H}(\boldsymbol{y},t,\boldsymbol{u}) = \begin{pmatrix} \beta\theta h \\ \beta\theta hv^1 \\ \beta\theta hv^2 \end{pmatrix},$$

$$\mathcal{F}(\boldsymbol{y},t,\boldsymbol{u}) = \begin{pmatrix} \beta\theta hv^1 & \beta\theta hv^2 \\ \beta\theta(hv^1v^1 + g\nu^3\beta^{11}h^2/2) & \beta\theta(hv^1v^2 + g\nu^3\beta^{12}h^2/2) \\ \beta\theta(hv^2v^1 + g\nu^3\beta^{21}h^2/2) & \beta\theta(hv^2v^2 + g\nu^3\beta^{22}h^2/2) \end{pmatrix},$$

and

$$\mathcal{P}(\boldsymbol{y},t,\boldsymbol{u}) =$$

$$\begin{pmatrix} \beta(\mathfrak{m}_r-\theta(y)\mathfrak{m}_i) \\ -\beta\theta h\gamma^1_{ab}v^av^b - gh\left[\beta\theta\beta^{1a}\left(\partial_a x^3+\frac{h}{2}\partial_a\nu^3\right)-\frac{h}{2}\nu^3\partial_a\beta\theta\beta^{1a}\right]-\beta\mathcal{K}|v|v^1 \\ -\beta\theta h\gamma^1_{ab}v^av^b - gh\left[\beta\theta\beta^{2a}\left(\partial_a x^3+\frac{h}{2}\partial_a\nu^3\right)-\frac{h}{2}\nu^3\partial_a\beta\theta\beta^{2a}\right]-\beta\mathcal{K}|v|v^2 \end{pmatrix}.$$

(b) *For any unitary vector* $\boldsymbol{n}\in\mathbb{R}^3$*, the eigenvalue problem [17]*

$$\left(\frac{\partial}{\partial u^i}\mathcal{F}^{ja}n_a-\lambda\frac{\partial}{\partial u^i}\mathcal{H}^j\right)r^i=0 \tag{35}$$

has three solutions:

$$\lambda_-=v^an_a-\sqrt{g\nu^3h},\quad \lambda_0=v^an_a,\quad \lambda_+=v^an_a+\sqrt{g\nu^3h}. \tag{36}$$

Proof. In order to prove the existence of the solution for (35), it is sufficient to show that

$$\frac{\partial}{\partial u^i}\mathcal{F}^{ja}n_a-\lambda\frac{\partial}{\partial u^i}\mathcal{H}^j=\beta\theta\begin{pmatrix}\delta & hn_1 & hn_2\\ v^1\delta+g\nu^3h\beta^{1a}n_a & h\delta+hv^1n_1 & hv^1n_2\\ v^2\delta+g\nu^3h\beta^{2a}n_a & hv^2n_1 & h\delta+hv^2n_2\end{pmatrix},$$

where $\delta=v^an_a-\lambda$. The solutions (36) results then from straightforward calculations.

Proposition 3. *The following properties hold for system* (33)*:*

(a) it preserves the steady state of a lake

$$x^3+h\nu^3=\text{constant};$$

(b) there is a conservative equation for the energy

$$\frac{\partial}{\partial t}h\beta\theta\mathcal{E}+\frac{\partial}{\partial y^a}h\beta\theta v^a\left(\mathcal{E}+g\frac{h}{2}\nu^3\right)=\beta\left(\left(\mathfrak{M}(-\frac{1}{2}|\boldsymbol{v}|^2+w\right)-\mathcal{K}|\boldsymbol{v}|^3\right), \tag{37}$$

where

$$\mathcal{E}:=\frac{1}{2}|\boldsymbol{v}|^2+g(x^3+\frac{h}{2}\nu^3),\quad \mathfrak{M}=\mathfrak{m}_r-\theta\mathfrak{m}_i$$

(c) Bernoulli's law. At a steady state, in the absence of mass source and friction force, the total energy

$$\mathcal{E}^{\mathrm{t}}=\frac{1}{2}|\boldsymbol{v}|^2+gx^3+p(\boldsymbol{y},h)$$

is constant along a current line

$$v^a\partial_a\mathcal{E}^{\mathrm{t}}=0. \tag{38}$$

3.1. FLOW ON ALMOST LOCAL FLAT SURFACE

The model equations (33) is a too complicate mathematical for many practical applications. It is a good base model to generate simplified models of certain realistics problem. A simplified version of the full model correspond to a given soil surface topograhy and a given structure of the plant cover. In the sequell we introduce a simplified variant of the full model that yet allows variation in the soil topography and plant porosity.

Let the soil surface be given by

$$x^1 = y^1, x^2 = y^2, x^3 = z(y^1, y^2), \boldsymbol{y} \in D \subset \mathbb{R}^2 \tag{39}$$

We denote the euclidian norm of gradient of surface by

$$|\nabla z|^2 = (\partial_1 z)^2 + (\partial_2 z)^2$$

The geometrical characteristics of the surface can be written as(see the Anexa):

$$\begin{aligned} &\beta_{ab} = \delta_{ab} + \partial_a z \partial_b z, \beta = \sqrt{1 + |\nabla z|^2} \\ &\nu^a = \frac{-\partial_a z}{\beta}, \nu^3 = \frac{1}{\beta} \\ &\gamma^c_{ab} = \frac{\partial_c z \partial^2_{ab} z}{\beta^2}, \kappa^a_b = \frac{\beta^{bc} \partial^2_{cb} z}{\beta} \end{aligned} \tag{40}$$

An almost local flat surface is one characterized by:

$$\partial^2_{ab} z \approx 0, a, b = 1, 2.$$

For such surface one assumes that:

$$\beta = \text{constant}, \gamma^a_{bc} = 0, \kappa^a_b = 0, a, b, c = 1, 2$$

One these ground the equations (33) can be approximate as:

$$\begin{aligned} \frac{\partial}{\partial t}\theta h + \partial_a (\theta h v^a) = &\quad \mathfrak{M}, \\ \frac{\partial}{\partial t}\theta h v_a + \partial_b \theta h v_a v^b + \theta h \partial_a w = &\quad -\mathcal{K}(h, \theta)|v| v_a. \end{aligned} \tag{41}$$

where

$$\mathcal{K}(h, \theta) = \alpha_p h(1 - \theta) + \theta \alpha_s, \mathfrak{M} = \mathfrak{m}_r - \mathfrak{m}_i \theta, \tag{42}$$

Note that the water depth is measured along the normal direction to the base flow surface in the case of slity inclined surface the vertical components of the unitary normal to the surface can approximat by, $\nu^3 = 1$ so that the potential of free water surface is given by

$$w = g(z(y^1, y^2) + h). \tag{43}$$

The model (41, 43) is most used model in the practical applications. It preserve the main properties of the full model.

Proposition 4. *The reduce model* (39) *equations of the water flow on vegetated hill is of the hyperbolic type with source terms.*
(a) *The conservative form of it is given by*

$$\begin{aligned} \frac{\partial}{\partial t}\theta h + \partial_a\left(\theta h v^a\right) = &\ \mathfrak{M}, \\ \frac{\partial}{\partial t}\theta h v_a + \partial_b\left(\theta h v_a v^b + \delta_a^b \theta g \frac{h^2}{2}\right) = &\ -hg\partial_a z - g\tfrac{h^2}{2}\partial_a\theta - \mathcal{K}(h,\theta)|v|v_a. \end{aligned} \tag{44}$$

(b) *For any unitary vectors* $\boldsymbol{n} \in \mathbb{R}^2$ *the eginvalues are given by*

$$\lambda_- = v^a n_a - \sqrt{gh}, \lambda_0 = v^a n_a, \lambda_+ = v^a n_a + \sqrt{gh}. \tag{45}$$

Proposition 5. *The system (39) has the properties:*
(a) *it preserve the steady state of a lake*

$$x^3 + h = \text{constant},$$

(b) *there exists a conservative form equation of the energy disipation*

$$\frac{\partial}{\partial t}\theta h\mathcal{E} + \frac{\partial}{\partial y^a}\theta h v^a\left(\mathcal{E} + g_{\text{gravit}}\frac{h}{2}\right) = \left(\left(\mathfrak{M}(-\frac{1}{2}|v|^2 + w\right) - \mathcal{K}|v|^3\right), \tag{46}$$

where

$$\mathcal{E} := \frac{1}{2}|v|^2 + g(x^3 + \frac{h}{2})$$

(c) *Bernoulli law. In a steady state in the absence of the mass source and without friction force the total energy, i.e*

$$\mathcal{E}^{\text{t}} = \frac{1}{2}|v|^2 + gx^3 + p(y,h)$$

is constant along of a current line

$$v^a\partial_a\mathcal{E}^{\text{t}} = 0. \tag{47}$$

The presence of the plants and the exitence of the frictional ineraction between water and soil induce and energetic lost. To put in evidence such phenomenon let us consider a domain Ω whos and let $\boldsymbol{n}$ be the normal unitary to the $\partial\Omega$ outward orientated. One assume that the $\partial\Omega$ consists in an impermeables portion and an exit portion $\partial\Omega = \Gamma_1 \cup \Gamma_2$ $\boldsymbol{n}\cdot\boldsymbol{v} = 0$ on Γ_1 and $\boldsymbol{n}\cdot\boldsymbol{v} > 0$ on the Γ_2, one of the two portion can be a void set.

Proposition 6 (Energy disipation)**.** *Assume that there is no mass production. Then the energy of* Ω *is a deacreasing function whith respect to time*

$$\partial_t \int_\Omega h\beta\theta\mathcal{E}\mathrm{d}x < 0 \tag{48}$$

To prove the assertion one integrates the energy dissipation equation (46)

$$\partial_t \int_\Omega h\beta\theta\mathcal{E}\mathrm{d}x + \int_{\partial\Omega} h\beta\theta\boldsymbol{v}\cdot\boldsymbol{n}\mathcal{E}^t\mathrm{d}s = -\int_\Omega \mathcal{K}|v|^3\mathrm{d}x$$

and and one observes that the second integrals in the left hand side is a positive quantity.

4. APPLICATIONS

We will presents three applications of the SWE-Veg model given by 41, 43. The first application deals with the Riemann problem and the next two applications reffer to the ability of the model to accuratelly predict the real phenomena.

Riemann problem. The Riemann Problem is a central topic in the theory of the hyperbolic systems, [14], [15], [16], . When solvable, the solution of it consists in a superposition of shock and rarefaction waves. This very special solutions can be used to define a class of numerical schemes, Riemann solver: [18], [19], [22], [24].

In the case of the SWE-Veg model a shock wave solution is defined as a measure solution that satisfies certain requirements, [20], [23], [9]. The Riemann solver is still composed by picewise smooth solutions, but this time the solver include a new steady shock wave located at the point discontinuity of the soil or porosity function [25], [26].

The Riemann problem for the shallow water equations with topography and vegetation consists in finding a solution in the class of functions with bounded variation for the equations 41 with the following initial conditions:

$$(h,u,z,\theta) = \begin{cases} (h^L,u^L,z^L,\theta^L) & x<0, \\ (h^R,u^R,z^R,\theta^R) & x>0 \end{cases} \tag{49}$$

In the papper [26] was proved that Riemann problem is locally solvable. In the figures (2), (3 and (4) we illustrate the solution of the RP for different initial data. All pictures contain the h profiles at the moment of time $t = 0.7s$. In all cases illustrate here the solutions include rarefaction wave, that propagate to the left and a shock wave that propagate to the right. If the data terrain

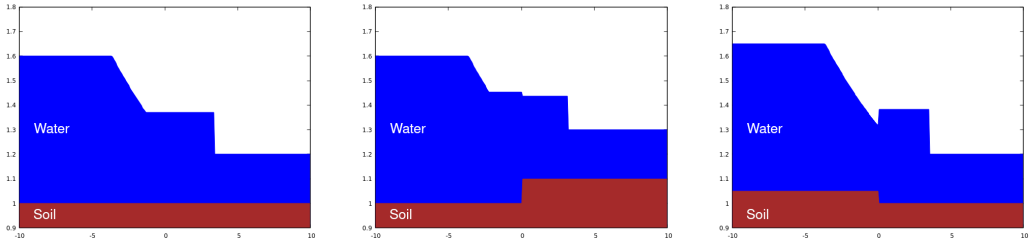

(a) (b) (c)

Fig. 2. Solutions of Riemann Probelm: $(u^L, \theta^L) = (u^R, \theta^R)$; (a) $(h^L, z^L) = (0.6, 1), (h^R, z^R) = (0.2, 1)$; (b) $(h^L, z^L) = (0.6, 1), (h^R, z^R) = (0.2, 1.1)$; (c) $(h^L, z^L) = (0.6, 1.05), (h^R, z^R) = (0.2, 1)$.

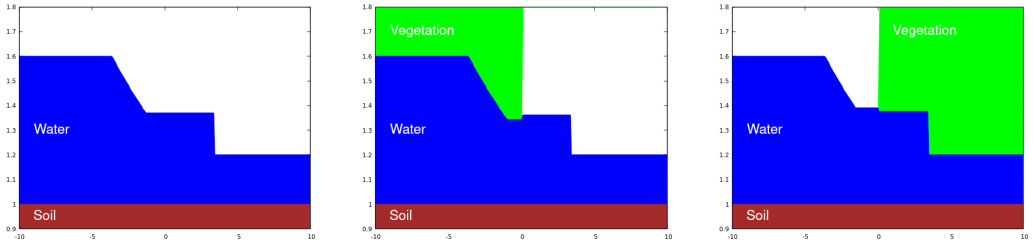

(a) (b) (c)

Fig. 3. Solutions of Riemann Probelm: $(u^L, z^L) = (u^R, z^R)$; (a) $(h^L, \theta^L) = (0.6, 1), (h^R, \theta^R) = (0.2, 1)$; (b) $(h^L, \theta^L) = (0.6, 0.9), (h^R, \theta^R) = (0.2, 1)$; (c) $(h^L, \theta^L) = (0.6, 1), (h^R, \theta^R) = (0.2, 0.9)$.

present a jump then a new shock wave is generated that is located at the discontiuity point, $x = 0$.

The global solvability of the Riemann problem for SWE-veg equations is an open problem. The problem was discused in the paper [26].

Comparision of the model prediction with the experimental data. Generally speaking, a mathematical model is a metaphor of the reality that it refers. He cannot quantify all the state variables but only a part of them, the variables that dominate and control the evolution or state of the system. With necessity the model must retain the dominant forces that govern the physical phenomenon and must ignore others that induce small effects in the state of it.

The SWE-Veg models are intended to predict the dynamics of water flow on the soil surface. Apparently this is not so complicated process, but really it is difficult to mathematically model it. The water-plant and water soil

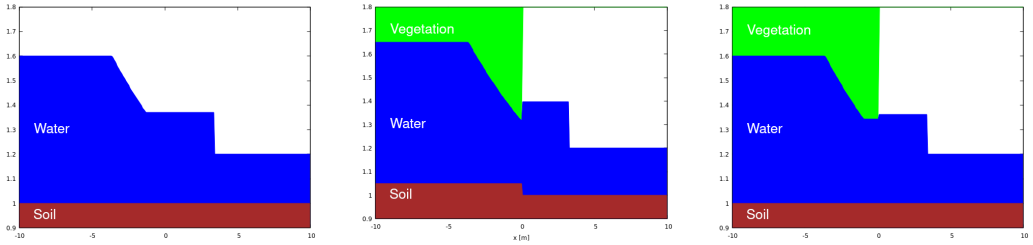

(a) (b) (c)

Fig. 4. Solutions of Riemann Probelm: $u^L = u^R$; (a) $(h^L, z^L, \theta^L) = (0.6, 1, 1), (h^R, z^R, \theta^R) = (0.2, 1, 1)$; (b) $(h^L, z^L, \theta^L) = (0.6, 1., 1), (h^R, z^R, \theta^R) = (0.2, 1.1, 1)$; (c) $(h^L, z^L, \theta^L) = (0.6, 1.05, 1), (h^R, z^R, \theta^R) = (0.2, 0, 1, 1)$.

interactions forces are hardly quantifiables and in certain circumstances new processes can become relevant, erosion and water infiltration, for examples

In spite of this difficulties the SWE-Veg model can predict the evolution of water dynamics variables with a satisfactory accuracy.

The model is versatil enough to cope with a large class of physical processes. By a proper choice of the model parameters α_p and α_s and a proper determination of the porosity function θ and soil altitude function z it can be used to simulate water flow for different, real or imaginary, scenarios.

We will illustrate the model ability to predict main water flow charcteristics by comparing its prediction with some experimental data. All results furnished by the model was obtained by using a numerical scheme exposed in [27].

We consider two experiments, one is the dam break simulation and another one is the water flow on a vegetated slope.

Water flow on vegetated slope

Briefly, the experimental installation consists of an 18m long and 1m width laboratory flume with a longitudinal bottom slope S = 1.05mm/m, see figure (5). = 1.1738. Figure (6) includes the numerical and experimental data for forth different steady configurations. The experimental data are extracted from the graphics The experimental results was reported in [28].

Dam break flow in an L-shaped channel

We consider the CADAM test case of the dam break flow propaga- tion in an impermeable L-shaped channel, [29], [30]. The layout of this experiment and the initial state of the water at rest are presented in Figure (7). The water level in reservoir is $h = 0.53[m]$ and $h = 0$ in the channel. The experimental data for bare soil are for [30]. We simulate the same problem but considering in addition a vegetated channel with $\theta = 0.99$, the numerical and experimental results are given in the figures (8) . One notes the vegetation effect to dammped the water oscilation and to slow down the speed of the propagation of the direct wave, see the data from gauge P4.

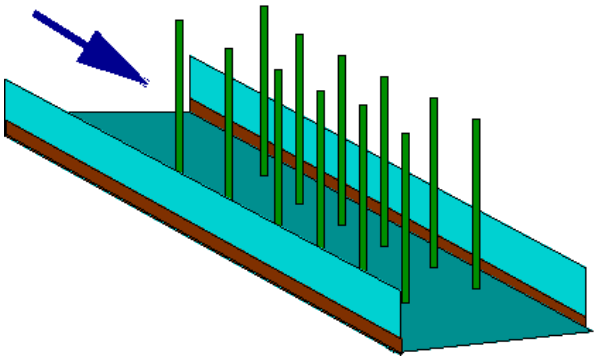

Fig. 5. Experimental instalation for water flow on vegetated slope

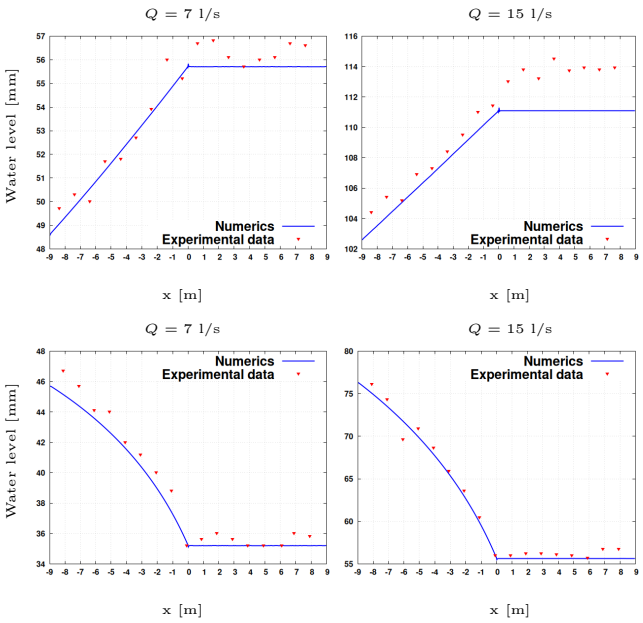

Fig. 6. Flow over a slope with vegetation

5. FINALY REMARKS AND FURTHER RESEARCH

The flow of water is a natural phenomenon that interests everyone. To predict the flow main characteristcs like water depth or water velocity of water coming from rain or generated by the floods is of the great important for hydrogist or agriculters. To predict the flow main characteristics like water depth or water velocity of water coming from rain or generated by the floods is

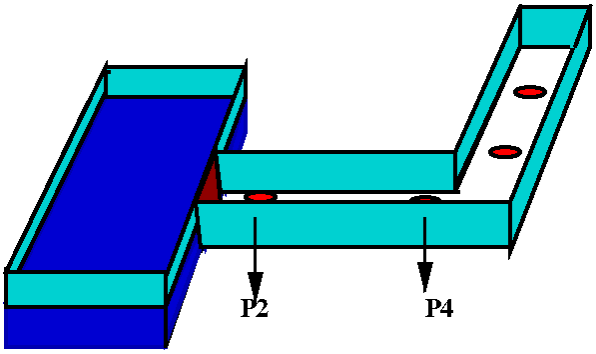

Fig. 7. Experimental instalation for dam break flow

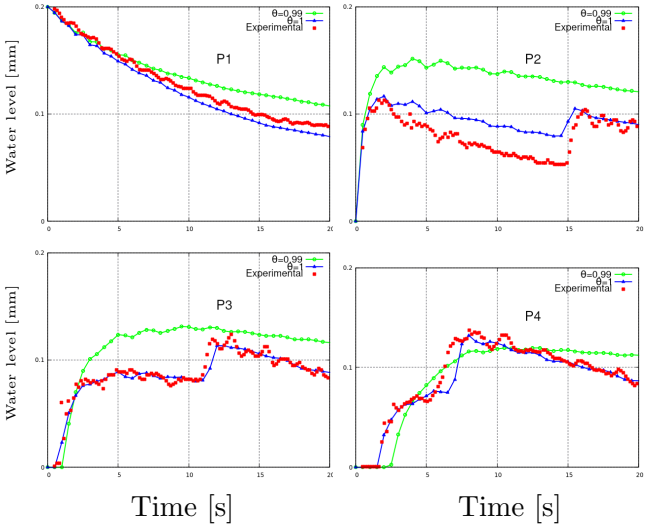

Fig. 8. Dam break flow in L-shaped channel

of the great important for hydrologist, agriculturists or or officials responsable with soil and water management. Given that there are a large variety of geographical context where the water flow is of the interes, there are a plethora of mathematical model used to study it . Some of them are empirical models and some of them are physical processes based models.

Independently of their character, all includes many simplified hypothesis in order to be solvable or to fit to a particular case.

In the paper we has try to show how one can obtain a class of shallow water model equations by using the general continuum mechanical principles.

This mathematical dedudicting way revels what was assumed as important and what was less important and was dropped out from the model. In this

way a person interesed in applications can judge in advance if a simplified version of the model is adequat for a given problem or one must consider a more complicated model.

A comparating study presented in the section Application show thta the simplified model (41), (43) is able to accurate predict the main characteristics of the water flow and it can be used for many application in hydrology or agrucukture.

It is very versatil and it can be relativelly ease programated.

The elements of differential geometry presented in the Annexa faciltate the readers to understend the mathematical tools used in the paper.

We belive that there are two main directions to extend the area of applications of the model: to develope more accurate and more economically, in time and computer memory, numerical schemes and to incorporate the surface curvature effects in the model.

References

[1] M.J. Baptist, V. Babovic, J. Rodriguez Uthurburu, M. Keijzer, R.E. Uittenbogaard, A. Mynett and A. Verwey, *On inducing equations for vegetation resistance*, Journal of Hydraulic Research, **45**(4), pp. 435–450, 2007.

[2] J. Bear, *Dynamics of Fluids in Porous Media*, Dover, 1988.

[3] R.A. Bagnold, *An Approach to the Sediment Transport Problem from General Physics*, Geological Survey Prof. Paper 422-I, Wash., 1966.

[4] L.P. Eisenhart, *An Introduction to Differential Geometry - With the Use of Tensor Calculus*, Kessinger Publishing, 2010.

[5] S.M. Hassanizadeh, W.G. Gray, *Mechanics and thermodynamics of multiphase flow in porous media including interphase boundaries*, Adv. Water Resources, **13**(4), pp. 169–186, 1990.

[6] R.J. Lowe, U. Shavit, J.L. Falter, J.R. Koseff and S.G. Monismith *Modeling flow in coral communities with and without waves: A synthesis of porous media and canopy flow approaches*, Limnol. Oceanogr., **53**(6), pp. 2668–2680, 2008.

[7] I. Müller, *Thermodynamics*, Boston : Pitman, 1985.

[8] H.M. Nepf, *Drag, turbulence, and diffusion in flow through emergent vegetation*, Water Resource Research, **35**(2), pp. 479–489, 1999. Resource Research, **35**(2), pp. 479–489, 1999.

[9] L. Cozzolino, V. Pepe, L. Cimorelli, A. D'Aniello, R. D. Morte, D. Pianese, *The solution of the dam-break problem in the porous shallow water equations*, Advances in Water Resources 114 (2018)

83 – 101. doi:https://doi.org/10.1016/j.advwatres.2018.01.026. URL http://www.sciencedirect.com/science/article/pii/S0309170817306966

[10] Kamel Mohamed, *A finite volume method for numerical simulation of shallow water models with porosity*, Computers&Fluids 104 (2014) 9–19.

[11] L. Cea, M.E. Vázquez-Cendón, *Unstructured finite volume discretisation of bed friction and convective flux in solute transport models linked to the shallow water equations*, Journal of Computational Physics 231 (2012) 3317–3339.

[12] S. Whitaker, *Flow in Porous Media I: A Theoretical Derivation of Darcy's Law*, Transport in Porous Media, **1**, pp. 3–25, 1986.

[13] S.L. Neitsch, J.G. Arnold, J.R. Kiniry, J.R. Williams, *Soil and Water Assessment Tool, Theoretical Documentation*, Texas Water Resources Institute Technical Report No. 406, 2009.

[14] Tai-Ping Liu, *The Deterministic Version of the Glimm Scheme*, Commun. math. Phys. 57, 135—148 (1977).

[15] Glimm, J., *Solutions in the large for nonlinear hyperbolic systems of equations*, Commun. Pure Appl.Math. **18**(1965), 697—-715.

[16] Lax,P.D., *Hyperbolic systems of conservation laws and the mathematical theory of shock waves*, Philadelphia SIAM Regional Conf. Ser. in Appl. Math. **11**(1973)

[17] C. M. Dafermos, *Solution of the Riemann problem for a class of hyperbolic systems of conservation laws by the viscosity method*, Arch. Rational Mech. Anal., **52**, pp. 1–9, 1973.

[18] P. L. Roe. "Approximate Riemann solvers, parameter vectors and difference schemes". Journal of Computational Physics. **43**(2)(1981), 357–372.

[19] Toro, E. F. (1999), *Riemann Solvers and Numerical Methods for Fluid Dynamics*, Springer-Verlag, 1999.

[20] Dal Maso, Gianni and G. LeFloch, Philippe and Murat, François, *Definition and weak stability of nonconservative products*, J. de Math. Pures Appl., **74** (1995), 483-548

[21] David L. George, *Augmented Riemann solvers for the shallow water equations over variable topography with steady states and inundation*, Journal of Computational Physics **227**(2008) 3089–3113.

[22] D. I. Ketcheson, R. J. LeVeque, M. J. del Razo, *Riemann Problems and Jupyter Solutions*, SIAM, 2020.

[23] P. G. LeFloch, M. D. Thanh, *The Riemann problem for the shallow water equations with discontinuous topography*, Commun. Math. Sci. **5**(4) (2007) 865–885.

[24] F. B. Francisco Alcrudo, *Exact solution of the Riemann problem for the shallow water equations with a bottom step*, Computers& Fluids, **30**(2001) 643 – 671.

[25] S. Ion, D. Marinescu, S. G. Cruceanu, *Riemann problem for shallow water equations with vegetation*, An. St. Univ. Ovidius **26** (2) (2018) 83 – 114.

[26] S. Ion, D. Marinescu, S. G. Cruceanu, *Constructive Approach of the Solution of Riemann Problem for Shallow Water Equations with Topography and Vegetation* , An. St. Univ. Ovidius **28** (2) (2020) 145 – 173.

[27] S. Ion, D. Marinescu, S. G. Cruceanu,*Numerical scheme for solving a porous Sain-Venant type model for water flow on vegetated hill slope*, Applied Numerical Mathematics, **172**(2020), 67-98.

[28] V. Dupuis, S. Proust, C. Berni, A. Paquier, *Combined effects of bed friction and emergent cylinder drag in open channel flow*, Environmental Fluid Mechanics **16**(6) (2016) 1173–11

[29] S. Soares Frazao, Y. Zech, *Dam break in a channel with 90*^{1} *bend*, J. Hydraul. Eng., **128**(2002), 956-968.

[30] S. Soares Frazao, X. Sillen and Y. Zech, *Dam break flow through sharp bends-physical model and 2D Boltzman model validation*, CADAM Meeting Wallingford, United Kingdom, March 1998; Belgium, 1999.

[31] V. Guinot, *Multiple porosity shallow water models for macroscopic modelling of urban floods*, Advances in Water Resources 37 (2012) 40 – 72. doi:https://doi.org/10.1016/j.advwatres.2011.11.002.

6. BASICS OF DIFFERENTIAL GEOMETRY IN EUCLIDEAN SPACE

6.1. CURVILINEAR COORDINATE

Let $O\boldsymbol{x}$ be a Cartesian coordinate system in the reference Euclidean space $\mathbb{E}^3$. Let $\{y^I\}_{I=\overline{1,3}}$ be another coordinate system and let

$$x^i = x^i(y^1, y^2, y^3), \quad \boldsymbol{y} \in D \tag{50}$$

be the transformation rule. By coordinate line, one understands the curves generated by the variation of a single variable y^I, while the rest are kept constants. The tangent vectors at the coordinate lines are defined by

$$\boldsymbol{e}_I = \partial_I \boldsymbol{x}. \tag{51}$$

The set of vectors $\{\boldsymbol{e}_I\}_{I=\overline{1,3}}$ give rise to a new base of tensor fields. For the vectors and tensors of rank 2, one writes

$$\boldsymbol{v} = v^I \boldsymbol{e}_I, \quad \mathbf{t} = \mathfrak{t}^{IJ} \boldsymbol{e}_I \boldsymbol{e}_J.$$

In the new coordinate system, the components of the metric tensor $\boldsymbol{g}$ are given by

$$g_{IJ} = \delta_{ij} e_I^i e_J^j \tag{52}$$

and

$$g^{IJ} = \delta^{ij} h_i^I h_j^J, \tag{53}$$

where

$$h_j^I = \partial_j y^I. \tag{54}$$

One has

$$e_I^j h_i^I = \delta_i^j, \quad e_I^j h_j^J = \delta_I^J \tag{55}$$

and then

$$g^{IK} g_{KJ} = \delta_J^I.$$

The volume element is

$$J = \varepsilon_{ijk} e_1^i e_2^j e_3^k, \tag{56}$$

with ε_{ijk} representing the Levi-Civita symbol. From (56) and (52), one obtains

$$\det \boldsymbol{g} = J^2, \tag{57}$$

where $\boldsymbol{g}$ is the matrix with the elements g_{IJ}.

The variation of the basis $\{\boldsymbol{e}_I\}_I$ with respect to the y coordinate is stored inside Christoffel's symbols Γ

$$\partial_I \boldsymbol{e}_J = \Gamma_{IJ}^L \boldsymbol{e}_L. \tag{58}$$

Alternatively, one can calculate the Γ coefficients by

$$\begin{aligned} \Gamma_{IJ}^L &= h_i^L \partial_J e_I^i, \\ \Gamma_{IJ}^L &= -e_I^i e_J^j \partial_i h_j^L, \\ \Gamma_{IJ}^L &= \frac{1}{2} g^{LK} \left(\partial_I g_{KJ} + \partial_J g_{KI} - \partial_K g_{IJ} \right). \end{aligned} \tag{59}$$

The first relation here results from the definition (58) and (55), the second relation results from the first one, and the last relation results from (58) and (52). Define now the covariant derivative of a vector by

$$v_{;L}^I = \partial_L v^I + v^K \Gamma_{LK}^I \tag{60}$$

and the covariant derivative of tensor by

$$t_{;L}^{IJ} = \partial_L t^{IJ} + t^{KJ} \Gamma_{LK}^I + + t^{IK} \Gamma_{LK}^J. \tag{61}$$

An elementary way to introduce the covariant derivative is to estimate the difference of vector fields between two neighbor points

$$\begin{aligned} \boldsymbol{v}(\boldsymbol{y} + \triangle \boldsymbol{y}) - \boldsymbol{v}(\boldsymbol{y}) =& v^I(\boldsymbol{y} + \triangle \boldsymbol{y}) \boldsymbol{e}_I(\boldsymbol{y})(\boldsymbol{y} + \triangle \boldsymbol{y}) - v^I \boldsymbol{e}_I(\boldsymbol{y}) \\ =& \left(\partial_L v^I(\boldsymbol{y}) + v^K(\boldsymbol{y}) \Gamma_{LK}^I(\boldsymbol{y}) \right) \boldsymbol{e}_I(\boldsymbol{y}) \triangle y^L + O(\triangle \boldsymbol{y}^2). \end{aligned}$$

6.2. BASIC NOTIONS OF DIFFERENTIAL GEOMETRY ON A SURFACE IN $\mathbb{E}^3$

For completeness, we present here the essential facts about the differential geometry of the surface in the euclidean space E^3; as a reference, one can consult the classical books [4]. Let $O\boldsymbol{x}$ be a Cartesian coordinate system in the reference Euclidean space $\mathbb{E}^3$. Let $\mathcal{S}$ be a surface in E^3 and let

$$x^i = b^i(y^1, y^2), \quad (y^1, y^2) \in D \in \mathbb{R}^2 \tag{62}$$

be a parameterization of $\mathcal{S}$. One defines the tangent vectors to the surface by

$$\tau_a^i = \frac{\partial b^i}{\partial y^a} \tag{63}$$

and the oriented normal direction to the surface by

$$\mathcal{N}_i = \varepsilon_{j\,k\,i}\tau_1^j\tau_2^k. \tag{64}$$

The unitary normal $\boldsymbol{\nu}$ to the surface is given by

$$\nu_i = \frac{\mathcal{N}_i}{||\boldsymbol{\mathcal{N}}||}. \tag{65}$$

Metric tensor $\boldsymbol{\beta}$ of the surface. The covariant components of $\boldsymbol{\beta}$ are given by

$$\beta_{ab} = \delta_{ij}\tau_a^i\tau_b^j \tag{66}$$

and the contravariant components β^{ab} of it are defined by the relations

$$\delta_b^a = \beta^{ac}\beta_{cb} = \beta_{bc}\beta^{ca}. \tag{67}$$

The area element of the surface is defined by

$$\mathrm{d}\sigma(y) = \beta(y)\mathrm{d}y^1\mathrm{d}y^2, \tag{68}$$

where

$$\beta = \sqrt{\varepsilon^{ab}\beta_{a1}\beta_{b2}}, \tag{69}$$

with ε^{ab} being the Levi-Civita symbol.

Note that

$$||\boldsymbol{\mathcal{N}}|| = \beta.$$

The curvature tensor $\boldsymbol{\kappa}$. The curvature tensor κ and the affine connection γ can be defined by the Gauss-Wiengarten equations

$$\begin{aligned} &\frac{\partial \boldsymbol{\tau}_a}{\partial y^b} = \gamma_{a\,b}^c\boldsymbol{\tau}_c + \kappa_{a\,b}\boldsymbol{\nu}, \quad \text{(Gauss)} \\ &\frac{\partial \boldsymbol{\nu}}{\partial y^a} = -\kappa_a^b\boldsymbol{\tau}_b. \qquad\qquad (Wiengarten) \end{aligned} \tag{70}$$

6.3. SURFACE BASED CURVILINEAR COORDINATE SYSTEM

A surface $\mathcal{S}$ based coordinate system in the space $\mathbb{E}^3$ is introduced as follows. Given a parameterization (62) of the surface, one defines the applications

$$x^i = b^i(y^1, y^2) + y^3\nu^i, \quad (y^1, y^2) \in \widetilde{D} \subset \mathbb{R}^2, \quad y^3 \in \widetilde{I} \in \mathbb{R}, \tag{71}$$

where $\widetilde{I}$ is an open neighborhood of zero. Assume that (71) defines a coordinate transformation from $\widetilde{D} \times \widetilde{I}$ to a space neighborhood Ω of the surface $\mathcal{S}$. The surface $\mathcal{S}$ in the new coordinate system is given by $y^3 = 0$. Furthermore, we have:

• the tangent vectors to the coordinate lines

$$\boldsymbol{e}_I = \frac{\partial \boldsymbol{x}}{\partial y^I} \Longrightarrow \left\{ \begin{array}{l} \boldsymbol{e}_a = q_a^b \boldsymbol{\tau}_b, \quad q_a^b := \delta_a^b - y^3\kappa_a^b, \quad a = \overline{1,2} \\ \boldsymbol{e}_3 = \boldsymbol{\nu} \end{array} \right. ; \tag{72}$$

• the coefficients of the metric tensor

$$g_{IJ} = \delta_{ij} e_I^i e_J^j \Longrightarrow \left\{ \begin{array}{ll} g_{ab} = q_a^c q_b^d \beta_{cd}, & g_{a3} = 0, \\ g_{3a} = 0, & g_{33} = 1, \end{array} \right. \tag{73}$$

with

$$\sqrt{\det \boldsymbol{g}} = \beta\Delta, \quad \Delta := 1 - 2y^3 K_M + (y^3)^2 K_G, \tag{74}$$

where $K_M = 1/2\kappa_a^a$ and $K_G = \epsilon_{a,b}\kappa_1^a\kappa_2^b$ are the mean curvature and the Gauss curvature of the surface, respectively; • the affine connection

$$\frac{\partial \boldsymbol{e}_I}{\partial y^J} = \Gamma_{IJ}^L \boldsymbol{e}_L \Longrightarrow \left\{ \begin{array}{ll} \Gamma_{ab}^c = \left(\gamma_{ab}^d - y^3\left(\partial_a\kappa_b^d + \kappa_b^f\gamma_{af}^d\right)\right) Q_d^c, & \Gamma_{a3}^c = -\kappa_a^e Q_e^c, \\ \Gamma_{ab}^3 = (\delta_a^c - y^3\kappa_a^c)\kappa_{cb}, & \Gamma_{a3}^3 = 0, \end{array} \right. \tag{75}$$

where Q is defined by

$$\boldsymbol{\tau}_a = Q_a^b \boldsymbol{e}_b \Longrightarrow \left\{ \begin{array}{ll} Q_1^1 = \dfrac{1 - y^3\kappa_2^2}{\Delta(y)}, & Q_1^2 = \dfrac{y^3\kappa_1^2}{\Delta(y)}, \\ Q_2^1 = \dfrac{y^3\kappa_2^1}{\Delta(y)}, & Q_2^2 = \dfrac{1 - y^3\kappa_1^1}{\Delta(y)}. \end{array} \right. \tag{76}$$

Obs. For any $y^3 \in I$, the tangent vectors $\boldsymbol{e}_a$, $a = \overline{1,2}$ belong to the tangent plane at the surface $y^3 = \text{const}$ and they are orthogonal to the normal $\boldsymbol{e}_3 = \boldsymbol{\nu}$. In the new coordinate system, the volume element is $\vartheta(y)\mathrm{d}y^1\mathrm{d}y^2\mathrm{d}y^3$, where

$$\vartheta(y) = \epsilon_{i\,j\,k} e_1^i e_2^j e_3^k = \sqrt{\det \boldsymbol{g}} = \left(1 - 2y^3 K_M + (y^3)^2 K_G\right)\beta. \tag{77}$$

6.4. INTEGRALS OF VECTORS AND SECOND ORDER TENSORS

Let V be a domain in $\mathbb{E}^3$ defined by

$$\boldsymbol{x} = \boldsymbol{b}(y^1, y^2) + y^3 \boldsymbol{\nu}, \quad (y^1, y^2) \in D, \quad u(y^1, y^2) < y^3 < w(y^1, y^2)$$

where D is a open closed domain with boundary ∂D, $u(y^1, y^2)$ and $w(y^1, y^2)$ are two functions that define some surfaces in $\mathbb{E}^3$. We are interested in calculating the flux of vectors or tensors through the boundary of V, to evaluate integral of vectors in V or to calculate integrals of vectors on surfaces. In $\mathbb{E}^3$, such integrals define global quantities of the same type with the integrands: scalars define scalars, vectors define vectors and second order tensors define second order tensors. If one uses curvilinear coordinates, such invariant properties are lost for vectors and tensors.

Let $\mathcal{S}$ and V be a surface and a domain in $\mathbb{E}^3$, respectively. Define the flux of $\boldsymbol{f}$ and $\boldsymbol{\Phi}$ through a surface by

$$\mathcal{F}_{\boldsymbol{f}}(S) := \int\limits_S f^i \, n_i \mathrm{d}\sigma,$$
$$\mathcal{F}^i_{\boldsymbol{\Phi}}(S) := \int\limits_S \Phi^{ij} \, n_j \mathrm{d}\sigma,$$

where $\boldsymbol{n}$ stands for outward oriented unitary normal to the surface.

Define by components the integral of a vector field $\boldsymbol{f}$ on V

$$\mathcal{I}^j_{\boldsymbol{f}}(V) := \int\limits_V f^j \mathrm{d}x$$

and the integral on the surface S

$$\mathcal{I}^j_{\boldsymbol{f}}(S) := \int\limits_S f^j \mathrm{d}\sigma.$$

Let $\mathcal{S}_r$ be the surface defined by some function $r(y^1, y^2)$

$$\boldsymbol{x} = \boldsymbol{b}(y^1, y^2) + r(y^1, y^2)\boldsymbol{\nu}, \quad (y^1, y^2) \in D.$$

One denotes the "vertical" boundary of V by

$$\begin{aligned} \Sigma = \{ \boldsymbol{x} \in \mathbb{E}^3 | \boldsymbol{x} = \boldsymbol{b}(y^1(s), y^2(s)) + y^3 \boldsymbol{\nu}(y^1(s), y^2(s)), \\ s \in (0, L), \ u(y^1(s), y^2(s)) < y^3 < w(y^1(s), y^2(s)) \} \end{aligned} \tag{78}$$

where $\big(y^1(s), y^2(s)\big)$, $s \in (0, L)$ is a parameterization of ∂D.

Let $\boldsymbol{f}$ and $\boldsymbol{\Phi}$ be a vector field and a second order tensor field in $\mathbb{E}^3$, respectively. Using the law of transformation of the coordinate system of a tensor field under coordinate transformation, one can write

$$f^i = f^I e^i_I, \quad \Phi^{ij} = e^i_I e^j_J \Phi^{IJ}.$$

Next lemma refers to various integrals.

Lemma 7. *Let $\boldsymbol{f}$ and $\boldsymbol{\Phi}$ be some smooth fields on a domain $\Omega \subset \mathbb{E}^3$. Let S_r, V and Σ be a surface, domain and portion of ∂V, respectively, as previously defined. Then:*

$$\begin{aligned}
\mathcal{I}^i_f(V) &= \iint\limits_D \left(\tau^i_a \int\limits_u^w q^a_b f^b \vartheta \mathrm{d}y^3 + \nu^i \int\limits_u^w f^3 \vartheta \mathrm{d}y^3 \right) \mathrm{d}y^1 \mathrm{d}y^2, \\
\mathcal{F}_f(S_r) &= \iint\limits_D \vartheta(y) \left(f^3 - f^a \frac{\partial r}{\partial y^a} \right) \Big|_{y^3=r} \mathrm{d}y^1 \mathrm{d}y^2, \\
\mathcal{F}_f(\Sigma) &= \iint\limits_D \frac{\partial r}{\partial y^a} \int\limits_u^w \vartheta f^a \mathrm{d}y^3 \mathrm{d}y^1 \mathrm{d}y^2, \\
\mathcal{F}^i_\Phi(S_r) &= \iint\limits_D \left[\left(\tau^i_c q^c_b \left(\Phi^{b3} - \frac{\partial r}{\partial y^a} \Phi^{ba} \right) \right. \right. \\
&\quad \left. \left. + \nu^i \left(\Phi^{33} - \frac{\partial r}{\partial y^a} \Phi^{3a} \right) \right) \vartheta(y) \right] \Big|_{y^3=r} \mathrm{d}y^1 \mathrm{d}y^2, \qquad (79) \\
\mathcal{F}^i_\Phi(\Sigma) &= \iint\limits_D \tau^i_c \left(\frac{\partial}{\partial y^a} \int\limits_u^w q^c_b \vartheta(y) \Phi^{ba} \mathrm{d}y^3 \right. \\
&\quad \left. + \gamma^c_{ae} \int\limits_u^w q^e_b \vartheta(y) \Phi^{ba} \mathrm{d}y^3 - \kappa^c_a \int\limits_u^w \vartheta(y) \Phi^{3a} \mathrm{d}y^3 \right) \mathrm{d}y^1 \mathrm{d}y^2 \\
&\quad + \iint\limits_D \nu^i \left(\kappa_{ca} \int\limits_u^w q^c_b \vartheta(y) \Phi^{ba} \mathrm{d}y^3 \right. \\
&\quad \left. + \frac{\partial}{\partial y^a} \int\limits_u^w \vartheta(y) \Phi^{3a} \mathrm{d}y^3 \right) \mathrm{d}y^1 \mathrm{d}y^2.
\end{aligned}$$

Proof. Let $(y^1(s), y^2(s))$, $s \in (0, L)$ be a parameterization of the boundary ∂D. On Σ, the tangent directions are given by

$$\begin{aligned} \boldsymbol{t}_s &= \boldsymbol{e}_a w^a, \\ \boldsymbol{e}_3 &= \boldsymbol{\nu}, \end{aligned}$$

where $w^a = \dfrac{\mathrm{d}y^a}{\mathrm{d}s}$ and the outward normal direction is given by

$$N_i := \epsilon_{jki} e_3^j t_s^k = \epsilon_{jki} \nu^j e_a^k w^a.$$

Thus, one can evaluate the flux as

$$\mathcal{F}_f(\Sigma) := \int_\Sigma f^i n_i \mathrm{d}\sigma = \int_0^L \int_{\widetilde{u}(s)}^{\widetilde{w}(s)} f^i N_i \mathrm{d}y^3 \mathrm{d}s,$$

with $\widetilde{w}(s) = w(y^1(s), y^2(s))$, $\widetilde{u}(s) = u(y^1(s), y^2(s))$. Then, one writes $\boldsymbol{f}$ in the local basis $\{\boldsymbol{e}_1, \boldsymbol{e}_2, \boldsymbol{e}_3\}$ and obtains

$$f^i N_i = (f^b e_b^i + f^3 \nu^i) N_i = \epsilon_{jki} \nu^j e_a^k e_b^i w^a f^b = \vartheta(y) \epsilon_{ab} w^a f^b$$

and

$$\mathcal{F}_f(\Sigma) = \int_0^L \int_{\widetilde{u}(s)}^{\widetilde{w}(s)} \vartheta(y) \epsilon_{ab} w^a f^b \mathrm{d}y^3 \mathrm{d}s = \int_0^L \epsilon_{ab} w^a \int_{\widetilde{u}(s)}^{\widetilde{w}(s)} \vartheta(y) f^b \mathrm{d}y^3 \mathrm{d}s.$$

Observe that $\epsilon_{ab} w^a = \epsilon_{ab} \dfrac{\partial y^a}{\partial s}$ is the normal direction to the boundary ∂D and use the flux-divergence theorem and to obtain

$$\mathcal{F}_f(\Sigma) = \iint_D \frac{\partial}{\partial y^a} \int_{u(y^1, y^2)}^{w(y^1, y^2)} \vartheta(y) f^a \mathrm{d}y^3 \mathrm{d}y^1 \mathrm{d}y^2. \tag{80}$$

On S_r, one has the tangent vectors

$$\boldsymbol{\zeta}_a = \frac{\partial \boldsymbol{x}}{\partial y^a} = \boldsymbol{e}_a + \frac{\partial r}{\partial y^a} \boldsymbol{\nu} \tag{81}$$

and normal direction

$$N_i = \epsilon_{jki} \left(e_1^j + \frac{\partial r}{\partial y^1} \nu^j \right) \left(e_2^k + \frac{\partial r}{\partial y^2} \nu^k \right). \tag{82}$$

Then, we obtain

$$f^i N_i = \vartheta(y)\left(f^3 - \frac{\partial r}{\partial y^a} f^a\right).$$

Consequently,

$$\mathcal{F}_f(S_r) = \iint\limits_D \vartheta(y)\left(f^3 - \frac{\partial r}{\partial y^a} f^a\right)\Big|_{y^3=r} \mathrm{d}y^1\mathrm{d}y^2. \tag{83}$$

Consider now a second order tensor Φ. The coordinate transformation (71) implies that the contravariant components of the tensor in the two coordinate system are related by

$$\Phi^{ij} = e^i_I e^j_J \Phi^{IJ}.$$

The main difficulty in this case is that the vectors of the basis depend on the variables (y^1, y^2, y^3) and there is no sense to find the components of the global vector quantity $\mathcal{F}_\Phi$ in the new system of coordinates. We proceed to find the Cartesian components of $\mathcal{F}_\Phi$, but calculated as functions of the contravariant components Φ^{IJ}.

On the surface Σ, one has

$$\Phi^{ij} N_j = e^i_I e^j_J \Phi^{IJ} N_j = \vartheta(y)\epsilon_{ab} w^a e^i_I \Phi^{Ib}$$

and the flux is given by

$$\mathcal{F}^i_\Phi(\Sigma) = \iint\limits_D \frac{\partial}{\partial y^a} \int\limits_u^w \vartheta(y) e^i_I \Phi^{Ia} \mathrm{d}y^3 \mathrm{d}y^1 \mathrm{d}y^2.$$

Using the relations (72) we get

$$\mathcal{F}^i_\Phi(\Sigma) = \iint\limits_D \frac{\partial}{\partial y^a}\left(\tau^i_c \int\limits_u^w q^c_b \vartheta(y)\Phi^{ba}\mathrm{d}y^3 + \nu^i \int\limits_u^w \vartheta(y)\Phi^{3a}\mathrm{d}y^3\right)\mathrm{d}y^1\mathrm{d}y^2.$$

Applying Weigartern formula, we can write

$$\begin{aligned}\mathcal{F}^i_\Phi(\Sigma) = &\iint\limits_D \left(\tau^i_c \frac{\partial}{\partial y^a}\int\limits_u^w q^c_b \vartheta(y)\Phi^{ba}\mathrm{d}y^3 + \nu^i \frac{\partial}{\partial y^a}\int\limits_u^w \vartheta(y)\Phi^{3a}\mathrm{d}y^3\right)\mathrm{d}y^1\mathrm{d}y^2\\ &+ \iint\limits_D \tau^i_c \left(\gamma^c_{ae}\int\limits_u^w q^e_b \vartheta(y)\Phi^{ba}\mathrm{d}y^3 - \kappa^c_a \int\limits_u^w \vartheta(y)\Phi^{3a}\mathrm{d}y^3\right)\mathrm{d}y^1\mathrm{d}y^2\\ &+ \iint\limits_D \nu^i \kappa_{ea}\int\limits_u^w q^e_b \vartheta(y)\Phi^{ba}\mathrm{d}y^3\mathrm{d}y^1\mathrm{d}y^2.\end{aligned}$$

Regrouping the terms, we obtain the result for $\mathcal{F}^i_{\Phi}(\Sigma)$.

Lemma 8. *Consider that the stress tensor of the fluid has the following form*

$$t^{ij} = -p\delta^{ij} + \tau^{ij}$$

and set

$$\mathcal{F}^i_{\text{stress}}(S_r) = \iint\limits_{S_r} t^{ij} n_j \mathrm{d}\sigma.$$

Then

$$\begin{aligned}\mathcal{F}^i_{\text{stress}}(S_r) = \iint\limits_D \Bigg[\tau^i_d q^d_a \Bigg((p - \widetilde{\tau}^{33}) g^{ab} \frac{\partial r}{\partial y^b} \\ + \widetilde{\tau}^{a3} \sqrt{1 + g^{bc} \frac{\partial r}{\partial y^b} \frac{\partial r}{\partial y^c}}\Bigg) \vartheta(y)\Bigg]\Bigg|_{y^3 = r(y^1, y^2)} \mathrm{d}y^1 \mathrm{d}y^2 \\ + \iint\limits_D \Bigg[\nu^i \Bigg(-p + \widetilde{\tau}^{33} + \frac{\partial r}{\partial y^a} \widetilde{\tau}^{a3} \\ \cdot \sqrt{1 + g^{bc} \frac{\partial r}{\partial y^b} \frac{\partial r}{\partial y^c}}\Bigg) \vartheta(y)\Bigg]\Bigg|_{y^3 = r(y^1, y^2)} \mathrm{d}y^1 \mathrm{d}y^2.\end{aligned} \tag{84}$$

In this lemma, $\widetilde{\tau}^{IJ}$ denotes the contravariant components of the viscous stress tensor in the frame given by the tangent vectors to the surface $y^3 = r(y^1, y^2)$ and the unit normal to the tangent plan (which points to the same direction as the unit normal $\boldsymbol{\nu}$ to the support surface).

Proof. Let $r(y^1, y^2)$ be a parameterization of the surface S_r and let $\boldsymbol{\zeta}_1$, $\boldsymbol{\zeta}_2$ and $\boldsymbol{n}$ be the tangent vectors and the unit normal given by (81) and (82), respectively. One can write

$$t^{ij} n_j = -pn^i + \tau^{ij} n_j = -pn^i + \widetilde{\tau}^{a3} \zeta^i_a + \widetilde{\tau}^{33} n^i. \tag{85}$$

Using the basis $\{\boldsymbol{e}_I\}$, the unit normal has the form

$$\begin{aligned}\boldsymbol{n} = n^a \boldsymbol{e}_a + n^3 \boldsymbol{\nu}, \quad n^a = -g^{ab} \frac{\partial r}{\partial y^b} \frac{\vartheta(y)}{||\boldsymbol{N}||}, \quad n^3 = \frac{\vartheta(y)}{||\boldsymbol{N}||}, \\ ||\boldsymbol{N}|| = \vartheta(y) \sqrt{1 + g^{ab} \frac{\partial r}{\partial y^a} \frac{\partial r}{\partial y^b}}, \quad y^3 = r(y^1, y^2)\end{aligned}$$

and the tangent vectors are expressed by

$$\boldsymbol{\zeta}_a = \boldsymbol{e}_a + \frac{\partial r}{\partial y^a} \boldsymbol{n}\boldsymbol{u}.$$

Since the area element is given by

$$\mathrm{d}\sigma = ||\boldsymbol{N}||\mathrm{d}y^1\mathrm{d}y^2,$$

then, we immediately obtain the conclusion of this lemma.

ROMAI J., v.19, no.1(2023), 107–112

ON SOME NEW UNIFORM ESTIMATES AND MAXIMAL THEOREMS FOR H^{P} SPACES

Romi F. Shamoyan

Department of Mathematics, Bryansk State Technical University, Bryansk, Russia

rsham@mail.ru

Abstract We obtain some new uniform estimates and maximal theorems in classical Hardy spaces in the unit disk related with Bergman projection extending some previously well-known inequalities for Hardy spaces.

Keywords: Bergman projection, Hardy spaces, unit disk, maximal theorems, uniform estimates.

2020 MSC: 32, 46.

1. INTRODUCTION

Let further $U = \{z \in \mathbb{C}, |z| < 1\}$, be the unit disk on a complex plane $\mathbb{C}$, T be the unit circle on $\mathbb{C}$, let dm_2 be the normalized Lebegues measure on $\mathbb{C}$, let futher U^n be the unit polydisk on $\mathbb{C} \times ... \times \mathbb{C}$.

And finnaly let H^p be the classical analytic Hardy class in the unit disk for all positive values of p, let $dm(\xi)$ be the normalized Lebegues measure on T. The goal of this short paper is to extend certain classical estimates of complex function theory, in the unit disk to several variables extending certain known one dimensional results to several variables using the so-called expanded Bergman projection which was recently studied in papers of the author.

The expanded Bergman projection for any analytic function in the unit disk we define as follows (see [5])

$$(T_{n,\alpha} f)(w) = C(n,\alpha) \int_U \frac{f(z)(1-|z|)^\alpha}{\prod_{k=1}^{n} (1 - \langle \bar{z}, w_k \rangle)^{\frac{\alpha+2}{n}}} dm_2(z), \quad \alpha > -1,$$

where $w = (w_1, \ldots, w_n) \in U^n, C(n,\alpha)$ is a Bergman constant from Bergman representation formula, is playing a crucial role during the study of diagonal map (see [2], [3], [5], [7] and references there).

We will now provide new estimates for this operator using, in particular, Stein type maximal functions from [6]. We at the same time extend previously known estimates.

In this paper we as usual denote by $\mathcal{D}^\alpha$ for any positive α the fractional derivative of analytic f function in the unit disk,

$$\mathcal{D}^\alpha f(z) = \sum_{k=0}^{\infty} (k+1)^\alpha a_k z^k,$$

for any analytic function f, $f(z) = \sum\limits_{k=0}^{\infty} a_k z^k$ (see [5]).

2. MAIN RESULT

The following theorem is the main result of this note.

Theorem 2.1. *(a) Let* $\Gamma_\gamma(\xi) = \left\{ z \in U : \left|1 - \bar{\xi} z\right| < \gamma(1 - |z|) \right\}, \gamma > 1, \xi \in T.$ *Let* $\beta \in (0, \frac{1}{2}), \alpha > \beta, n = 2.$ *Then*

$$\int_T \left(\sup_{z_1 \in \Gamma_\gamma(\xi)} \sup_{z_2 \in \Gamma_\gamma(\xi)} \left| \mathcal{D}^\alpha_{z_2} T_{n,0}(f)(z_1, z_2) \right| (1 - |z_1|)^{\alpha - \beta} (1 - |z_2|)^\beta dm(\xi) \right)^2 \leqslant C \left\| f \right\|^2_{H^2(U)}.$$

(b) Let $p > 2, \frac{1}{p} + \frac{1}{q} = 1, t \in (-2, -1), \alpha > \max(t + \frac{2}{q}, 0), n = 2.$ *Then*

$$\sup_{z_1, z_2 \in U} |T_{n,\alpha} f(z_1, z_2)| (1 - |z_1|)^{t+2} (1 - |z_2|)^{\frac{\alpha - t}{2} - \frac{1}{q}}$$
$$\leq C \left(\int_T \sup_{z \in \Gamma_\gamma(\xi)} |f(z)| (1 - |z|)^{\frac{\alpha}{2}} \right)^p dm(\xi).$$

Proof. Let $T_{2,0}(f) = \Phi(z_1, z_2)$. Then using Hölder's inequality we obtain

$$|\Phi(z_1, z_2)| \leq C \int_U \frac{|f(w)|}{|1 - \langle \bar{w}, z_1 \rangle| \, |1 - \langle \bar{w}, z_2 \rangle|} dm_2(w)$$
$$\leq C \left(\int_U \frac{|f(w)|^2 (1 - |w|)^{2\beta}}{|1 - \langle \bar{w}, z_1 \rangle|^2} dm_2(w) \right)^{\frac{1}{2}} \left(\int_U \frac{(1 - |w|)^{-2\beta}}{|1 - \langle \bar{w}, z_2 \rangle|^2} dm_2(w) \right)^{\frac{1}{2}}.$$

Hence since $\beta \in (0, \frac{1}{2})$ and $\alpha > \beta$,

$$\left| \mathcal{D}^\alpha_{z_2} \Phi(z_1, z_2) \right| \leq C \left(\int_U \frac{|f(w)|^2 (1 - |w|)^{-2\beta}}{|1 - \langle \bar{w}, z_1 \rangle|^2} dm_2(w) \right)^{\frac{1}{2}} \left(\int_U \frac{(1 - |w|)^{2\beta}}{|1 - \langle \bar{w}, z_2 \rangle|^{2+2\alpha}} dm_2(w) \right)^{\frac{1}{2}},$$

and we have

$$\sup_{z_1, z_2 \in \Gamma_\gamma(\xi)} \left| \mathcal{D}^\alpha_{z_2} \Phi(z_1, z_2) \right| (1 - |z_2|^{\alpha - \beta})(1 - |z_1|^\beta)$$
$$\leq C \sup_{z_1 \in \Gamma_\gamma(\xi)} \left(\int_U \frac{|f(w)|^2 (1 - |w|)^{-2\beta}}{|1 - \langle \bar{w}, z_1 \rangle|^2} dm_2(w) (1 - |z_1|)^{2\beta} \right)^{\frac{1}{2}} = G_1(f), \text{ (see[4])}.$$

Note that

$$(\left|1-\left\langle |\lambda|\,\bar{\xi},z\right\rangle\right|) \asymp (\left|1-\left\langle \bar{\lambda},z\right\rangle\right|),\ \ z\in U, \lambda\in\Gamma_\beta(\xi).$$

Hence

$$G_1(f)(\xi)\le C\sup_{0<r<1}\left(\int_U \frac{(1-|z|)^{-2\beta}\,|f(z)|^2\,(1-r)^{2\beta}}{\left|1-\left\langle r\bar{\xi},z\right\rangle\right|^2}dm_2(z)\right)^{\frac{1}{2}}=\widetilde{G_1}(f,\xi,\beta).$$

Obviously for $\gamma\in(1,2-2\beta), \beta\in(0,\frac{1}{2})$,

$$\widetilde{G_1}(f,\xi,\beta)\le C\sup_{0<r<1}\left(\int_T \frac{(1-r)^{\gamma-1}\,|f(r\xi)|^2}{|1-\langle r\xi,\varphi\rangle|^{\gamma}}dm(\xi)\right)^{\frac{1}{2}}.$$

Hence it is enough to use estimates for Stein-type maximal functions [6]

$$\left\|\sup_{0<r<1}\left(\int_T \frac{(1-r)^{\alpha-1}\,|f(r\varphi)|^p}{|1-\langle r\bar{\varphi},\xi\rangle|^{\alpha}}d(\varphi)\right)^{\frac{1}{p}}\right\|_{L^p}\le C\,\|f\|_{H^p},$$

$f\in H^p,\ p>1,\ \beta\in(0,\frac{1}{p}),\ \alpha\in(1,2-\beta p)$ to get what we need. So the proof of first estimate is complete.

Let us prove the second estimate. First, we have the following chain of known estimates (see for example [4]).

$$\int_U d\mu(z)\le C\int_T\int_{\Gamma_t(\xi)}\frac{d\mu(z)}{1-|z|}dm(\xi), \tag{1}$$

$$\int_T |M_{H-L}f(\xi)|^p\,d\xi\le C\int_T |f(\xi)|^p\,d\xi,\ p>1, \tag{2}$$

where M_{H-L} is a classical maximal Hardy-Littlewood operator.

$$\int_U |f(z)|^{\widetilde{p}}\,dm_2(z)\le C\int_T\left(\sup_{z\in\Gamma_\gamma(\xi)}|f(z)|\right)^{\widetilde{p}}C(\mu)(\xi)d\xi, \tag{3}$$

where μ is a positive Borel measure, $0<\widetilde{p}<\infty$, f is measurable in U and as usual $C(\mu)(\xi)=\sup\limits_{\xi\in I}\frac{1}{|I|}\int_{\triangle I}d\mu(\xi), \triangle I=\{z=r\xi,\xi\in I, 1-|z|<r<1\}, I\subset T$.
Using (1) we have

$$|\Phi(z_1,z_2)|\le C(\alpha)\int_U\frac{|f(w)|\,(1-|w|^{\alpha})}{(1-\langle z_1,\bar{w}\rangle)^{\frac{\alpha+2}{2}}(1-\langle z_2,\bar{w}\rangle)^{\frac{\alpha+2}{2}}}dm_2(w),$$

where $z_1, z_2 \in U$ and $C(\alpha)$ is a Bergman projection constant. Further using (1) and applying twice Hölder's inequality we get

$$|\Phi(z_1,z_2)| \le C \left(\int_T \left(\int_{\Gamma_\alpha(\xi)} \frac{|f(w)|^2 (1-|w|)^{2\alpha-t} dm_2(w)}{(1-|w|)^2 |1-\langle z_1,\bar{w}\rangle|^{\alpha+2}} \right)^{\frac{p}{2}} d\xi \right)^{\frac{1}{p}} \times$$

$$\times \left(\int_T \left(\int_{\Gamma_\alpha(\xi)} \frac{(1-|w|)^t dm_2(w)}{|1-\langle z_2,\bar{w}\rangle|^{\alpha+2}} \right)^{\frac{q}{2}} dm(\xi) \right)^{\frac{1}{q}} \le B(f)(1-|z_2|)^{-\left(\frac{\alpha-t}{2}-\frac{1}{q}\right)},$$

$p>2, \alpha > t+\frac{2}{q}, t \in (-2,-1), \alpha > \frac{t}{2}, \frac{1}{p}+\frac{1}{q}=1.$

Using Fubini's theorem, duality argument

$$B(f) = \sup_{\|\varphi\|_{L^{(\frac{p}{2})'}}} \int_T \int_{\Gamma_\alpha(\xi)} \frac{|f(w)|^2 (1-|w|)^{2\alpha-t} dm_2(w)}{(1-|w|)^2 |1-\langle z_1,\bar{w}\rangle|^{\alpha+2}} |\psi(\xi)|\, dm(\xi)$$

$$= \sup_{\|\varphi\|_{L^{(\frac{p}{2})'}}} \int_U \frac{|f(w)|^2 (1-|w|)^{2\alpha-t}}{|1-\langle z_1,\bar{w}\rangle|^{\alpha+2}} \int_T |\psi(\xi)|\, \chi_{\Gamma_\alpha(\xi)}(z) d\xi \frac{dm_2(w)}{(1-|w|)^2}.$$

Hence using (3) and the estimate

$$\sup_{z\in\Gamma_\eta} \frac{1}{1-|z|} \int_T |\psi(\xi)|\, \chi_{\Gamma_\tau(\xi)}(z) dm(\xi) \le C M_{H-L}(\varphi)(\xi), \text{ (see[4])},$$

we have $(\widetilde{f} = f(1-|w|)^{\frac{\alpha}{2}})$

$$B(f) \le \sup_{\varphi} \int_T (A_\infty(\widetilde{f})(\xi))^2 M_{H-L}(\varphi)(\xi) C \left(\frac{(1-|w|)^{\alpha-t-1}}{|1-\langle z,w\rangle|^{\alpha+2}} \right)(\xi) d\xi$$

$$\le \sup_{\varphi} \int_T (A_\infty(\widetilde{f})(\xi))^2 M_{H-L}(\varphi)(\xi) d\xi \sup_{\widetilde{w}\in U} \int_U \frac{(1-|w|)^{\alpha-t-1}(1-|\widetilde{w}|)^N dm_2(w)}{|1-\langle z_1,\widetilde{w}\rangle|^{\alpha+2} |1-\langle \widetilde{w},w\rangle|^{N+1}},$$

where M_{H-L} is a maximal Hardy-Littlewood function. We used the fact that

$$\|C(F)\|_{L^\infty} = \sup_{\widetilde{w}\in U} \int_U \frac{|F(z)|\, dm_2(z)}{|1-\langle \widetilde{w},z\rangle|^N} (1-|\widetilde{w}|)^{N-1}, \ N>1.$$

From last estimate, Hölder's inequality and (2) we fimally get

$$|\Phi(z_1,z_2)|\,(1-|z_1|)^{t+2}(1-|z_2|)^{\frac{\alpha-t}{2}-\frac{1}{q}} \le C \left\| \widetilde{f} \right\|_{L^p},$$

$t \in (-2,-1), p>2$. The proof of Theorem 1 is complete. ∎

Remark 2.1. *Putting $n = 1, \alpha = 0, \beta = 0$ in first estimate of Theorem 1 we get the following well-known estimate for H^p classes (see [5], Chapter 1)*

$$\int_T \sup_{z \in \Gamma_\gamma(\xi)} |\Phi(z)|^2 \, dm(\xi) \leq C \, \|\Phi\|^2_{H^2(U)} .$$

Putting $n = 1, \alpha = 0, t = -2$ in the second statement of Theorem 1 we get the well-known estimate (see [1], Theorem 2.5, [4], [5])

$$\sup_{|z|<1} |\Phi(z)| \, (1 - |z|)^{\frac{1}{p}} \leq C \int_T \sup_{w \in \Gamma_\gamma(\xi)} |\Phi(w)|^p \, dm(\xi) = \|\Phi\|^p_{H^p} .$$

We similarly show the following results for multifunctional case, some are valid even in the unit ball.

We assume that parameters α and β in the following theorems are positive .

Theorem 2.2. *Let $\alpha + \beta < \frac{1}{2}, \alpha > \beta, \beta < \frac{1}{2}$. Then we have that*

$$\int_T \left(\sup_{z_1 \in \Gamma_\gamma(\xi)} \sup_{z_2 \in \Gamma_\gamma(\xi)} \left| \mathcal{D}^\alpha_{z_2} (T_{2,0} \tilde{f})(z_1, z_2) \right| (1 - |z_1|)^{\alpha - \beta} (1 - |z_2|)^{\beta + \alpha} \right)^2 d\xi \leq$$
$$\leq C \, \|f_1\|^2_{H^2(U)} \, \|f_2\|^2_{H^{\frac{m-1}{\alpha}}} \ldots \|f_m\|^2_{H^{\frac{m-1}{\alpha}}} ,$$

where $\tilde{f} = \prod_{j=1}^{m} f_j$; $m \geq 2$; $m \in \mathbb{N}$.

Theorem 2.3. *Let $\alpha + \beta < \frac{1}{2}, \alpha > \beta, \beta < \frac{1}{2}$. Then*

$$\int_T \left(\sup_{z_1 \in \Gamma_\gamma(\xi)} \sup_{z_2 \in \Gamma_\gamma(\xi)} \left| \mathcal{D}^\alpha_{z_2} (T_{2,0}) (\tilde{f})(z_1, z_2) \right| (1 - |z_1|)^{\alpha - \beta} (1 - |z_2|)^{\beta + \alpha} \right)^2 dm(\xi) \leq$$
$$\leq \widetilde{C} \, \|f_1\|^2_{H^2(U)} \, \|f_2\|^2_{\frac{\alpha}{m-1}} \ldots \|f_m\|^2_{\frac{\alpha}{m-1}} ,$$

where $\|f\|_t = \sup_{z \in U} |f(z)| \, (1 - |z|)^t$; $t \geq 0$; $\tilde{f} = \prod_{j=1}^{m} f_j$; $m \geq 2$.

We will show these results in the second part of this paper related with this topic.

References

[1] A. V. Aleksandrov, *Essay on non locally convex Hardy classes*, Lecture notes in Mathematics, Springer-Verlag, Complex Analysis and spectral theory. edited by V. V. Havin and N. K. Nikolski (1981), 1-99.

[2] E. Amar, C. Menini, *A counterexample to the corona theorem for operators on* $H^2(D^n)$, Pacific Journal of Mathematics, v. 206, no 2, 2002.

[3] D. Clark, *Restrictions of* H^p *functions in the polydisk*, American Journal of Mathematics, (110)(1988), 1119-1152.

[4] R. Coifman, Y. Meyer, E. Stein, *Some new functional classes and their applications to harmonic analysis*, Journal of Functional Analisys, (62)(1985), 304-335.

[5] A. E. Djrbashian, F. A. Shamoyan, *Topics in the Theory of* A^p_α *Spaces*, Leipzig, Teubner, 1988.

[6] I. Verbitsky, *Multipliers in spaces with fractional norms and inner functions*, Siberian Math. Journal, (Russian), no 2, 1985, 49-72.

[7] G. Ren, J. Shi, *The diagonal mapping in mixed norm spaces*, Studia Math., 163, 103-117, 2004.